SISSA ISAS

SCUOLA INTERNAZIONALE SUPERIORE DI STUDI AVANZATI
INTERNATIONAL SCHOOL FOR ADVANCED STUDIES

Variational Study of Two Strongly Correlated Fermi Systems: Fractional Quantum Hall Effect and Atomic ^{3}He at Zero Temperature

Thesis submitted for the degree of
"Doctor Philosophiæ"

CANDIDATE
Orion Ciftja

SUPERVISOR
Prof. Stefano Fantoni

Trieste—October 1997

Table of Contents

1 Introduction

This thesis includes a study on the strongly correlated Fermi systems, and can be thought as consisting of two parts. The first part deals with electronic correlations in two-dimensions (2D), namely the fractional quantum Hall effect (FQHE), while the second one is a Variational Monte Carlo (VMC) study on the ground state properties of liquid and solid ^{3}He in 3D.

In the first part we study the FQHE by means of self-consistent integral techniques, like the hyper-netted-chain (HNC) and Fermi-hyper-netted-chain (FHNC) theory. Such theories are very useful to study strongly correlated Bose and Fermi systems in the thermodynamic limit.

Firstly we studied the Laughlin states of the FQHE, by applying the Bose HNC and then a suitable approximation for the elementary diagrams, which was fairly accurate.

Then, a new class of variational wave functions, denoted as extended shadow wave function (ESWF) was studied in relation to the particle-hole conjugated states of the FQHE.

The generalized theory of the composite fermions (CF) was investigated by means of the FHNC and effective hyper-netted-chain (EFHNC) method.

Attempts were made to study the half-filled case, too.

In the second part we explored by means of a VMC simulation some issues related to a new class of variational wave functions which include the spin correlations explicitely on it.

This variational wavefunction which uses the spin coherent representation, to represent the spin correlations was used to study the properties of ^{3}He liquid and solid.

In both cases, the interaction potential between ^{3}He atoms was taken to be of the Aziz (HFDHE2) form.

Furthermore, we explored the effects of triplet correlations on it, finding a significant improvement on the ground state energy for ^{3}He liquid and solid.

2 A new Hyper–Netted–Chain treatment for Laughlin states

2.1 The 2D Bose HNC theory

Fractional quantum Hall effect (FQHE) [1], [2] is observed in two-dimensional (2D) electronic systems in the extreme quantum limit of very high magnetic field $B(> 5T)$, low temperature $T(< 2K^0)$ and high-mobility of electrons in the samples ($\mu > 10^5 cm^2/Vs$). Under these extreme conditions when the lowest Landau level (LLL) is fractionally filled the FQHE resistencies appear quantized, $\rho_{xy}(plateau) = \frac{h}{e^2}\frac{1}{\nu}$ and $\rho_{xx}(plateau) = 0$, where h is the Planck constant, ϵ the magnitude of the electronic charge and ν is the LLL filling factor.

The filling factors where FQHE was observed [3] are such that they appear with odd denominators: $\nu = 1/3, 2/5, 3/7, 4/9 \ldots$ or $1/5, 2/9 \ldots$ but FQHE is not confined only to the LLL. It is observed also in higher Landau levels ($n = 1, 2 \ldots$), where n is the quantum number of each Landau level.

For instance, in higher Landau levels a fractional Hall plateau $\rho_{xy}(plateau) = \frac{h}{e^2}\frac{1}{(5/2)}$, corresponding to an even denominator filling factor was found. There are indications that other even denominator filling factors, like the very interestig case of $\nu = 1/2$ exists and work in such direction is current research.

The first step in the explanation of the FQHE would be the study of the properties of a 2D system of interacting electrons in a uniform positive background, with the magnetic field $\vec{B}$ so high and temperature T so low, such that only the lowest Landau level (LLL) would be partially filled. The filling factor ν of the LLL can be written as :

$$\nu = 2\pi l_0^2 \rho \ , \tag{2.1}$$

where $l_0 = \sqrt{\hbar/(eB)}$ is the so-called magnetic length, ρ is the 2D electronic density, $\hbar$ is the reduced Planck constant and $e > 0$ is the magnitude of the electron charge.

The unit of Coulomb potential energy is $\frac{1}{4\pi\epsilon_0}\frac{e^2}{\epsilon l_0}$ which is the energy scale throughout and ϵ is the dielectric constant of the neutralizing background. Where FQHE has been generally observed can be verified that :

$$\frac{1}{4\pi\epsilon_0}\frac{e^2}{\epsilon l_0} \leq \hbar\omega_c \tag{2.2}$$

so the admixture of states in higher Landau levels can be ignored .

Magnetic field $\vec{B}$ is considered such that all electronic spins $\{\vec{s}_i\}$ are frozen along the applied field $\vec{B}$ and have no interesting dynamics .

Electrons with charge $-e(e > 0)$ are considered as usual to be confined in the $x - y$ plane. They are subjected to a strong magnetic field perpendicular to the plane. Considering the symmetric gauge: $\vec{A} = \left[-\frac{B}{2}y, \frac{B}{2}x, 0\right]$ the magnetic field $\vec{B} = \vec{\nabla} \times \vec{A}$ is of the form: $\vec{B} = [0, 0, B]$. The many-electron system is described by the Hamiltonian:

$$\hat{H} = \hat{K} + \hat{V} \ , \tag{2.3}$$

where

$$\hat{K} = \frac{1}{2m_e}\sum_{i=1}^{N}[-i\hbar\vec{\nabla}_i + e\vec{A}(\vec{r}_i)]^2 \tag{2.4}$$

and

$$\hat{V} = \sum_{i<j}^{N} v(|\vec{r}_i - \vec{r}_j|) - \rho \sum_{i=1}^{N} \int d^2r\ v(|\vec{r}_i - \vec{r}|) + \frac{\rho^2}{2} \int d^2r_1 \int d^2r_2\ v(|\vec{r}_1 - \vec{r}_2|) \qquad (2.5)$$

In the above expressions $e > 0$, m_e - is the electron mass, N is the total number of the electrons on the system, $z_j = x_j + iy_j$ - is the location of the j-th electron in complex coordinates, $v(|\vec{r}_i - \vec{r}_j|) = \frac{1}{4\pi\epsilon_0} \frac{e^2}{\epsilon|z_i - z_j|}$ is the interaction potential and the three terms in the formula for $\hat{V}$ are respectively the electron-electron, electron-background and background-background interaction energy.

For LLL filling factor $\nu = 1/m$ with $m = 1, 3, \ldots$ odd, Laughlin [4] has proposed the following variational wave function to describe the ground state:

$$\psi_m(z_1 \ldots z_N) = \prod_{i<j}^{N} (z_i - z_j)^m \prod_{j=1}^{N} \exp(-\frac{|z_j|^2}{4l_0^2}) \qquad (2.6)$$

To determine which m minimizes the energy , Laughlin wrote the probability distribution of the 2D electrons described by ψ_m as : $|\psi_m|^2 = \exp[-\beta H_m]$, with

$$\beta H_m = -2m \sum_{i<j}^{N} \ln|z_i - z_j| + \sum_{i=1}^{N} \frac{|z_i|^2}{2l_0^2} \qquad (2.7)$$

From here he identified $\beta = 1/m$ and mapping the problem into a classical 2D one component plasma (OCP) [5] he found that energy is minimized when plasma 2D electrons spread out uniformly in a disk where 2D electronic density ρ_m corresponds to a filling factor $\nu = 1/m$ where m is an odd integer.

Let us recall some of the properties of the 2D OCP where N particles are confined to a disk of radius R uniformly filled by the neutralizing background of charge density $\rho_0 = \frac{Ne}{\pi R^2}$.

The total interaction potential includes the electron-electron, electron-background and background-background parts:

$$V_N(\vec{r}_1 \ldots \vec{r}_N) = V_{ee}(\vec{r}_1 \ldots \vec{r}_N) + V_{eb}(\vec{r}_1 \ldots \vec{r}_N) + V_{bb}(\vec{r}_1 \ldots \vec{r}_N) \qquad (2.8)$$

They are respectively:

$$V_{ee}(\vec{r}_1 \ldots \vec{r}_N) = -\frac{1}{2\pi\epsilon_0} e^2 \sum_{i<j}^{N} \ln(|\vec{r}_i - \vec{r}_j|) \ , \tag{2.9}$$

$$V_{eb}(\vec{r}_1 \ldots \vec{r}_N) = \frac{1}{2\pi\epsilon_0} N \frac{e^2}{2} \sum_{i=1}^{N} (\frac{r_i}{R})^2 + const \ , \tag{2.10}$$

$$V_{bb}(\vec{r}_1 \ldots \vec{r}_N) = -\frac{1}{2\pi\epsilon_0} \frac{\rho_0^2}{2} (\pi R^2)^2 [\ln(R) - \frac{1}{4}] \tag{2.11}$$

and

$$const = \frac{1}{2\pi\epsilon_0} \frac{\rho_0^2}{2} (\pi R^2)^2 [2\ln(R) - 1] \tag{2.12}$$

Summing all the interacting energy parts we have the following

potential for the 2D OCP:

$$V_N(\vec{r}_1 \ldots \vec{r}_N) = -\frac{1}{2\pi\epsilon_0} e^2 \sum_{i<j}^{N} \ln(|\vec{r}_i - \vec{r}_j|) + \frac{1}{2\pi\epsilon_0} N \frac{e^2}{2} \sum_{i=1}^{N} (\frac{r_i}{R})^2 + \frac{1}{2\pi\epsilon_0} \frac{N^2 e^2}{2} [\ln(R) - 3/4] \ . \tag{2.13}$$

Monte Carlo (MC) calculations of Caillol et al [5] have demonstrated that 2D OCP is a hexagonal crystal when the dimensionless plasma parameter $\Gamma = e^2\beta$ is greater than 140 and a fluid otherwise. Laughlin maped his FQHE states to a 2D OCP with coupling parameters of the form : $\Gamma = 2m$. The most interesting feature in the intermediate coupling regime of the 2D OCP is that calculations can be done exactly for one special value [6] of coupling constant, namely : $\Gamma = 2$.

The 2D classical plasma provides a strong support that the Laughlin ground state function is indeed a translationally invariant incompresible liquid up to $\nu_c \approx 1/7$, where a 2D hexagonal Wigner crystal ground state function is calculated to be more preferable.

For $\nu = 1/3$ and $\nu = 1/5$, Laughlin [4] , using a modified hyper-netted chain (MHNC) technique described by [5] found that the interaction energy per particle defined as: $u(\nu =$

$1/m) = \frac{1}{N}\frac{<\psi_m|\hat{V}|\psi_m>}{<\psi_m|\psi_m>}$ was such that, $u(\nu = 1/3) = (-0.4156 \pm 0.0012)\ \frac{1}{4\pi\epsilon_0}\frac{e^2}{\epsilon l_0}$ and $u(\nu = 1/5) = (-0.3340 \pm 0.0028)\ \frac{1}{4\pi\epsilon_0}\frac{e^2}{\epsilon l_0}$.

Later , almost exact results for the interaction energy per particle were obtained by Levesque et al [7] performing Monte Carlo calculations on 256 electrons and obtaining : $u(\nu = 1/3) = (-0.410 \pm 0.0001)\ \frac{1}{4\pi\epsilon_0}\frac{e^2}{\epsilon l_0}$ and $u(\nu = 1/5) = (-0.3277 \pm 0.0002)\ \frac{1}{4\pi\epsilon_0}\frac{e^2}{\epsilon l_0}$.

Laughlin's model accounts the FQHE at $\nu = 1/m$ and $\nu = 1 - 1/m$, (by electron-hole symmetry) [8] for m-odd .

The elementary charged excitations in a stable state $\nu = 1/m$ are quasiparticles and quasi-holes with fractional charge $\pm e/m$. If one electron is added to the system, it amounts to adding m elementary excitations. The wave function at $\nu = p/q$ changes by a complex phase factor $e^{i\pi\nu}$, upon the interchange of 2 quasiparticles, so quasiparticles in the Laughlin model obey fractional statistics , but they also can be described by wave functions obeying Bose or Fermi statistics.

When filling factor ν is slightly shifted from the stable value $1/m$, where m is odd, the ground state of the system is expected to consist of a small density of quasiparticles or quasiholes with fractional charge $\pm e/m$ interacting via Coulomb interaction.

When filling factor ν is slightly less than $1/m$, quasiholes are formed, while when it is slightly higher than $1/m$, quasielectrons are formed .

Due to the absence of an energy scale, like the band width of a periodic solid or the Fermi energy of an electron liquid in the absence of a magnetic field, the Coulomb interaction induces such strong correlations amongst the electrons that cannot be accounted for in a perturbative way. It has been shown that these correlations are very well approximated by *Jastrow* factors, similarly to the case of liquid ^{4}He and ^{3}He.

Integral equation techniques, such as Hyper–Netted–Chain (HNC) for bosons or Fermi–Hyper–Netted–Chain (FHNC) for fermions, allow for realistic evaluations of the distribution

functions and related quantities for Jastrow correlated wave functions. Infact, they are particularly useful when calculations must be performed strictly in the thermodynamic limit. They have been extensively and succesfully used in the study of quantum liquids.

In the following, we study the Laughlin states ψ_m using the Bose hyper-netted-chain (HNC) method which is a standard technique to study the strongly interacting Bose systems.

Let us make a general brief description of the one-component HNC method. Suppose we have a one-component non-ideal Bose system described by a Hamiltonian that has the kinetic energy part $\hat{T}$ and the interaction potential one $\hat{V}$:

$$\hat{H} = \hat{T} + \hat{V} \tag{2.14}$$

The simplest variational Bose many-body wavefunction for the ground state will be of the Jastrow form and symmetric under the particle exchange:

$$\Psi(\vec{r}_1 \ldots \vec{r}_N) = \prod_{i<j}^{N} f(|\vec{r}_i - \vec{r}_j|) \tag{2.15}$$

The most important physical quantity we want to calculate is the pair-distribution function defined as :

$$g(\vec{r}_1, \vec{r}_2) = \frac{N(N-1)}{\rho^2} \frac{\int d\vec{r}_3 ... d\vec{r}_N \, |\Psi(\vec{r}_1 \ldots \vec{r}_N)|^2}{\int d\vec{r}_1 ... d\vec{r}_N \, |\Psi(\vec{r}_1 \ldots \vec{r}_N)|^2} \, , \tag{2.16}$$

where the integration includes summation over the discrete spin coordinates of all the particles.

Let us define :

$$|f(|\vec{r}_i - \vec{r}_j|)|^2 = e^{u(|\vec{r}_i - \vec{r}_j|)} \tag{2.17}$$

where $u(r_{ij})$ is the (pseudo)potential between particles i and j and $r_{ij} = |\vec{r}_i - \vec{r}_j|$.

Closely related to the pair distribution function is the long ranged pair correlation function defined as : $h(r_{12}) = g(r_{12}) - 1$, which heals out to 0 as the interparticle distance grows very large.

For the Bose HNC case, everything is reduced on the ability to sum all possible irreducible cluster diagrams of $|\Psi|^2$ in the numerator of $g(\vec{r}_1, \vec{r}_2)$ which are of following classes and types :

a) Composite (non-nodal) diagrams , denoted as non-nodal diagrams .

b) Simple (nodal) diagrams , of the type of simple chain or netted chain, denoted as nodal diagrams.

c) Simple (non-nodal) diagrams , of the type elementary (or bridge) , from now denoted as elementary diagrams .

The full set of Bose HNC equations is written as follows:

$$X(r_{12}) = \exp[u(r_{12}) + N(r_{12}) + E(r_{12})] - N(r_{12}) - 1 \ , \tag{2.18}$$

$$N(r_{12}) = \rho \int d^2 r_3 \ X(r_{13}) \ [X(r_{32}) + N(r_{32})] \ , \tag{2.19}$$

$$g(r_{12}) = 1 + X(r_{12}) + N(r_{12}) \tag{2.20}$$

The generation of diagrams contibuting to $g(r_{12})$ must go through a self consistent procedure. As a first approximation (and a good one) the contribution of the elementary diagrams is set to 0, $E(r_{12}) = 0$. The subscript "0" at HNC/0 denotes such approximation. Defining the 2D Fourier transform and its inverse:

$$\tilde{F}(q) = \int d^2 r \ e^{i\vec{q}\vec{r}} \ F(r) \ , \tag{2.21}$$

$$F(r) = \frac{1}{(2\pi)^2} \int d^2q \; e^{-i\vec{q}\vec{r}} \; \tilde{F}(q) \tag{2.22}$$

the summation of the nodal diagrams is easily done in the Fourier space,

$$\tilde{N}(q) = \rho \frac{\tilde{X}(q)^2}{1 - \rho \tilde{X}(q)} \tag{2.23}$$

The equations are solved by a self-consistent procedure which starts by setting $N(r_{12}) = 0$ in the first iteration. Then $X(r_{12})$ is computed. Performing a Fourier transform on $X(r_{12})$, $\tilde{X}(q)$ is found and, as consequence, $\tilde{N}(q)$ is calculated from Eq.(2.23). By inverse-Fourier transforming $N(q)$ we find the new $N(r_{12})$ which closes the first full iterative step. The process goes on until the desired convergency is achieved.

For the Laughlin states let us write the square modulus of the trial many-body wave function:

$$|\psi_m(z_1 \ldots z_N)|^2 = \prod_{i<j}^{N} |z_i - z_j|^{2m} \prod_{i=1}^{N} \exp[-\frac{|z_i|^2}{2l_0^2}] \tag{2.24}$$

Using the HNC theory one can express the pair function $g(r)$ as a series of cluster terms, associated with linked diagrams. The difference with respect to the case of the standard Jastrow wave function, in which the single particle term is not present, is that the diagrams are not irreducible and each vertex brings the *uncorrelated* one–body density $\rho_0(r)$ as a vertex correction. It has been proved [9] that such a series can be recast into a series of irreducible diagrams with the full one–body density $\rho(r)$ being the vertex correction. Since the full density is a constant, then the HNC equations for the pair function are exactly the same as for a Jastrow wave function without the single particle term and at density $\rho = \nu/(2\pi l_0^2)$, so

$$|\psi_m(z_1 \ldots z_N)|^2 = \prod_{i<j}^{N} |z_i - z_j|^{2m} \tag{2.25}$$

can be easily identified as a Bose wavefunction, with

$$u(|z_i - z_j|) = 2m \ln(|z_i - z_j|) \tag{2.26}$$

In order to handle the 2D logarithmic interaction , the standard procedure is to separate the (pseudo)potential, the nodal function and the non-nodal function in their short-range and the long-range parts. The HNC equations become more complicated but their form remains the standard one.

Let us write:

$$u(r_{12}) = u_s(r_{12}) + u_l(r_{12}) \ , \tag{2.27}$$

$$N(r_{12}) = N_s(r_{12}) - u_l(r_{12}) \ , \tag{2.28}$$

$$X(r_{12}) = X_s(r_{12}) + u_l(r_{12}) \ . \tag{2.29}$$

The splitting is done in such a way that:

$$u(r_{12}) + N(r_{12}) = u_s(r_{12}) + N_s(r_{12}) \ , \tag{2.30}$$

$$N(r_{12}) + X(r_{12}) = N_s(r_{12}) + X_s(r_{12}) \ , \tag{2.31}$$

The main short and long-range (pseudo)potentials for this case are taken:

$$u_s(r_{12}) = -2mK_0(Qr_{12}) \ , \tag{2.32}$$

$$u_l(r_{12}) = 2mK_0(Qr_{12}) + 2m \ln(r_{12}) \ , \tag{2.33}$$

where $K_0(x)$ is the modified Bessel function, Q is the cutoff parameter of order $1/l_0$ and the relation:

$$\int d^2r \ e^{i\vec{q}\vec{r}} \ [\ln(r) + K_0(Qr)] = \frac{-2\pi Q^2}{q^2(q^2+Q^2)} \ , \tag{2.34}$$

holds.

The Bose HNC final set of equations is solved by initially setting $N_s(r_{12}) = 0$ in the following equation:

$$X_s(r_{12}) = \exp[u_s(r_{12}) + N_s(r_{12}) + E(r_{12})] - N_s(r_{12}) - 1 \ , \tag{2.35}$$

Then we perform a 2D Fourier transform of $X_s(r_{12})$, obtaining $\tilde{X}_s(q)$. Later, we compute $\tilde{X}(q) = \tilde{X}_s(q) + \tilde{u}_l(q)$, so that $\tilde{N}(q)$ is computed from the standard HNC Eq.(2.23). Easily $\tilde{N}_s(q) = \tilde{N}(q) + \tilde{u}_l(q)$, and an inverse 2D Fourier transform on it, produces the new $N_s(r_{12})$. This procedure goes on until the desired accuracy is reached and the pair distribution function may be obtained from:

$$g(r_{12}) = 1 + X_s(r_{12}) + N_s(r_{12}) \tag{2.36}$$

Because the Laughlin wave function is treated as a Bose case, and it lies entirely in the LLL, the kinetic energy per particle will be

$$\frac{1}{N}\frac{<\Psi_m|\hat{K}|\Psi_m>}{<\Psi_m|\Psi_m>} = \frac{1}{2}\hbar\omega_c. \tag{2.37}$$

Instead the potential energy per particle is computed from the following formula:

$$\frac{1}{N}\frac{<\Psi_m|\hat{V}|\Psi_m>}{<\Psi_m|\Psi_m>} = \frac{\rho}{2}\int d^2r \ v(|\vec{r}|) \ [g(r) - 1] \tag{2.38}$$

where $v(|\vec{r}|) = \frac{1}{4\pi\epsilon_0}\frac{e^2}{\epsilon|\vec{r}|}$.

2.2 Scaling Approximation for the Laughlin states

HNC theory has also been adopted in the study of the FQHE, to evaluate the pair distribution function for the variational wave function proposed by Laughlin [4].

It is well known that the (F)HNC techniques are intrinsically approximated because there is a set of cluster terms (corresponding to the so called *elementary diagrams*) which cannot

be fully included in any closed form. Whereas the approximation of totally neglecting these terms [(F)HNC/0] leads to reliable results for the ground state energies, realistic evaluations of other quantities, like for instance the pair distribution function or the magnetoroton spectrum, require better approximations. Therefore, it is important to find numerical procedures to include efficiently the main contributions from the elementary diagrams.

In this thesis we propose a new *scaling* procedure for the inclusion of elementary diagrams in (F)HNC calculations to be used in the study of the FQHE, and we apply it to the Laughlin case.

The HNC/0 approximation neglects $E(r)$ completely. The HNC/4 approximation includes the elementary diagrams of the simplest structure, namely the four point elementary diagram $E_4(r)$. Higher order approximations include the five–points elementary structures (HNC/5), and so on. It is known that the series, HNC/0, HNC/4, ..., converges very slowly to the exact result. It is also known that the various elementary structures $E_4(r)$, $E_5(r)$, .., roughly scale with each other. Based on this property, the scaling approximation:

$$E(r) = \alpha E_4(r), \tag{2.39}$$

has been successfully used [10] in variational calculations on liquid ^{4}He.

In this section we apply this approximation to calculate the pair function, the energy per particle and the magnetoroton spectrum for the Laughlin wave function. For a given filling factor $\nu = 1/m$ we solve the HNC equations in HNC/0 approximation. Then we compute the four–point elementary diagram:

$$E_4(r_{ij}) = \frac{\rho^2}{2} \int [h(r_{ik})h(r_{il})h(r_{jk})h(r_{jl})h(r_{kl})] d^2r_k d^2r_l, \tag{2.40}$$

where $h(r) = g(r) - 1$. From the correspondence [4] of $|\Psi_m|^2$, with the partition function of a *charge neutral* two-dimensional plasma, it follows that [5] HNC/0 theory automatically

m	HNC/0	HNC/4	HNC/S	MHNC	MC
3	-0.4055	-0.4063	-0.4100	-0.4156	-0.410
5	-0.3240	-0.3247	-0.3274	-0.3340	-0.3277

Table 2.1: Interaction energies per particle in units of $\frac{1}{4\pi\epsilon_0}\frac{e^2}{\epsilon l_0}$.

satifies the *charge neutrality* and the *perfect screening* sum rules,

$$\rho \int d^2r\ [g(r) - 1] = -1\ , \tag{2.41}$$

$$\rho \int d^2r\ r^2[g(r) - 1] = -2l_0^2\ , \tag{2.42}$$

but violates the *compressibility* sum rule. Therefore we fix the scaling parameter α by imposing the *compressibility* sum rule [5] :

$$\rho \int d^2r\ r^4[g(r) - 1] = -16l_0^4(1 - m/2). \tag{2.43}$$

With the estimated $E(r)$ we solve again the HNC equation for a new $g(r)$ and we iterate the process until convergence is reached.

This approximation is much better than that used by Laughlin [4] in his original calculations, named Modified HNC (MHNC) [5]. MHNC approximation assumes that, for any given filling factor, $E(r)$ scales with respect to the corresponding function: $E^{(m=1)}(r)$ for filling $\nu = 1$, which is exactly known.

In fact the assumption that the shape of $E(r)$ does not change significantly with the filling factor is not justified, as shown in Fig. 2.1.

The results obtained for the energy per particle for $m = 3, 5$ are given in Table 2.1.

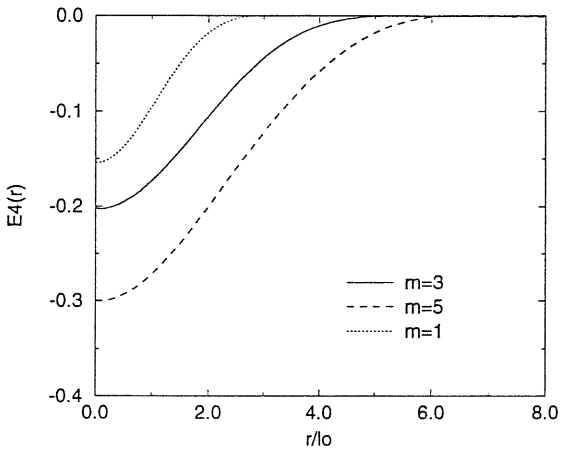

Figure 2.1: Lowest order elementary (bridge) function $E_4(r)$ for Laughlin states $\nu = 1/3$ (solid) and $\nu = 1/5$ (dashed) compared to the exact $E(r)$ for the $\nu = 1$ state (dotted).

Our scaling approximation (HNC/S) is compared with HNC/0, HNC/4 and with the MHNC results of Ref. [4] and the Monte Carlo (MC) results of Ref. [7]. One can see that the HNC/S results are in much better agreement with the MC ones than the other approximation schemes.

The values found for the scaling coefficient α, 6.25 for filling 1/3 and 5.2 for filling 1/5 are quite large, consistently with the fact that HNC/4 is a rather poor approximation. MHNC approximation gets worse for higher value of m.

In Fig. 2.2 we plot the pair distribution functions obtained for $\nu = 1/3$ and $\nu = 1/5$ by using HNC/0 and HNC/S techniques together with that given in Ref. [11] which fits the Monte Carlo data.

The agreement between the HNC/S pair function and the MC one is impressive especially

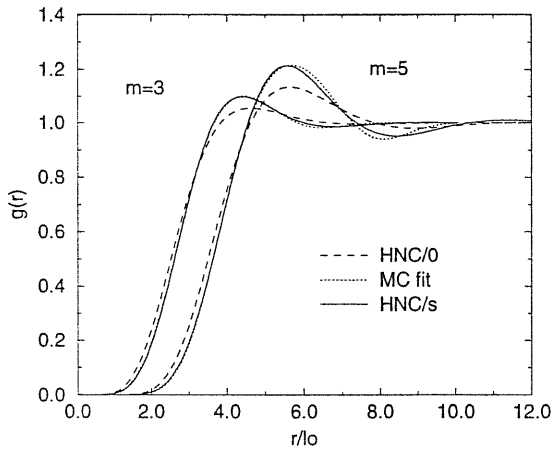

Figure 2.2: Comparison of $g(r)$ obtained from HNC/0 (dashed), HNC/S (solid) and the best MC data fitting of Ref. [11] , (dotted) for the Laughlin states $\nu = 1/3$ and $\nu = 1/5$.

in the small r regime. The r^2, r^4 and r^6 coeficients of $g(r)$ at small r compares very well with the MC results of Ref. [11].

We also investigated the collective excitations in the single mode approximation (SMA), using the wave function [11, 12]:

$$\Phi_{\vec{k}}^{(m)} = \overline{\rho}_{\vec{k}}\, \Psi_m, \tag{2.44}$$

where $\overline{\rho}_{\vec{k}}$ is the projection of the density operator $\rho_{\vec{k}} = \sum_{j=1}^{N} \exp(i\vec{k}\cdot\vec{r}_j)$ onto the subspace of the lowest Landau level. In Fig. 2.3 we plot the excitation energies $\Delta(k)$ obtained with both HNC/S and HNC/0 at filling $\nu = 1/3$.

One can see that the effect of the elementary diagrams is quite sizeable for such a quantity, and HNC/0 approximation gives a higher gap. Similar results are found also at filling

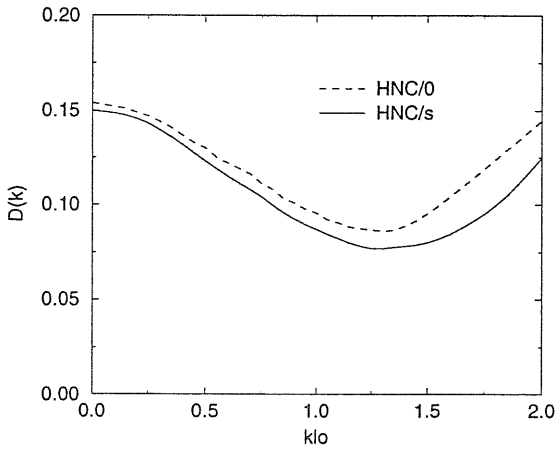

Figure 2.3: The SMA collective excitation gap $D(k)$ in units $\frac{1}{4\pi\epsilon_0}\frac{e^2}{\epsilon l_0}$ obtained from the HNC/0 and HNC/S pair distribution functions $g(r)$, for the Laughlin state $\nu = 1/3$.

$\nu = 1/5$.

3 The Extended Shadow Wave Functions for FQHE Hierarchical States

3.1 Introduction to the Extended Shadow Wave Function

The description of strong interparticle correlations in both Bose and Fermi systems with continuous degrees of freedom is a long-standing problem of current interest. More recently, the shadow wave function (SWF) has been proposed [13, 14] as a new variational ansatz to compute the properties of solid and liquid ^{4}He at T = 0 K.

The SWF in the Bose case is given by

$$\Psi^B_{SWF}(\vec{r}_1, \cdots, \vec{r}_N) = \prod_{i<j}^{N} f_{pp}(r_{ij}) \int \prod_{i=1}^{N} \chi(|\vec{r}_i - \vec{s}_i|) \prod_{i<j}^{N} f_{ss}(s_{ij})\, d\vec{S} \; . \tag{3.1}$$

The quantity $\vec{S}$ denotes the set of coordinates $[\vec{s}_i]$, so-called "shadow" variables, associated with the particles. The respective correlation factors may be written as

$$f_{pp}(r_{ij}) = e^{-\frac{U_{pp}(r_{ij})}{2}} \; , \tag{3.2}$$

and

$$f_{ss}(s_{ij}) = e^{-U_{ss}(s_{ij})} \; , \tag{3.3}$$

where $U_{pp}(r_{ij})$ and $U_{ss}(s_{ij})$ represent, respectively, the particle-particle and the shadow-shadow (pseudo)potential. The structure of $f_{ss}(s_{ij})$ is the same as that of $f_{pp}(r_{ij})$, namely it heals out to unity at large intershadow distances, whereas the "correlation" $\chi(x)$ between a particle and its associated shadow heals out to zero. [13]

Physically, the shadow variables $\vec{s}_i$ can be thought of as mimicking the quantum correlation "holes" which the particles carry around themselves in the dense system.

The physical interpretation of a SWF as well as the request of more variational freedom and of full symmetry under exchange of any particle with any hole, suggests further extended forms for the SWF, so that a new type of so-called extended shadow wave function (ESWF) was proposed. [15]

The ESWF is of the form

$$\Psi^B_{ES}(\vec{r}_1, \cdots, \vec{r}_N) = \prod_{i<j}^{N} f_{pp}(r_{ij}) \int \prod_{i,j}^{N,M} f_{ps}(|\vec{r}_i - \vec{s}_j|) \prod_{i<j}^{M} f_{ss}(s_{ij})\, d\vec{S}\ , \tag{3.4}$$

where N and M are, respectively, the number of particles and the number of shadows. The extension which Eq.(3.4) represents over the standard SWF of Eq.(3.1) concerns two aspects.

First, in the ESWF all shadows are correlated with all real particles rather than being in a one to one correspondence as in Eq.(3.1), allowing the possibility that the number and location of "holes" becomes different from those of the real particles. This form also allows for a description of lattice vacancies.

The second aspect, which is however related to the first, is that all three "correlation" functions, $f_{pp}(x)$, $f_{ps}(x)$, and $f_{ss}(x)$, must heal out to unity at large values of x.

In the case of an ESWF, the cluster diagrams of the pair distribution function are characterized by only three different types of points: p, s^R, s^L, where p denotes particle and $s^{R,L}$ denotes, respectively, right or left shadow coordinates. In fact, the normalization of

an ESWF is given by

$$< \Psi^B_{ES} | \Psi^B_{ES} >= \int \Big[\prod_{i<j}^{N} f^2_{pp}(r_{ij}) \prod_{i,j}^{N,M} f_{ps}(|\vec{r}_i - \vec{s}^L_j|) \times \prod_{i<j}^{M} f_{ss}(s^L_{ij}) \prod_{i,j}^{N,M} f_{ps}(|\vec{r}_i - \vec{s}^R_j|) \prod_{i<j}^{M} f_{ss}(s^R_{ij}) \Big] d\vec{S}^L d\vec{S}^R d\vec{R} \ , \tag{3.5}$$

and coincides with the partition function of a classical three-component system (p, s^R, s^L) interacting via the following (pseudo)potentials:

$$U_{pp} = -\ln(f^2_{pp}) \ , \tag{3.6}$$

$$U_{ps^R} = U_{ps^L} = -\ln(f_{ps}) \ , \tag{3.7}$$

$$U_{s^R s^R} = U_{s^L s^L} = -\ln(f_{ss}) \ , \tag{3.8}$$

and

$$U_{s^R s^L} = 0 \ . \tag{3.9}$$

The normalization integral (3.5) contains as integrand the square

$$\Psi^B_{ES}(\vec{r}_1, \cdots, \vec{r}_N) \times \Psi^B_{ES}(\vec{r}_1, \cdots, \vec{r}_N)$$

of the extended shadow wave function Ψ^B_{ES} as defined in expression (3.4). The real particle coordinates $\vec{r}_1, \cdots, \vec{r}_N$ must, of course, be taken to be identical in both factors. However, two indepedent sets of shadow coordinates, over both of which must be integrated in formula (3.5), are needed for explicitly representing the square of wave function Ψ^B_{ES}. In Eq.(3.5) these two independent sets of shadow particles are distinguished by the superscripts L and R, referring to "left" and "right" shadows, respectively. Every real particle is correlated with every other real particle as well as with every "left" and "right" shadow. Every "left"

shadow is correlated in turn with every other "left" shadow. The same applies to the "right" shadows. Correlations between "left" and "right" shadows are absent.

3.2 The Three-component HNC Method for FQHE

The hierarchical states [16, 17] may be described microscopically by electronic wave functions which can be expressed as an ESWF.

A possible way of constructing wave functions for the second level of the hierarchy is to first particle-hole conjugate [18, 19] the Laughlin parent state $\Psi_{\nu_0}(z_1, \cdots, z_N)$ with filling factor $\nu_0 = 1/m$, where $m = 3, 5$:

$$\Psi_{1-1/m}(z_1, \cdots, z_N) = \hat{C}\ [\Psi_{1/m}(z_1, \cdots, z_N)] = \int d\vec{S}_M\ \Psi^*_{1/m}(\vec{S}_M)\ \Phi_{\nu=1}(z_1, \cdots, z_N; \vec{S}_M) \tag{3.10}$$

The short-hand notation $\vec{S}_M$ represents the coordinates $\vec{s}_1, \cdots, \vec{s}_M$ of the M holes, where N and M satisfy [19] the relation $N + M = mM$. The second hierarchy state Ψ_ν is then obtained by multiplying $\Psi_{1-1/m}(z_1, \cdots, z_N)$ with $\prod_{j<k}^{N}(z_j - z_k)^p$, where p must be an even integer such that

$$\frac{1}{\nu} = \frac{1}{1-\nu_0} + p\ . \tag{3.11}$$

It follows that

$$\Psi_\nu = \prod_{j<k}^{N} (z_j - z_k)^{p+1}\, e^{-\sum_{j=1}^{N} \frac{|z_j|^2}{4l_0^2}}$$
$$\times \int \prod_{j,k}^{N,M} (z_j - s_k) \prod_{j<k}^{M} (s_j^* - s_k^*)^m (s_j - s_k)\, e^{-\sum_{j=1}^{M} \frac{|s_j|^2}{2l_0^2}}\, d\vec{S}\ , \tag{3.12}$$

where $l_0 = \sqrt{\frac{\hbar}{eB}}$ is the magnetic length and z_k and s_k are given in complex notation $x_k + iy_k$. For instance, the Laughlin parent state $\nu_0 = \frac{1}{3}$ with $m = 3$ generates for $p = 2$ the daughter state $\nu = \frac{2}{7}$, whereas for $p = 0$ it produces the state $\nu = \frac{2}{3}$. Similarly, the Laughlin state $\nu_0 = \frac{1}{5}$ generates for $p = 0$ the daughter state $\nu = \frac{4}{5}$, and so on.

Seen from the perspective of the ESWF approach, the hole variable $\vec{s}_i$ may be interpreted as a shadow variable. The analytic form of the shadow-shadow and shadow-particle correlations is, in the present case fixed by the lowest Landau level constraint. In this sense, this is a variational wave function with no adjustable parameters.

A comparison between Ψ_ν and Ψ^B_{ES} shows that Ψ_ν can be identified (after removal of the exponential factor which is relevant only in the trivial long wavelength limit) with a Ψ^B_{ES}, where

$$f_{pp}(jk) = (z_j - z_k)^{p+1} \ , \tag{3.13}$$

$$f_{ps}(jk) = (z_j - s_k) \ , \tag{3.14}$$

and

$$f_{ss}(jk) = (s^*_j - s^*_k)^m (s_j - s_k) \ . \tag{3.15}$$

Normalization of Ψ_ν yields

$$\begin{aligned} < \Psi_\nu | \Psi_\nu > = \int \Big[\prod_{j<k}^{N} |z_j - z_k|^{2(p+1)} \prod_{j,k}^{N,M} (z^*_j - s^{L*}_k) \prod_{j<k}^{M} (s^L_j - s^L_k)^m \\ \times (s^{L*}_j - s^{L*}_k) \prod_{j,k}^{N,M} (z_j - s^R_k) \prod_{j<k}^{M} (s^{R*}_j - s^{R*}_k)^m (s^R_j - s^R_k) \Big] d\vec{R} d\vec{S}^L d\vec{S}^R \ . \end{aligned} \tag{3.16}$$

Writing

$$|z_j - z_k|^{2(p+1)} = e^{-U_{pp}} \ , \tag{3.17}$$

$$(z_j - s^R_k) = e^{-U_{pR}} \ , \tag{3.18}$$

and

$$(s^{R*}_j - s^{R*}_k)^m (s^R_j - s^R_k) = e^{-U_{RR}} \ , \tag{3.19}$$

we see that the normalization condition for Ψ_ν coincides with the partition function of a three-component (p, R, L) system interacting via the (pseudo)potentials

$$U_{pp} = -2(p+1)\ln|z_j - z_k| \ , \tag{3.20}$$

$$U_{pR} = U_{pL} = -\ln|z_j - s_k^R| - i\theta_{jR,kR} \ , \tag{3.21}$$

$$U_{RR} = U_{LL} = -(m+1)\ln|s_j^R - s_k^R| + i(m-1)\theta_{jR,kR} \ , \tag{3.22}$$

and

$$U_{RL} = 0 \ , \tag{3.23}$$

where $\tan(\theta_{jk}) = y_{jk}/x_{jk}$.

For our p, R, L system we can apply a three-component HNC treatment.

This will improve upon the one-component HNC calculation of MacDonald et al., [18] based on the introduction of an ad-hoc effective potential mimicking the effect of the hole variables. While this is an approximation [18] (which we will presently overcome) it did allow inclusion of elementary diagrams in a simple way.

In the present work, for the sake of simplicity, we neglect the elementary diagrams, so we use the so-called HNC/0 approximation.

There is a major difference from the previously known HNC/0 treatments, since here the correlations $f_{ps}(jk)$ and $f_{ss}(jk)$, and consequently, several other HNC/0 quantities are complex functions and depend on both the x_{jk}- and y_{jk}-component of the interparticle coordinate z_{jk}.

The long range parts $U_{ps}^l(jk)$ and $U_{ss}^l(jk)$ bring an angular dependence into all the HNC quantities. However, it turns out that the nodal functions $N_{\alpha\beta}(jk)$ and non-nodal functions

$X_{\alpha\beta}(jk) = g_{\alpha\beta}(jk) - 1 - N_{\alpha\beta}(jk)$ have a long range behavior exactly given by $-U^l_{\alpha\beta}(jk)$ and $U^l_{\alpha\beta}(jk)$, so that all pair distribution functions $g_{\alpha\beta}(jk)$ are short-ranged. [15]

The multi-component HNC/0 method is a generalization of the one-component one and an iteration scheme similar to that can be adopted here.

In the case of a multi-component system the corresponding HNC/0 quantities are given by the following equations:

$$X_{\alpha\beta}(r_{12}) = e^{-U_{\alpha\beta}(r_{12})+N_{\alpha\beta}(r_{12})} - 1 - N_{\alpha\beta}(r_{12}) \,, \tag{3.24}$$

$$N_{\alpha\beta}(r_{12}) = \sum_\gamma \rho_\gamma \int X_{\alpha\gamma}(r_{13})[X_{\gamma\beta}(r_{32}) + N_{\gamma\beta}(r_{32})]\, d\vec{r}_3 \,, \tag{3.25}$$

and

$$g_{\alpha\beta}(r_{12}) = 1 + X_{\alpha\beta}(r_{12}) + N_{\alpha\beta}(r_{12}) \tag{3.26}$$

where ρ_γ represents the densities of the different types of particles of the multi-component system.

We recall that the different "particles" identified as p (particle), R (right shadow), and L (left shadow) have densities ρ_p, ρ_R, and ρ_L.

Since Ψ^B_{ES} is symmetric under the exchange of shadow variables $\vec{s}_i$, irrespective of $\vec{r}_i$, there are only four independent HNC/0 quantities, i.e, N_{pp}, $N_{pR} = N_{pL}$, $N_{RR} = N_{LL}$, and N_{RL}. Among the three components p, R, L there are only four independent pairings: (pp), (pR), (RR), and (RL).

Introducing the two-dimensional (2D) Fourier transforms

$$\tilde{F}_{pp}(q) = \rho_p \int e^{i\vec{q}\vec{r}} F_{pp}(r)\, d\vec{r} \,, \tag{3.27}$$

$$\tilde{F}_{ps}(q) = \sqrt{\rho_p \rho_s} \int e^{i\vec{q}\vec{r}} F_{pr}(r)\, d\vec{r} \,, \tag{3.28}$$

and

$$\tilde{F}_{ss}(q) = \rho_s \int e^{i\vec{q}\vec{r}} F_{ss}(r)\, d\vec{r}\,, \tag{3.29}$$

with $\rho_s = \rho_R = \rho_L$, the general formula of Eq.(3.25) becomes

$$\tilde{N}_{\alpha\beta}(q) = \sum_{\gamma} \tilde{X}_{\alpha\gamma}(q)[\tilde{X}_{\gamma\beta}(q) + \tilde{N}_{\gamma\beta}(q)]\,. \tag{3.30}$$

As R and L are hermitian conjugated we have: $\tilde{F}_{pp}(q) = \tilde{F}^*_{pp}(q)$, $\tilde{F}_{pR}(q) = \tilde{F}^*_{pL}(q)$, $\tilde{F}_{RR}(q) = \tilde{F}^*_{LL}(q)$, $\tilde{F}_{RL}(q) = \tilde{F}^*_{LR}(q)$, whereas $\tilde{F}_{pR}(q) = \tilde{F}_{Rp}(q)$, $\tilde{F}_{pL}(q) = \tilde{F}_{Lp}(q)$.

Keeping this in mind, we determine after some algebra all relations between HNC/0 quantities in the Fourier space for the four possible independent pairings: (pp), (pR), (RR), and (RL):

$$\tilde{X}_{pR}(q) + \tilde{N}_{pR}(q) = \frac{\tilde{X}_{pR}(q)[1 - \tilde{X}^*_{RR}(q)] + \tilde{X}^*_{pR}(q)\tilde{X}^*_{RL}(q)}{D(q)}\,, \tag{3.31}$$

$$\tilde{X}_{RR}(q) + \tilde{N}_{RR}(q) = \frac{[1 - \tilde{X}_{pp}(q)][1 - \tilde{X}^*_{RR}(q)] - \tilde{X}^*_{pR}(q)^2}{D(q)} - 1\,, \tag{3.32}$$

$$\tilde{X}^*_{RL}(q) + \tilde{N}^*_{RL}(q) = \frac{\tilde{X}^*_{RL}(q)[1 - \tilde{X}_{pp}(q)] + |\tilde{X}_{pR}(q)|^2}{D(q)}\,, \tag{3.33}$$

and

$$\tilde{X}_{pp}(q) + \tilde{N}_{pp}(q) = \frac{|1 - \tilde{X}_{RR}(q)|^2 - |\tilde{X}_{RL}(q)|^2}{D(q)} - 1\,, \tag{3.34}$$

where the denominator $D(q)$ is given by

$$\begin{aligned} D(q) \;=\; & [1 - \tilde{X}_{pp}(q)][|1 - \tilde{X}_{RR}(q)|^2 - |\tilde{X}_{RL}(q)|^2] - |\tilde{X}_{pR}(q)|^2[\tilde{X}_{RL}(q) + \tilde{X}^*_{RL}(q)] \\ & -\tilde{X}_{pR}(q)^2[1 - \tilde{X}^*_{RR}(q)] - \tilde{X}^*_{pR}(q)^2[1 - \tilde{X}_{RR}(q)]\,. \end{aligned} \tag{3.35}$$

As in a standard HNC/0 treatment our (pseudo)potentials of the form $U(z) = a\ln(z) + \theta$ are separated into short-range and long-range parts:

$$U^s(z) = -aK_0(Qz) \ , \tag{3.36}$$

and

$$U^l(z) = a[\ln(z) + K_0(z)] + \theta \ , \tag{3.37}$$

where $K_0(x)$ is the modified Bessel function and Q is the cutoff parameter of the order of $1/l_0$.

As a consequence, all nodal and non-nodal functions for all independent pairings (pp), (pR), (RR), and (RL) are split into their short- and long-range parts.

3.3 Results for the Hierarchical states

A three-component HNC/0 scheme has been implemented using ESWF for the hierarchy states corresponding to $\nu = 2/7$, $\nu = 2/3$, and $\nu = 4/5$. For numerical convenience the distances were expressed in dimensionless units r/l_0.

In Fig. 3.1 we plot the pair distribution function $g(r)$ for $\nu = 2/7$ as a function of r/l_0 and compare it with that of Ref. [18].

It clearly shows characteristics of a liquid state.

The ground state interaction energy per particle, is found to be $u(2/7) = -0.374\ \frac{1}{4\pi\epsilon_0}\frac{e^2}{\epsilon l_0}$, which is in close agreement with the value $-0.377(3)\ \frac{1}{4\pi\epsilon_0}\frac{e^2}{\epsilon l_0}$ of Morf and Halperin. [20]

In Fig. 3.2 we plot the structure factor $S(q)$ for $\nu = 2/7$ as a function of ql_0.

A further test of the ESWF and a useful source of information for future research is the study of small r behavior of the pair distribution functions [21]. Diagonalizing numerically the Hamiltonian for a finite system of 4 to 6 fermions, Yoshioka [22] obtained the coefficients of expansion of $g(r)$ for small r which seem to vary continuously as function of ν. For small

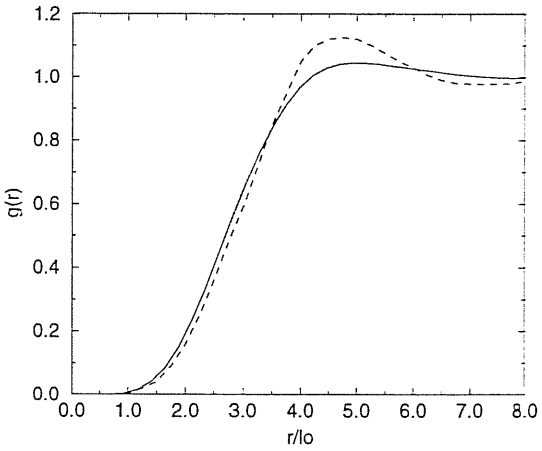

Figure 3.1: Pair distribution function obtained from the ESWF (solid), compared to that of MacDonald et al. Ref. [18] (dashed), for the FQHE state $\nu = 2/7$.

r around the origin $r = 0$, we can expand our $g(r)$ obtained from the three-component HNC/0 method in the following way:

$$g(r) = \sum_{i=0}^{\infty} c_i \left(\frac{r}{l_0}\right)^{2i} . \tag{3.38}$$

We least-square-fitted $g(r)$ in the region $0 \leq r \leq 1.7\, l_0$ to obtain the coefficients c_i.

For $\nu = 2/7$ we found $c_0 = 0$, $c_1 = 0$, $c_2 = 0$, $c_3 = 0.008185$, $c_4 = -0.001455$, whereas for $i > 4$ the coefficients c_i are zero within the limit of our numerical accuracy. The same procedure applied to the state $\nu = 4/5$ gives: $c_0 = 0$, $c_1 = 0.481689$, $c_2 = -0.133997$, $c_3 = 0.024499$, $c_4 = -0.002222$.

For the state $\nu = 2/3$ we obtain instead: $c_0 = 0$, $c_1 = 0.435377$, $c_2 = -0.117703$, $c_3 = 0.021723$, $c_4 = -0.001994$. These results agree rather closely with the finite-size calculations by Yoshioka. [22]

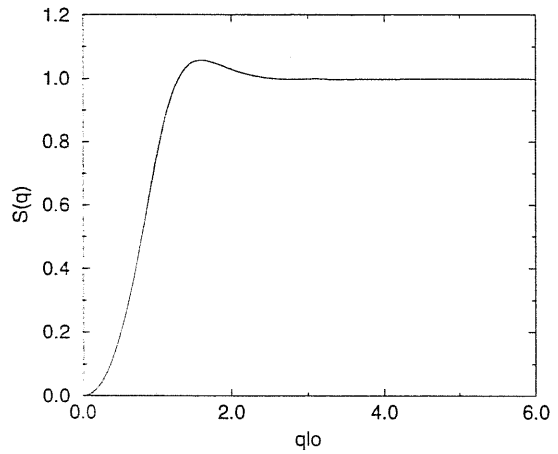

Figure 3.2: Static structure factor $S(q)$ for $\nu = 2/7$, obtained from the ESWF.

The small r behavior of different FQHE pair distribution functions as a function of r/l_0 is plotted in Fig. 3.3.

Indeed, there are only small differences between states $\nu = 4/5$ and $\nu = 2/3$, as expected.

In Fig. 3.4 we plot the resulting $g(r)$ for the state $\nu = 2/3$, obtained from the ESWF, and compare it with that of Ref. [20].

The $g(r)$ for $\nu = 2/3$ is in rather good agreement with that obtained by Morf and Halperin [20] using non-antisymmetrized wave functions.

For instance, the ground state energy per particle was found to be $u(2/3) = -0.510\ \frac{1}{4\pi\epsilon_0}\frac{e^2}{\epsilon l_0}$, very close to the result $-0.509(5)\ \frac{1}{4\pi\epsilon_0}\frac{e^2}{\epsilon l_0}$ of Morf and Halperin. [20] The ground state energy per particle of the state $\nu = 4/5$ was found to be $u(4/5) = -0.548\ \frac{1}{4\pi\epsilon_0}\frac{e^2}{\epsilon l_0}$.

Accurate energy values for the states $\nu = 2/3$ and $\nu = 4/5$ are obtained from those at $\nu = 1/3$ and $\nu = 1/5$.

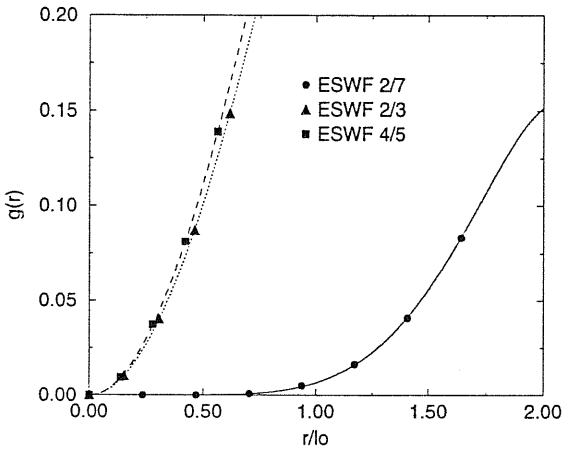

Figure 3.3: Small r behaviour for several FQHE states.

Using the MC simulation data of Levesque et al. [7] , via Eq.(3.39) of particle-hole symmetry, we compute $u(2/3)$ and $u(4/5)$,

$$\nu u(\nu) = (1-\nu)u(1-\nu) + \sqrt{\frac{\pi}{8}}(1-2\nu)\,\frac{1}{4\pi\epsilon_0}\frac{e^2}{\epsilon l_0}\,, \tag{3.39}$$

yielding $u(2/3) = -0.518\ \frac{1}{4\pi\epsilon_0}\frac{e^2}{\epsilon l_0}$ and $u(4/5) = -0.5519\ \frac{1}{4\pi\epsilon_0}\frac{e^2}{\epsilon l_0}$, in reasonable agreement with our approximate values $-0.510\ \frac{1}{4\pi\epsilon_0}\frac{e^2}{\epsilon l_0}$ and $-0.548\ \frac{1}{4\pi\epsilon_0}\frac{e^2}{\epsilon l_0}$ for functions of the ESWF type.

Finally in Table 3.1 we make an overall comparison of the ground state energy per particle obtained using the ESWF, the results of M.W.C. Dharma-wardana [23] from a parametrization fit, and those of Morf and Halperin. [20]

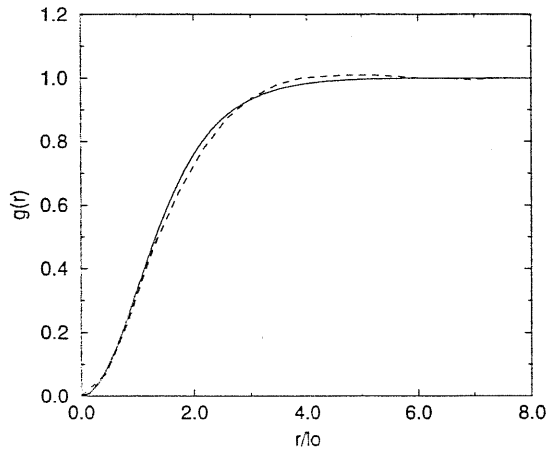

Figure 3.4: Pair distribution $g(r)$ obtained from the ESWF (solid), compared to that of Morf and Halperin, Ref. [20] (dashed), for the state $\nu = 2/3$.

3.4 Conclusion

The main approximation in this calculation is to neglect the elementary function $E(r)$. It is known that this mainly affects the magnitude of the peak of the pair distribution function. It has also been shown that the scaling approximation applied to the four-point elementary diagrams provides almost exact results [24] for the one-component HNC. The extension of the scaling procedure to the three-component case is not completely straightforward. It is expected that the elementary diagrams which need to be scaled will be the E_{pp} ones. The scaling coefficient may be obtained by requiring consistency on the available sum rules like, for instance, the kinetic energy sum rule.

The extension of ESWF to higher fractions in the hierarchical scheme requires larger multi-component systems. The study of ground state wave functions of the composite fermion

ν	2/3	4/5	2/7
$u(\nu)$ (ESWF)	-0.510	-0.548	-0.374
$u(\nu)$ (Ref. [23])	-0.518	-0.552	-0.379
$u(\nu)$ (Ref. [20])	-0.509(5)	not available	-0.377(3)

Table 3.1: Ground-state energies per particle $u(\nu)$ in units of $\frac{1}{4\pi\epsilon_0}\frac{e^2}{\epsilon l_0}$ for filling factors $\nu = 2/3, 4/5, 2/7$. The first row displays our ESWF results. The results of Dharma-wardana Ref. [23] are reported in the second row; $u(2/3)$ and $u(4/5)$ are obtained by applying particle-hole conjugation to the corresponding estimates of Ref. [23].

type [25] asks for the use of Fermi Hypper–Netted–Chain (FHNC) rather than HNC techniques. [26]

4 The Fermi Hyper-Netted–Chain theory for Laughlin quantum Hall states

4.1 Introduction to the FHNC

Integral equation techniques such as the Hyper-Netted–Chain (HNC) theory for bosons [5, 27] or the Fermi Hyper-Netted–Chain (FHNC) formalism for fermions [26, 28] permit an accurate evaluation of the radial distribution function and related quantities associated with a Jastrow and Jastrow-Slater wave function. In particular, they are extremely useful for calculations that are performed in the thermodynamic limit. They have been extensively and successfully applied in studies of quantum fluids such as liquid ^{4}He, ^{3}He, and nuclear matter. Recently, these methods have been also applied to problems in the newly developing areas of condensed matter theory such as the physics related to the FQHE. For a completely spin-polarized system of electrons the dominant sequence of fractional Hall states occurs for filling factors of the LLL, $\nu = p/(2p+1)$, where $p \neq 0$ is an integer.

Laughlin's interpretation [4] of the fractions $\nu = 1/m$ of the FQHE, where $m = 1, 3, 5 \ldots$, is well established and experimentally confirmed with high accuracy. He proposed a trial many-electron wave function of Jastrow type

$$\psi_m = \prod_{j<k}^{N} (z_j - z_k)^m \prod_{j=1}^{N} \exp\left(-\frac{|z_j|^2}{4l_0^2}\right) . \tag{4.1}$$

Here, z_j is a complex coordinate, $z_j = x_j + iy_j$, and $l_0 = \sqrt{\frac{\hbar}{eB}}$ is the magnetic length. This wave function describes a translationally invariant isotropic and incompressible liquid at a density $\rho = \nu/2\pi l_0^2$, corresponding to the lowest Landau level with filling factor $\nu = 1/m$. Laughlin studied the properties of the trial wave function (4.1), by using a modified version of the HNC theory, which is a well established technique for dealing with Bose quantum fluids.

Further applications of the HNC scheme to the FQHE have been performed by Chakraborty to study the elementary excitations [29] and Pietilainen and Chakraborty for the collective ones [30].

More recently, Jain [25] proposed a simple picture for understanding the origin of the FQHE by introducing the idea of a new kind of particle, called a *composite fermion* (CF), that consists of an electron carrying an even number of vortices. In this interpretation he describes the electronic ground state for fillings $\nu = p/(q_e p + 1)$ in terms of trial composite fermion wave functions of the form

$$\Psi_{CF} = \hat{P}_{LLL} \prod_{j<k} (z_j - z_k)^{q_e} \, |\Phi_p> \ . \tag{4.2}$$

Here, $\hat{P}_{LLL}$ is the projection operator onto the lowest Landau-level, $|\Phi_p>$ is an antisymmetric ground state of noninteracting electrons, $q_e = 0, 2, 4 \ldots$ is an even number of vortices attached to each electron, and $p = 1, 2, 3, \ldots$ is a positive integer.

The calculation , at various FQHE fillings, of relevant groundstate quantities, like the radial distribution function, $g(r)$, the static structure factor, $S(q)$ and the interaction energy per particle $u(\nu)$ for the CF wavefunction, requires the use of the Fermi version of the HNC theory, namely the FHNC method. Therefore it is important to study the FHNC theory in

connection with the FQHE.

As far as the Ψ_{CF} wavefunction is concerned, the presence of the LLL projection operator $\hat{P}_{LLL}$, limits the testing cases to those fillings where the CF wavefunctions are identical to the Laughlin ones, i.e $\nu = 1/(q_e + 1)$. For such cases there is no mixing with higher Landau levels and:

$$\frac{1}{N} < \hat{K} >= \frac{1}{N} \frac{< \Psi_{CF}|\hat{K}|\Psi_{CF} >}{< \Psi_{CF}|\Psi_{CF} >} \approx \frac{1}{2}\hbar\omega_c \ . \tag{4.3}$$

In addition, FHNC scheme is a powerful tool to compute $\frac{1}{N} < \hat{K} >$ for the unprojected CF trial wavefunctions, providing a tool to estimate their spuriosity. We also check the validity of an approximation to the FHNC theory, known as Effective HNC (EFHNC) or Lado approximation, which simplifies enormously the problem of inclusion of elementary diagrams in the integral equation schemes.

Rewriting Eq.(4.1) as a product of a Bose Jastrow part with a Fermi Slater–determinant of single–particle states in the LLL, we readdress the problem by performing a Fermi analysis, applying the FHNC and EFHNC approaches to it.

4.2 FHNC theory for the Laughlin states

Let us consider a many–body wave function of the form

$$|\Psi >= \prod_{i<j}^{N} f(r_{ij}) \ |\Phi > \ . \tag{4.4}$$

The ket $|\Phi >$ represents a determinant of single–particle states $\varphi_\alpha(\vec{r})$ and $f(r_{ij}) = f(|\vec{r}_i - \vec{r}_j|)$ is the dynamic correlation factor. The fermions may have internal spin degrees of freedom, a single state may be therefore occupied by g_s particles, where g_s denotes the spin degeneracy of each state.

Because of the "healing" property of the factor $f^2(r_{ij}) - 1 = h(r_{ij}) \to 0$ as $r_{ij} \to \infty$ the spatial correlations present in the wave function may be ordered in powers of the function

$h(r_{ij})$,

$$|\Psi|^2 = [1 + \sum_{i<j}^{N} h(r_{ij}) + \sum_{i<j}^{N} \sum_{k<l}^{N} h(r_{ij})h(r_{kl}) + \ldots] \, |\Phi|^2 \, . \tag{4.5}$$

The (reduced) single–particle density matrix for the dynamically uncorrelated state is given by

$$\hat{\rho}(\vec{r}_1, \vec{r}_2) = g_s \sum_{\alpha} \varphi_{\alpha}^*(\vec{r}_1)\varphi_{\alpha}(\vec{r}_2) \, , \tag{4.6}$$

where g_s is the spin degeneracy of the quantum state α.

As it should be, we have $\hat{\rho}(\vec{r}, \vec{r}) = \rho$, where ρ is the particle density of the Fermi system. The central ingredient of the FHNC formalism is the statistical exchange factor

$$l(\vec{r}_1, \vec{r}_2) = \frac{\hat{\rho}(\vec{r}_1, \vec{r}_2)}{\rho} \, . \tag{4.7}$$

Expression (4.1) describes a completely spin–polarized system, i.e., $g_s = 1$. Within the permutation expansion method of Fantoni and Rosati [26], $|\Phi|^2$ may be expanded in the number of permutations of particles or the number of exchange factors. After insertion into the expansion (4.5) the product may be ordered according to the number of particles involved. The resulting cluster terms contain both kinds of correlations and may be represented by cluster diagrams. As in the Bose case, the associated radial distribution function $g(r)$ is then given by the sum of all irreducible diagrams obeying well-defined topological rules [26].

One defines *nodal*, *non-nodal* (composite), and *elementary* diagrams as in the Bose case, but there are now four different types for each of them. The four different classes of nodal and elementary diagrams are generally denoted by *dd* (direct-direct), *de* (direct-exchange), *ee* (exchange-exchange), and *cc* (circular-exchange).

The resulting radial distribution function $g(r)$ is computed from the set of self-consistent FHNC equations given in Appendix A.

For a 2D electronic system in a transverse magnetic field $\vec{B} = (0, 0, B)$ described in the symmetric gauge by a vector potential $\vec{A} = \frac{1}{2}\vec{B} \times \vec{r}$, the single–particle states $|0, \alpha >$ of the lowest Landau level are represented by the wave functions

$$\varphi_\alpha(z) = c_\alpha z^\alpha \exp(-|z|^2/4l_0^2) \,, \tag{4.8}$$

where $c_\alpha = \frac{1}{\sqrt{2\pi l_0^2 2^\alpha \alpha!}} \frac{1}{l_0^\alpha}$ and $\alpha = 0, 1, 2 \ldots$

To apply the FHNC formalism we must — in a first step — separate the ground state wave function into an appropriate determinant of an orthonormal set of single–particle wave functions, describing only statistical correlations present in a system of noninteracting fermions and a factor representing the dynamical correlations generated by the interactions among the particles. To illustrate the idea let us consider the simplest case $\nu = 1$,

$$\psi_{\nu=1} = \prod_{j<k}^{N} (z_j - z_k) \prod_{j=1}^{N} \exp\left(-\frac{|z_j|^2}{4l_0^2}\right) . \tag{4.9}$$

This wave function can be cast into the form of a Vandermonde determinant of single–particle states. The associated one–body density matrix is

$$\hat{\rho}_{\nu=1}(z_1, z_2) = g_s \sum_{\alpha=0}^{N-1} \varphi_\alpha^*(z_1)\varphi_\alpha(z_2) = \rho_1 \ \exp\left[-\frac{\pi}{2}\rho_1(|z_1|^2 + |z_2|^2)\right] \exp\left(\pi\rho_1 z_1^* z_2\right) . \tag{4.10}$$

We observe the property $\hat{\rho}_{\nu=1}(z, z) = \rho_1$, where $\rho_1 = 1/(2\pi l_0^2)$ is the correct density that corresponds to $\nu = 1$. The spatial distribution function, in this case, has the explicit form

$$g_{\nu=1}(z_1, z_2) = 1 - \exp\left(-\pi\rho_1|z_1 - z_2|^2\right) . \tag{4.11}$$

For states $\nu = 1/m$, with $m = 3, 5$ we must, however, employ the FHNC technique [31], due to the presence of dynamical correlations.

For these filling factors the corresponding Laughlin wave function may be factorized into a Vandermonde determinant and a dynamically correlated function of Jastrow type. However,

to ensure that the associated density matrix $\hat{\rho}_\nu(z_1, z_2)$ has the correct behavior one has to modify the fermionic part as a determinant of single–particle wave functions of form

$$\varphi'_\alpha(z) = c'_\alpha \; z^\alpha \; \exp(-\frac{\pi}{2}\rho_m|z|^2) \; , \tag{4.12}$$

where $c'_\alpha = c_\alpha \; \frac{1}{\sqrt{m^{\alpha+1}}}$.

In this case we have

$$\hat{\rho}_\nu(z_1, z_2) = \rho_m \exp\left[-\frac{\pi}{2}\rho_m(|z_1|^2 + |z_2|^2)\right] \; \exp\left(\pi\rho_m z_1^* z_2\right) \; . \tag{4.13}$$

We may easily verify that $\hat{\rho}_\nu(z, z) = \rho_m$ with $\rho_m = \nu\rho_1$ and $\nu = 1/m$.

After some elementary algebra we may finally write

$$l_\nu(z_1, z_2) = \exp\left(-\frac{\pi}{2}\rho_m|z_1 - z_2|^2\right) \; \exp\left[-i\phi(z_1, z_2)\right] \; . \tag{4.14}$$

The phase factor $\phi(z_1, z_2)$ in Eq.(4.14) is

$$\phi(z_1, z_2) = \pi\rho_m r_1 r_2 \sin(\theta_1 - \theta_2) \; . \tag{4.15}$$

Due to the peculiar form of the statistical exchange factor (4.14) the FHNC scheme becomes rather involved, mainly for the two following reasons. (i) The appearance of a complex input function (4.14) in the FHNC equations makes the numerical treatment more susceptible, (ii) the phase $\phi(z_1, z_2)$ is not invariant under translations, i.e., depends on the coordinates z_1 and z_2 separatly, rather than only on the difference $|z_1 - z_2|$. As a consequence, the convolutions appearing in the set of chain equations cannot be simplified by transforming the integral into product form in the associated Fourier space as usually done in studies of quantum fluids such as liquid helium.

The HNC or FHNC relations of Appendix A provide a close set of equations for the nodal and non–nodal components only, if the elementary contributions (described by elementary diagrams) are known.

Several different approximation schemes are available for an appropriate evaluation of the elementary portions. However, at present we neglect such diagrams adopting the so-called FHNC/0 approximation. In this approximation we set $E_{\alpha,\beta} = 0$, where the indices are (α,β)= (dd), (de), (ee) and (cc). The FHNC/0 equations may be solved by an iterative procedure. We start by setting all $N_{\alpha,\beta} = 0$. The generated cyclic function $X_{cc}(i,j)$ is complex and has the same phase factor as the statistical exchange functions $l(i,j)$. In a second iterative cycle the output function $X_{\alpha,\beta}(i,j)$ is inserted on the r.h.s of equations (A6–A10) etc., until convergence is achieved.

After performing some algebra we find that also quantity $N_{cc}(i,j)$ has exactly the same phase factor, at each step of the iterative procedure.

Writing $l_\nu(z_i,z_j) = l_{ef}(z_i,z_j)\ \exp\left[-i\phi(z_i,z_j)\right]$, with

$$l_{ef}(z_i,z_j) = \exp(-\frac{\pi}{2}\rho_m|z_i - z_j|^2)\ , \tag{4.16}$$

we have

$$N_{cc}(1,2) = e^{i\phi(1,2)}\ \rho \int d\vec{r}_3 F_1(r_{13})F_2(r_{32})e^{i\pi\rho(\vec{r}_{13}\times\vec{r}_{32})}\ , \tag{4.17}$$

$$F_1(r) = -l_{ef}(r) + X_{cc}(r) + N_{cc}(r)\ , \tag{4.18}$$

and

$$F_2(r) = X_{cc}(r)\ . \tag{4.19}$$

Next, we separate the pseudopotential associated with the Laughlin state, $U(r_{12}) = 2(m-1)\ln(|z_1 - z_2|)$, into a short– and a long–ranged part, respectively,

$$U_s(r_{12}) = -2(m-1)K_0(Qr_{12})\ , \tag{4.20}$$

$$U_l(r_{12}) = 2(m-1)K_0(Qr_{12}) + 2(m-1)\ln(r_{12})\ . \tag{4.21}$$

Function $K_0(x)$ is the standard modified Bessel function and the wave number Q is a cut-off parameter of order $1/l_0$. Furthermore, all nodal and non-nodal functions are separated into their respective short– and long–range parts and the FHNC/0 scheme may be subsequently applied without difficulties.

4.3 The Effective Hyper-Netted-Chain Approximation

The square modulus of the many body wave function of Eq.(4.4), is expanded as in Eq.(4.5). Within the EFHNC method, one views the square of the wave function as some positive–valued function and writes it in the form

$$|\Phi|^2 = \exp\left[\sum_{i<j}^{N} w_2(r_{ij}) + \sum_{i<j<k}^{N} w_3(\vec{r}_i, \vec{r}_j, \vec{r}_k) + \ldots\right] . \tag{4.22}$$

i.e., one emphasizes that the Pauli principle introduces many-body correlations between particles in analogy to the pseudopotential describing the dynamic correlations. Retaining only two–body correlations [32], we have, approximately,

$$|\Phi|^2 \approx \exp\left[\sum_{i<j}^{N} w(r_{ij})\right] . \tag{4.23}$$

In a next step of a systematic approximation scheme, one may include triplet correlation factors, etc., until the required accuracy is achieved.

This approximation greatly simplifies the analysis of the problem [33]. Ignoring the kinetic energy (in the FQHE case it is quenched) the Fermi problem is effectively reduced to a Bose problem since the square of the Fermi wave function is of the form of a Bose wave function,

$$|\Psi|^2 = \prod_{i<j}^{N} f(r_{ij})^2 \prod_{i<j}^{N} \exp\left[w(r_{ij})\right] = \prod_{i<j}^{N} \tilde{f}(r_{ij})^2 , \tag{4.24}$$

with the effective correlation factor

$$\tilde{f}(r_{ij}) = f(r_{ij}) \ \exp[\frac{1}{2}w(r_{ij})] \ . \tag{4.25}$$

Thus, we may simply adopt the Bose HNC formalism for evaluating the radial distribution function $g(r_{ij})$.

To construct the potential $w(r)$ for a given determinant we require that the HNC evaluation of $g(r)$ recovers the *exact* radial distribution function of the noninteracting system, i.e., it should hold

$$g_{HNC}(r_{ij}) = g_{exact}(r_{ij}) = 1 - \frac{1}{g_s} \ |l_{exact}(r_{ij})|^2 \ . \tag{4.26}$$

The static structure function associated with the spatial distribution function $g(r)$ is defined by

$$S(k) = 1 + \rho[g(r) - 1]^F \ , \tag{4.27}$$

where $[f(r)]^F$ denotes the two–dimensional Fourier transform of a function $f(r)$. The inverse transform is

$$g(r) = 1 + \frac{1}{\rho}[S(k) - 1]^{F^{-1}} \ . \tag{4.28}$$

Consequently, the prescription leads us to the pseudopotential

$$w(r) = \ln[g_{exact}(r)] - \frac{1}{\rho}[\frac{(S_{exact}(k) - 1)^2}{S_{exact}(k)}]^{F^{-1}} \ , \tag{4.29}$$

where the spatial distribution function $g_{exact}(r)$ and the associated structure function $S_{exact}(k)$ correspond to the dynamically uncorrelated determinant.

Employing Eq.(4.14) we have

$$|l_\nu(z_1, z_2)|^2 = \exp\left(-\pi\rho_m|z_1 - z_2|^2\right) \ , \tag{4.30}$$

and, consequently,

$$g_{exact}(r) = 1 - \exp\left(-\frac{r^2}{2l_0^2 m}\right) = 1 - \exp\left(-\pi\rho_m r^2\right) \ , \tag{4.31}$$

$$S_{exact}(k) = 1 - \exp(-\frac{k^2 l_0^2 m}{2}) = 1 - \exp(-\frac{k^2}{4\pi\rho_m}) \ . \tag{4.32}$$

With these expressions as input Eq.(4.29) provides an explicit expression for the potential $w(r)$ and, consequently, due to Eq.(4.24) and (4.25), we arrive at:

$$|\Psi|^2 = \prod_{i<j}^{N} \exp\left[\tilde{u}(r)\right] \ , \tag{4.33}$$

where $\tilde{u}(r) = 2(m-1)\ln(r) + w(r)$. We may now employ the familiar boson HNC/0 formalism.

Decomposing the function $w(r)$ into a short– and a long–range portion,

$$w(r_{12}) = w_s(r_{12}) + w_l(r_{12}) \ , \tag{4.34}$$

we may write

$$w_s(r_{12}) = \ln\left[g_{exact}(r_{12})\right] \tag{4.35}$$

and

$$w_l(r_{12}) = -\frac{1}{\rho} \left\{ \frac{[S_{exact}(k)-1]^2}{S_{exact}(k)} \right\}^{F^{-1}} \ . \tag{4.36}$$

This decomposition achieves an analogous convenient separation $\tilde{u}(r)$ of the pseudo-potential,

$$\tilde{u}_s(r_{12}) = -2(m-1)K_0(Qr_{12}) + w_s(r_{12}) \ , \tag{4.37}$$

$$\tilde{u}_l(r_{12}) = 2(m-1)K_0(Qr_{12}) + 2(m-1)\ln(r_{12}) + w_l(r_{12}) \ . \tag{4.38}$$

Consequently, the k-space representation of the long-ranged part of the pseudo-potential $\tilde{u}_l(k)$, may be analytically performed and poses no computational problems for applying the standard HNC/0 theory.

m	FHNC/0	HNC/0	EFHNC/0	MC
3	-0.4026	-0.4056	-0.4060	-0.4100
5	-0.3228	-0.3244	-0.3243	-0.3277

Table 4.1: Interaction energies per particle in units of $\frac{1}{4\pi\epsilon_0}\frac{e^2}{\epsilon l_0}$ for the Laughlin states $\nu = 1/3$ and $\nu = 1/5$.

4.4 Results

We have performed numerical calculations on the ground state energy, the spatial distribution function and the static structure function corresponding to correlated states of Laughlin type describing the fractional quantum Hall effect, in FHNC/0 and EFHNC/0 approximation. In the case $\nu = 1$, the FHNC/0 approximation reproduces the exact result. For other Laughlin states $\nu = 1/m$ the FHNC/0 and EFHNC/0 results provide very accurate approximations for the ground state interaction energy per particle. For both Fermi and Bose case, the interaction energy per particle is given by the relation:

$$u(\nu) = \frac{1}{N}\frac{<\Psi_m|\hat{V}|\Psi_m>}{<\Psi_m|\Psi_m>} = \frac{\rho_m}{2}\int v(r)[g(r)-1]d^2r \ , \tag{4.39}$$

where $v(r) = \frac{1}{4\pi\epsilon_0}\frac{e^2}{\epsilon r}$.

For comparison, the FHNC/0 and EFHNC/0 results, the familiar HNC/0 results, and the Monte Carlo (MC) results, reported by Levesque et al. [7], which correspond to the Laughlin states $\nu = 1/3$ and $1/5$ are listed in Table 4.1.

The HNC/0 and the FHNC/0 data are rather close to each other, the HNC/0 result on the energy being slightly lower than the energy in FHNC/0 approximation. The differences between the HNC/0 and the EFHNC/0 data are almost negligible. We may understand this finding, by observing the relationship between the function $\tilde{u}_l(k)$ in EFHNC/0 approximation and the function $u_l(k)$ appearing in the HNC/0 scheme. It is easily checked that

both quantities have exactly the same long–wavelength limit,

$$\lim_{k\to 0} \tilde{u}_l(k) = \lim_{k\to 0} u_l(k) = -\frac{\gamma}{k^2} \ , \tag{4.40}$$

where $\gamma = 4\pi m$. Their respective short-range parts $\tilde{u}_s(r)$and $u_s(r)$ are compared in Fig. 4.1.

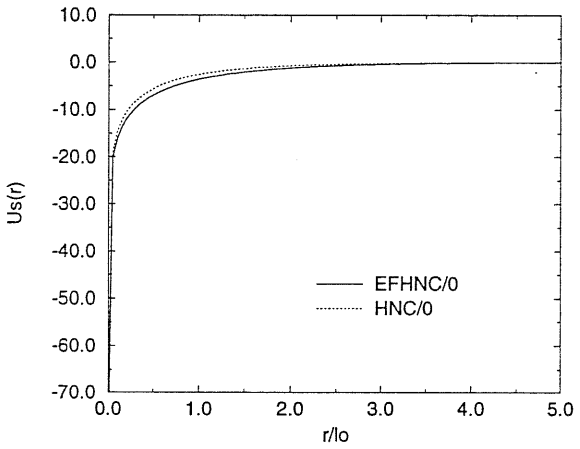

Figure 4.1: Comparison of the numerical results on the short-ranged parts of the pseudopotential $\tilde{u}_s(r)$, in the EFHNC/0 approximation (solid), and the pseudopotential $u_s(r)$, in HNC/0 approximation, for the filling factor $\nu = 1/3$.

We see that they are very close to each other, indicating that the EFHNC/0 scheme provides a good approximation.

In Fig.4.2 we plot the numerical results on the radial distribution function $g(r)$ obtained for $\nu = 1/3, 1/5$ within the FHNC/0 and EFHNC/0 approximation scheme.

The data are compared with the respective HNC/0 results and those of Girvin et al. [11] fitting the MC data.

The value of the ground state energy per particle is only marginally affected by inclusion

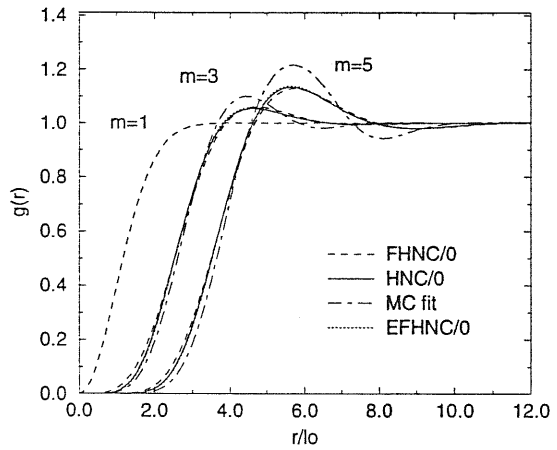

Figure 4.2: Numerical results on the radial distribution function $g(r)$ for the Laughlin state $\nu = 1, 1/3, 1/5$. We show the analytic results (dashed-dotted) and the results from FHNC/0 (dashed), HNC/0 (solid), and EFHNC/0 (dotted) approximation.

of the elementary contributions. The influence of the elementary pieces on the detailed shape of the radial distribution function is somewhat larger. Within the FHNC there are four different classes of elementary diagrams, whereas there is only one class in the HNC and EFHNC case. The scaling approximation [24] in the HNC case has been proven to be sufficiently adequate to account for the effect of the elementary diagrams. We have verified that a similar feature holds in the EFHNC case. A systematic numerical calculation within the EFHNC/S reproduces the MC results [7].

The structure factors $S(q)$ for the same Laughlin states are plotted in Fig.4.3 as functions of the variable ql_0, in FHNC/0 and EFHNC/0 approximation. They are also compared with the respective HNC/0 results.

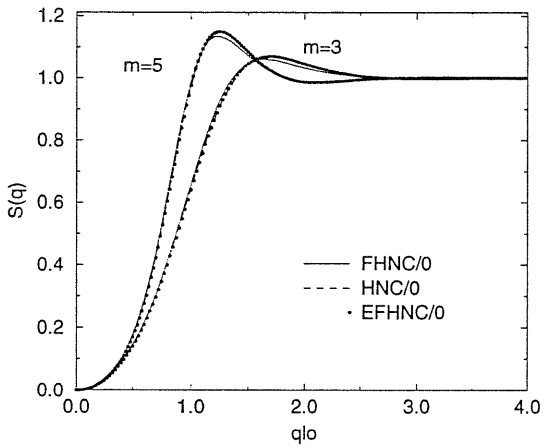

Figure 4.3: The static structure factor $S(q)$ obtained from FHNC/0 (solid), HNC/0 (dashed) and EFHNC/0 (dots) approximation, for the Laughlin states $\nu = 1/3$ and $\nu = 1/5$.

Thus the FHNC and EFHNC formalism permits to treat strongly correlated Fermi systems in the thermodynamic limit at a high level of precision, providing valuable tools to study the properties of the more general class of wave functions of the composite fermion type [25].

4.5 Conclusions

The above analysis of Laughlin quantum Hall states should be considered as a first successful accuracy test towards a general treatment of correlations arising from more complicated Fermi wavefunctions such those of CF type. The results obtained from the FHNC and EFHNC analysis are similar to the results derived by the bosonic HNC treatment and are very close to the best Monte Carlo estimates. The mixing of higher Landau levels into the unprojected CF wavefunction , a problem never studied in the thermodynamic limit, and

only in a few cases [34] studied by MC techniques, can also be addressed in this spirit. The EFHNC method opens the way to an alternative possibility for incorporation of the presently neglected elementary diagrams, thus permiting us to go beyond the FHNC/0 approximation, improving systematically the results for any FQHE filling.

5 The Composite Fermion Quantum Hall States

5.1 Introduction on the Composite Fermion Theory

For fully spin-polarized (spinless) electrons, the most pronounced FQHE states occur when filling of the lowest Landau level (LLL) is: $\nu = 1/m$, where $m = 1, 3, 5 \ldots$ and they are very well described by the Laughlin wavefunction.

The origin of the electronic states at so-called higher-order FQHE states at $\nu = p/q$ has been less clear. Jain [25, 35] has proposed a remarkably simple picture to understand the origin of the FQHE, by introducing the idea of a new kind of particle called composite fermion (CF), which is an electron carrying an even number of vortices of the wave function. The fundamental property of the CF-s is that they experience an effective field $B^* = B - q_e\phi_0\rho$, where $\phi_0 = h/e$ is the quantum of the magnetic flux and q_e is an even integer.

Thus the liquid of strongly correlated electrons at B is equivalent to a liquid of weakly interacting CF-s at B^*, or otherwise the FQHE is regarded as the integer quantum Hall effect (IQHE) of novel composite fermions.

The stable fractional filling factors obtained in this way are: $\nu = p/(q_e p \pm 1)$, where $q_e = 0, 2, 4 \ldots$ is the even number of vortices attached to each electron and $p = 1, 2, 3 \ldots$ is the corresponding number of CF Landau levels.

For sake of simplicity we confine the discussion below to the special filling factors $\nu = p/(q_e p + 1)$, where the corresponding CF filling factor is $\nu^* = p$.

Let us denote the ground state of noninteracting electrons at $\nu^* = p$, by $|\Phi_p>$. The corresponding wave function for the CF-s is obtained by attaching q_e vortices to each electron in the state $|\Phi_p>$, which amounts to correlate $|\Phi_p>$ by a a multiplication with a Jastrow factor $\prod_{j<k}(z_j - z_k)^{q_e}$. Thus the electronic ground state at $\nu = p/(q_e p + 1)$ is described by the trial CF wave function:

$$|\Psi_{CF}>= \hat{P}_{LLL} \prod_{j<k} (z_j - z_k)^{q_e} \, |\Phi_p> \, , \tag{5.1}$$

firstly introduced by Jain [25], where $\hat{P}_{LLL}$ is the lowest–Landau–level projection operator. For the special case of the ground state at $\nu = 1/(q_e + 1)$, namely for $p = 1$ the CF wave function is identical to the Laughlin wave function [4], which has already been known to be a very accurate representation of the exact ground state at $\nu = 1, 1/3, 1/5$. There is also a strong evidence for the validity of the CF theory from several numerical studies performed mainly on few electron systems [36, 37].

Exact calculations, in particular, are limited to systems with few electrons and extrapolation to the thermodynamic limit is not totally unambiguous. The difficulty gets more and more severe as $\nu \to 1/2$. The Fermi–Hyper–Netted–Chain technique (FHNC) seems very attractive in this respect, as it treats the many particle fermionic system exactly in the thermodynamic limit.

In this section we apply for the first time the Fermi-Hyper-Netted-Chain (FHNC) theory and the Effective-Hyper-Netted-Chain (EFHNC) method to the unprojected CF wavefunctions of the FQHE corresponding to filling factors $\nu = p/(q_e p + 1)$, where $q_e = 0, 2, 4$ and $p = 1, 2, 3, \ldots$.

This represents a first step towards a more systematic study in which the projection onto

the LLL will be taken into account. We find that FHNC theory provides a simple and powerful tool to deal with unprojected CF wavefunctions, both for groundstate properties and excited ones. The results obtained so far are consistent with previous calculations performed on systems with a finite number of electrons.

5.2 Application of the Fermi-Hyper-Netted-Chain theory for the composite fermion states

We have seen that integral equation techniques, such as Hyper–Netted–Chain (HNC) theory for bosons [5, 27] or Fermi–Hyper–Netted–Chain (FHNC) for fermions [26], allow for a realistic evaluation of the radial distribution function and related quantities for Jastrow and Jastrow-Slater wavefunctions. In particular, they are extremely useful when calculations must be performed strictly in the thermodynamic limit.

FHNC theory can always be applied on Fermi systems described by a many body wave function of the form:

$$|\Psi >= \prod_{i<j}^{N} f(r_{ij}) \; |\Phi > \quad . \tag{5.2}$$

The ket $|\Phi >$ is a Slater determinant of single particle states $\varphi_\alpha(\vec{r})$ for fermions and $f(r_{ij}) = f(|\vec{r}_i - \vec{r}_j|)$ is the so called dynamical correlation factor. More elaborated trial wavefunctions, containing, for instance, triplet and/or backflow correlations, can also be handled.

The radial distribution function $g(r_{12})$ is expressed as a sum of irreducible cluster diagrams constructed with (i) the "bosonic" bond $h(r_{ij}) = f(r_{ij})^2 - 1$, and (ii) the "statistical exchange" bond $l(\vec{r}_i, \vec{r}_j) = \hat{\rho}(\vec{r}_i, \vec{r}_j)/\rho$, where ρ is the particle density, $\hat{\rho}(\vec{r}_i, \vec{r}_j)$ is the uncorrelated one-body density matrix:

$$\hat{\rho}(\vec{r}_i, \vec{r}_j) = g_s \sum_\alpha \varphi^*_\alpha(\vec{r}_i)\varphi_\alpha(\vec{r}_j) \; , \tag{5.3}$$

and $g_s = 1$ is the spin degeneracy for the case being.

In the above equation, the sum over α is extended over all occupied single particle states $\varphi_\alpha(\vec{r})$.

For a magnetic field $\vec{B}$ in the z direction, with a symmetric gauge vector potential $\vec{A} = \frac{1}{2}\vec{B} \times \vec{r}$, the eigenstates of the ideal Hamiltonian:

$$\hat{H}_0 = \frac{1}{2m_e}(-i\hbar\vec{\nabla} + e\vec{A})^2 \ , \tag{5.4}$$

for the various Landau levels $n = 0, 1, 2, \ldots$, are given by:

$$|n, m >= \varphi_{n,m}(z) = \frac{1}{\sqrt{2^n n!}} \exp(\frac{zz^*}{4l_0^2}) \ (2l_0\frac{\partial}{\partial z})^n \ [\varphi_{0,m}(z) \ \exp(-\frac{zz^*}{4l_0^2})] \ , \tag{5.5}$$

where

$$\varphi_{0,m}(z) = \frac{1}{\sqrt{2^m m!}} \ (\frac{z}{l_0})^m \ \varphi_{0,0}(z) \ , \tag{5.6}$$

$$\varphi_{0,0}(z) = \frac{1}{\sqrt{2\pi l_0^2}} \ \exp(-\frac{zz^*}{4l_0^2}) \ , \tag{5.7}$$

and $m = 0, 1, 2 \ldots$ is the angular momentum quantum number.

The manifold of states with energy $\hbar\omega_c(n + 1/2)$ constitutes the n-th Landau level.

The first step in order to apply the FHNC theory is the knowledge of an orthonormal set of single particle wavefunctions which fully describe the unperturbed Fermi system.

To illustrate the idea, let us firstly consider the simple case $\nu = 1$, obtained for $p = 1$ and $q_e = 0$.

The CF wavefunction $|\Psi_{CF}^{\nu=1} >$, is in this case the Vandermonde determinant of single particle states $\varphi_{0,m}(z)$ of Eq.(5.6).

The density matrix for the case $\nu = 1$ is:

$$\hat{\rho}_{\nu=1}(z_1,z_2)=\sum_{m=0}^{N_s-1}\varphi^*_{0,m}(z_1)\varphi_{0,m}(z_2)=\frac{1}{2\pi l_0^2}\ \exp(-\frac{1}{4}\frac{|z_1-z_2|^2}{l_0^2})\ \exp[-\frac{1}{4l_0^2}(z_1^*z_2-z_1z_2^*)]\ , \tag{5.8}$$

where N_s is the degeneracy of each Landau level.

We observe that $\hat{\rho}_{\nu=1}(z,z)=\rho_1$, where $\rho_1=1/2\pi l_0^2$ is the density which corresponds to $\nu=1$.

For the case $\nu=1$, q_e in Eq.(5.1) is equal to zero and the uncorrelated radial distribution function is simply:

$$g_{\nu=1}(z_1,z_2)=1-e^{-\pi\rho_1|z_1-z_2|^2}\ . \tag{5.9}$$

For CF states, at filling $\nu=1/(q_e+1)$ (the Laughlin states) one need the full machinary of FHNC. In this case only the LLL orbitals are occupied, therefore the statistical exchange term results to be:

$$l_\nu(z_1,z_2)=\exp(-\frac{1}{4}\frac{|z_1-z_2|^2}{l_0^2})\ \exp[i\phi(z_1,z_2)]\ , \tag{5.10}$$

with the phase factor $\phi(z_1,z_2)$ given by:

$$\phi(z_1,z_2)=\frac{1}{2l_0^2}r_1r_2\sin(\theta_2-\theta_1)=\frac{1}{2l_0^2}(\vec{r}_2\times\vec{r}_1)_z\ . \tag{5.11}$$

It is known that the FHNC technique is intrinsically approximated because there is a set of cluster diagrams (corresponding to the so called *elementary* diagrams) which cannot be fully included in any closed form. Several schemes have been devised to include such cluster diagrams at various levels of approximation. The simplest approximation of totally neglecting these terms (FHNC/0) already leads to reliable results and we adopted it in this paper.

The full formalism of FHNC/0 theory for the Laughlin states has been reported elsewhere [38]. Here we limit ourselves to generalize such a scheme to the unprojected CF states.

As in a standard computation, we separate the CF (pseudo)potential: $U(r_{12}) = 2q_e \ln(|z_1 - z_2|)$ in his short and long-ranged parts:

$$U_s(r_{12}) = -2q_e K_0(Qr_{12}) \ , \tag{5.12}$$

$$U_l(r_{12}) = 2q_e K_0(Qr_{12}) + 2q_e \ln(r_{12}) \ , \tag{5.13}$$

$K_0(x)$ is the modified Bessel function and Q is a cut-off parameter of order of $1/l_0$. Furthermore, all nodal and non-nodal functions are splitted into their short and long range parts so that FHNC/0 scheme can directly be applied.

Knowing that the general CF state of the form $\nu = p/(q_e p + 1)$ is described by the trial CF wave function of Eq. (5.1), the one-body density matrix is written as:

$$\hat{\rho}_\nu(z_1, z_2) = \sum_{n=0}^{p-1} \sum_{m=0}^{N_s-1} \varphi^*_{n,m}(z_1)\ \varphi_{n,m}(z_2) \tag{5.14}$$

One can easily prove that the contribution to $\hat{\rho}_\nu(z_1, z_2)$ coming from the n-th Landau level is:

$$\sum_{m=0}^{N_s-1} \varphi^*_{n,m}(z_1)\varphi_{n,m}(z_2) = L_n(\frac{|z_1 - z_2|^2}{2l_0^2}) \sum_{m=0}^{N_s-1} \varphi^*_{0,m}(z_1)\varphi_{0,m}(z_2) \ , \tag{5.15}$$

where $L_n(x)$ are the Laguerre polynomials of order n.

After some algebra, the statistical exchange term turns out to be:

$$l_\nu(z_1, z_2) = \{\sum_{n=0}^{p-1} L_n(\frac{|z_1 - z_2|^2}{2l_0^2})/p\} \exp(-\frac{|z_1 - z_2|^2}{4l_0^2}) \exp[\frac{i}{2l_0^2}(\vec{r}_2 \times \vec{r}_1)_z] \ . \tag{5.16}$$

The systematic knowledge of the statistical exchange term $l_\nu(z_1, z_2)$ for all the fractional states $\nu = p/(q_e p + 1)$, enables us to readily apply the FHNC theory to all the unprojected CF states.

The intrinsic LL mixing of the CF wavefunctions implies a projection onto the LLL. The Jastrow factor already provides a good projection [39], which is particularly effective as far as ground state properties are concerned. However, to study other quantities, such as the excitation spectrum, the full LLL projection seems to be needed.

Unfortunately, such projection leads to a wavefunction which cannot be directly treated within the FHNC formalism, because the structure of a determinant of single particle orbitals is lost.

One can adopt the projection technique used by Bonesteel [34] to calculate the excitation gaps of $\nu = 1/3, 1/5, 1/7$, which however is limited to Slater determinants spanning two Landau levels only. The extension of such technique to more LL-s appears to be numerically unaccessible.

A more general projection scheme, applied to few electron systems in a spherical geometry [37] , seems to be more promising. Such a scheme brings in a many-body dependency on all single particle orbitals, which however can be handled by introducing state-dependent correlations in the wavefunction, in close analogy to "backflow" correlations [40] of liquid ^{3}He.

5.3 The Effective Hyper–Netted-Chain Method

The Effective Hyper-Netted-Chain (EFHNC) method [38], also known as Lado approximation [32], described in Chapter 4, can be applied to the unprojected CF wave function too.

This prescription leads us to the (pseudo)potential,

$$w(r) = \ln[g_{exact}(r)] - \frac{1}{\rho}[\frac{(S_{exact}(k)-1)^2}{S_{exact}(k)}]^{F^{-1}} , \tag{5.17}$$

where $S_{exact}(k) = 1 + \rho[g_{exact}(r) - 1]^F$, $[f(r)]^F$ denotes the 2D Fourier transform of a function $f(r)$ and $[f(k)]^{F^{-1}}$ is the 2D inverse Fourier transform of $f(k)$.

For a Slater determinant with p filled Landau levels we get:

$$g_{exact}(r) = 1 - \exp(-\frac{r^2}{2l_0^2})\{\sum_{n=0}^{p-1} L_n(\frac{r^2}{2l_0^2})/p\}^2 . \tag{5.18}$$

With these expressions as input, Eq.(5.17) provides an explicit expression for the potential $w(r)$ and, consequently, we obtain:

$$|\Psi_{CF}|^2 = \prod_{i<j}^{N} \exp[\tilde{u}(r)] , \tag{5.19}$$

where $\tilde{u}(r) = 2q_e \ln(r) + w(r)$. We may now employ the familiar boson HNC formalism. Decomposing the function $w(r)$ into a short– and a long–range portion,

$$w(r_{12}) = w_s(r_{12}) + w_l(r_{12}) , \tag{5.20}$$

we may write

$$w_s(r_{12}) = \ln[g_{exact}(r_{12})] , \tag{5.21}$$

and

$$w_l(r_{12}) = -\frac{1}{\rho}\{\frac{[S_{exact}(k)-1]^2}{S_{exact}(k)}\}^{F^{-1}} . \tag{5.22}$$

This decomposition achieves an analogous convenient separation for the (pseudo)potential $\tilde{u}(r)$,

$$\tilde{u}_s(r_{12}) = -2q_e K_0(Qr_{12}) + w_s(r_{12}) , \tag{5.23}$$

$$\tilde{u}_l(r_{12}) = 2q_e K_0(Qr_{12}) + 2q_e \ln(r_{12}) + w_l(r_{12}) . \tag{5.24}$$

Finally, the k-space representation of the long-ranged part of the (pseudo)potential $\tilde{u}_l(k)$, may be analytically obtained and the standard HNC theory can be employed.

5.4 The quasi-particle–quasi-hole excitation spectrum of the CF state

In this section we report a method used to compute the quasiparticle-quasihole excitations for the unprojected CF wavefunction within the FHNC theory. The low energy neutral excitations are obtained by promoting a single CF to the next higher CF Landau level (LL). For instance, a low energy band of excited states above the $\nu = 1/(q_e + 1)$ ground state is constructed by promoting a CF from the lowest pseudo-Landau level, to the first excited pseudo-Landau level.

The excitation gaps can be calculated, by adopting a technique firstly introduced by Friedman and Pandharipande [41] in the context of nuclear matter.

Supose we have p Landau levels filled. The statistical exchange correlation associated with $|\Phi_p>$, is $l_{q_e}(p, r_{12})$ and the interaction energy per particle $u_{q_e}(p)$ is a functional of $f(r)$ and $l_{q_e}(p, r)$.

Promoting a CF from the p-th LL to the $(p+1)$-th one, will produce a correlated wavefunction $|\Psi_{ph}>$, which is orthogonal to $|\Psi_{CF}>$ because of angular momentum conservation. The quasiparticle-quasihole excitation brings a new statistical exchange term in the cluster diagrams of the radial distribution function, given by:

$$l^{ph}_{q_e}(p, z_1, z_2) = \frac{1}{\rho}\{\sum_{n=0}^{p-1}\sum_{m=0}^{N_s-1}\varphi^*_{n,m}(z_1)\varphi_{n,m}(z_2) + \frac{1}{N_s}\sum_{m=0}^{N_s-1}\varphi^*_{p,m}(z_1)\varphi_{p,m}(z_2) - \frac{1}{N_s}\sum_{m=0}^{N_s-1}\varphi^*_{p-1,m}(z_1)\varphi_{p-1,m}(z_2)\} \quad (5.25)$$

In calculating the energy per particle, $u^{ph}_{q_e}(p) = \frac{1}{N}\frac{<\Psi_{ph}|\hat{V}|\Psi_{ph}>}{<\Psi_{ph}|\Psi_{ph}>}$ corresponding to $|\Psi_{ph}>$, the quasiparticle-quasihole exchange term $l^{ph}_{q_e}(p, z_1, z_2)$ must occur only once in any FHNC cluster diagram, so that the excitation energy, $\Delta_{q_e}(p) = u^{ph}_{q_e}(p) - u_{q_e}(p)$ is of the order of $1/N_s$, as it should.

The calculation of $\Delta_{q_e}(p)$ can be done by introducing a "mixed" statistical exchange correlation

$$l_{q_e}(x, p, r_{12}) = l_{q_e}(p, r_{12}) + x[l_{q_e}(p+1, r_{12}) - l_{q_e}(p, r_{12})] \tag{5.26}$$

where the fraction x of CF-s removed from the p-th LL, and placed to the next higher $(p+1)$-th level, is considered as a smallness parameter.

The derivative with respect to x of the excitation energy $\Delta^{ph}_{q_e}(x, p)$, gives the quasiparticle-quasihole gap for a general CF state $\nu = p/(q_e p + 1)$, namely:

$$\Delta_{q_e}(p) = \frac{\partial}{\partial x}\{u^{ph}_{q_e}[l_{q_e}(x, p, r), f(r)] - u^{ph}_{q_e}[l_{q_e}(p, r), f(r)]\} \tag{5.27}$$

The calculation of $u^{ph}_{q_e}[l_{q_e}(x, p, r), f(r)]$ is done in the same way as the calculation for $u^{ph}_{q_e}[l_{q_e}(p, r), f(r)]$, namely employing the same FHNC code.

5.5 Results and Conclusions

In this section we report the results obtained for the groundstate interaction energy per particle, radial distribution function and quasiparticle-quasihole excitation spectrum for several unprojected CF wavefunctions.

The radial distribution function $g(r)$ has been calculated by using the FHNC/0 and EFHNC/0 approximation as described in the previous sections. Table 5.1 and Table 5.2 present the ground state energies per particle of the two series of FQHE states, $\nu = 1/3, 2/5, 3/7 \ldots$

ν	FHNC/0	EFHNC/0	Ref. [42]
1/3	-0.40257	-0.4056	-0.409828(27)
2/5	-0.43054	-0.4309	-0.432804(62)
3/7	-0.44510	-0.4452	-0.442281(62)
4/9	-0.45300	-0.4531	-0.447442(115)
5/11	-0.45796	-0.4580	-0.450797(175)
6/13	-0.46137	-0.4614	–
7/15	-0.46386	-0.46389	–
8/17	-0.46576	-0.46578	–

Table 5.1: Interaction energies per particle $u(\nu)$ expressed in units $\frac{1}{4\pi\epsilon_0}\frac{e^2}{\epsilon l_0}$, computed by using unprojected CF wavefunctions, for fillings $\nu = p/(2p+1)$. The values in the second and third column refer to the FHNC/0 and EFHNC/0 approximations, in the fourth column we report the estimates of Jain and Kamilla Ref. [42] obtained using projected CF wavefunctions in the spherical geometry

and $\nu = 1/5, 2/9, 3/13$.

One can see that, the results obtained with the two schemes are almost identical. At $\nu = 1/2$ both FHNC/0 and EFHNC/0 give an interaction energy per particle of -0.479(9) $\frac{1}{4\pi\epsilon_0}\frac{e^2}{\epsilon l_0}$.

Our results are in good agreement with the most recent estimates by Jain and Kamilla [42] obtained with projected CF wavefunctions for rather large systems in the standard spherical geometry.

There are two approximations [43] in our calculations. One concerns the neglect of elementary diagrams, the other is the missing LLL projection of the CF wavefunction. The inclusion of elementary diagrams can be easily peformed within the EFHNC scheme. We

ν	FHNC/0	EFHNC/0	Ref. [42]
1/5	-0.32281	-0.3243	-0.327499(5)
2/9	-0.33743	-0.33748	-0.342782(35)
3/13	-0.34380	-0.34384	-0.348349(19)

Table 5.2: Same as in Table 5.1 for fillings $\nu = p/(4p+1)$.

ν	Δ_{unp}(FHNC)	Δ_{unp}	Δ_{proj}	Δ
1/3	0.04	0.048(2)	0.106(3)	0.1036(2)
1/5	0.01	0.014(2)	0.025(3)	0.0244(3)

Table 5.3: The energy gaps for $\nu = 1/3, 1/5$, computed using the FHNC theory for the unprojected CF wavefunction are given in the second column. The results of Bonesteel, Ref. [34] from a VMC calculation for 42 electrons for the unprojected and projected case are shown in the third and forth columns. The extrapolated exact diagonalization results of Fano et al. Ref. [44] are given in the fifth column. The excitation gap energies are all expressed in units of $\frac{1}{4\pi\epsilon_0}\frac{e^2}{\epsilon l_0}$.

have done that by using the scaling approximation [24], finding that the ground state interaction energies is lowered by $\sim 1\%$. As far as the LLL projection is concerned our results show that their absence has small influence on the groundstate properties of the system and slightly increases with ν approaching 1/2.

The radial distribution function $g(r)$ for all fractional Hall states $\nu = 1/3, 2/5, 3/7 \ldots$ and $\nu = 1/5, 2/9, 3/13$, obtained using unprojected CF wavefunctions is plotted in Fig. 5.1 and Fig. 5.2 respectively.

The excitation gaps for Laughlin states obtained using the FHNC theory, for the unprojected CF wavefunctions, are given in Table 5.3.

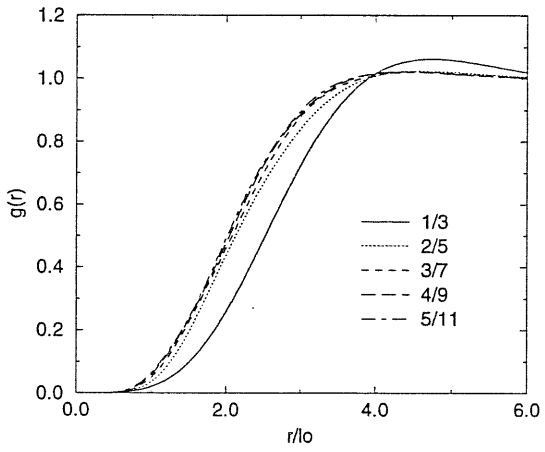

Figure 5.1: Radial distribution function $g(r)$, computed from the FHNC/0 theory for the series of FQHE fillings: $\nu = 1/3, 2/5, 3/7, 4/9, 5/11$, for the unprojected CF wavefunctions.

They are compared with the corresponding results of Bonesteel [34] from a VMC simulation for 42 electrons for the unprojected and projected case and the extrapolated exact diagonalization results of Fano et al [44].

As expected, the lack of projection of the CF excited state onto the LLL, leads to an underestimation of the excitation gap by a factor of about 2.

Within the Effective Hyper-Netted-Chain (EFHNC) method, one can calculate analytically the small r behaviour for different filling factors. As an explicit example we took the case of $\nu = 1/3$ and $\nu = 2/5$, which have the same Jastrow factor but different Slater determinant functions. One has that $g(r \rightarrow 0) \approx \exp[\tilde{u}_s(r \rightarrow 0)]$.

Using Eq.(5.23) and the formula $\lim_{r\rightarrow 0} K_0(Qr) = -\ln(\frac{Qr}{2}) - \gamma$, where $\gamma = 0.5772...$ is the socalled Euler constant, we get:

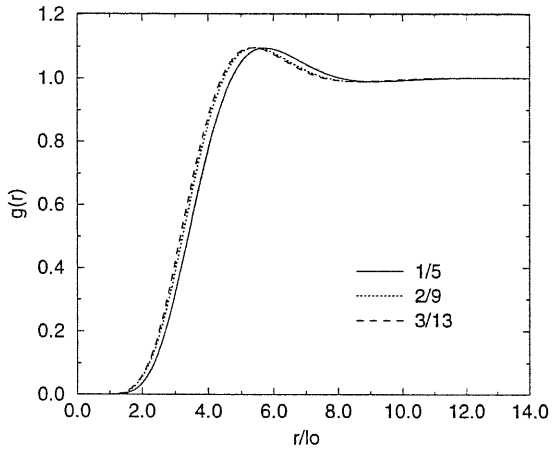

Figure 5.2: Radial distribution function $g(r)$, for the states $\nu = 1/5, 2/9, 3/13$, computed from the FHNC/0 theory for the unprojected CF wavefunctions.

$$g(r \to 0) \approx \exp[2q_e \ln(\frac{Qr}{2}) + 2q_e\gamma + w_s(r \to 0)] \; . \tag{5.28}$$

For filling $\nu = 1/3$, $w_s(r \to 0) \approx 2\ln(\frac{r}{l_0}) - \ln(2)$, implying

$$\ln[g(r \to 0)] \sim (2q_e + 2)\ln(\frac{r}{l_0}) \; . \tag{5.29}$$

Therefore the leading term in the small r behaviour of $g(r)$ is $(r/l_0)^6$ for $\nu = 1/3$.

The same calculation for filling $\nu = 2/5$, gives: $w_s(r \to 0) \approx 2\ln(\frac{r}{l_0})$. It turns out that also the state $\nu = 2/5$ has the same small r behaviour in $g(r)$ as the case $\nu = 1/3$. One can prove that $(r/l_0)^6$ is the leading term of $g(r)$ at small r also for the succesive fillings $\nu = 3/7, \ldots$.

The log-log plot of the small r behaviour of $g(r)$ obtained numerically from our EFHNC/0

calculations for the cases $\nu = 1/3$ and $\nu = 2/5$ is shown in Fig. 5.3.

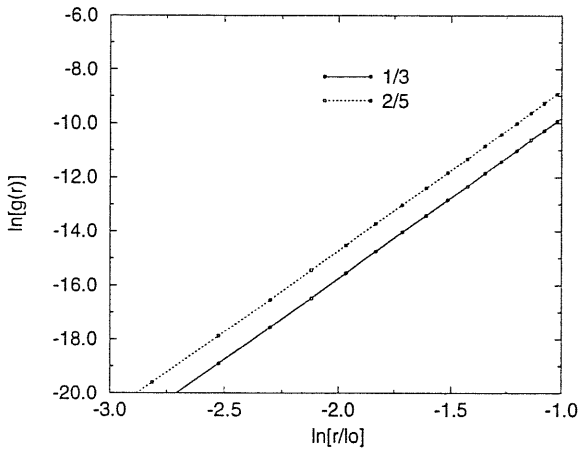

Figure 5.3: Small r behaviour for fillings $\nu = 1/3$ (circled) and $\nu = 2/5$ (squared). We show a plot of $\ln[g(r)]$ versus $\ln[r/l_0]$. One observes the same small r behaviour $g(r) \approx (r/l_0)^6$ for both cases. From the EFHNC/0 method such conclusion was found analytically too.

The explanation of this anomaly lies in the missing projection onto the LLL. The absence of such projection mainly affects the small r behaviour of the radial distribution function. Such a leading term is the one fixed by the Laughlin part of the wave function and is not modified by the inclusion of higher Landau levels through the Slater determinant part. Therefore we expect that the main effect of projection into the LLL is the correction of such tendency.

6 A Fermi unprojected wavefunction, for the half filled state of the FQHE

6.1 The peculiarity of the half-filled state

The fractional quantum Hall effect (FQHE) [3] results from a strongly correlated incompressible liquid state formed at special densities ρ_e of a two-dimensional (2D) electronic system, subject to a strong transverse magnetic field $\vec{B}$.

For a completely spin-polarized (spinless) system of electrons the dominant sequence of fractional Hall states occurs for filling factors of the lowest Landau level (LLL), $\nu = p/(2p+1)$, where $p \neq 0$ is an integer.

The first step in the FQHE explanation would be the study of the properties of a 2D fully spin-polarized (spinless) system of N interacting electrons emerged in a uniform positive background, with the magnetic field $\vec{B}$ high and temperature T low, such that only the lowest Landau level (LLL) would be partially filled.

At $T = 0$, the interaction energies $\sim \nu^{1/2} \frac{1}{4\pi\epsilon_0} \frac{e^2}{\epsilon l_0}$, where $l_0 = \sqrt{\frac{\hbar}{eB}}$ is the magnetic length and ϵ is the dielectric constant of the background, are weak compared with the Landau level splitting $\hbar\omega_c$, and so all electrons are considered to remain in the LLL.

Electrons with charge $-\epsilon$ ($e > 0$) are considered as usual to be confined in the $x - y$ plane. Working in the symmetric gauge: $\vec{A} = \left[-\frac{B}{2}y, \frac{B}{2}x, 0\right]$ the magnetic field $\vec{B} = \vec{\nabla} \times \vec{A}$ is perpendicular to the $x - y$ plane, $\vec{B} = [0, 0, B]$.

The many-electron system is described by the Hamiltonian:

$$\hat{H} = \hat{K} + \hat{V} \tag{6.1}$$

with

$$\hat{K} = \frac{1}{2m_e} \sum_{j=1}^{N} [-i\hbar\vec{\nabla}_j + e\vec{A}(r_j)]^2 \tag{6.2}$$

and

$$\hat{V} = \sum_{j<k}^{N} v(|\vec{r}_j - \vec{r}_k|) - \rho_e \sum_{j}^{N} \int d^2r \; v(|\vec{r}_j - \vec{r}|) + \frac{{\rho_e}^2}{2} \int d^2r_1 \int d^2r_2 \; v(|\vec{r}_1 - \vec{r}_2|) \tag{6.3}$$

where m_e - is the electron's mass, $z_j = x_j + iy_j$ - the location of the j-th electron in complex coordinates, $v(|\vec{r}_j - \vec{r}_k|) = \frac{1}{4\pi\epsilon_0} \frac{e^2}{\epsilon|z_j - z_k|}$ is the interaction potential and $\hat{V}$ contains the electron-electron, electron-background and background-background interaction potential.

From a theoretical point of view, the occurrence of Hall plateaus at filling factors of the form $\nu = 1/m$, $m = 1, 3, 5$ can be understood through the original ideas of Laughlin [4] which described these states by a trial many-electron wavefunction of the Jastrow type:

$$\psi_m = \prod_{j<k}^{N} (z_j - z_k)^m \prod_{j=1}^{N} \exp\left(-\frac{|z_j|^2}{4l_0^2}\right) . \tag{6.4}$$

By construction, this wavefunction lies entirely into the LLL and describes a translationally invariant isotropic and incompressible liquid of electrons at a density $\rho = \frac{\nu}{2\pi l_0^2}$, corresponding to the LLL filling factor $\nu = 1/m$, where $m = 1, 3, \ldots$

By contrast, the behaviour of such a system in the vicinity of a filling factor with even denominator, like $\nu = 1/2$, is not well understood.

A Laughlin-like Bose wavefunction,

$$\psi^{Bose}_{\nu=1/2} = \prod_{j<k}^{N}(z_j - z_k)^2 \prod_{j=1}^{N} \exp(-|z_j|^2/4l_0^2) \tag{6.5}$$

does not correctly describe such a situation, and a new theory is needed for such fillings.

6.2 The Chern-Simons transformation

At $\nu = 1/2$ the typical features of the FQHE, as quantized $\sigma_{xy} = \nu \frac{e^2}{h}$ and vanishing σ_{xx} are not observed, but nevertheless this state show a broad minimum [45] in ρ_{xx} and exhibits, additionally, anomalous behaviour in surface accoustic wave propagation [46], indicating a different type of correlation. Numerical work by Haldane [47], suggested that $\nu = 1/2$ is not incompressible.

Recently a theory of a compressible Fermi-liquid-like behaviour at $\nu = 1/2$, was proposed by Halperin, Lee and Read [48].

According to this theory a 2D electronic system subjected to an external perpendicular magnetic field $\vec{B}$, with LLL filling factor 1/2, can be transformed to a mathematically equivalent system of fermions interacting with a Chern-Simons gauge field such that the average effective magnetic field acting on the fermions is zero.

Let me mention some fundamental properties of this transformation, suposing that $|\Phi(z_1 \ldots z_N)>$ is a solution of the Schroedinger equation $\hat{H}\Phi = E\Phi$. Then for an even number $2m$, where now $m = 1, 2, 3, \ldots$, the wavefunction:

$$\Psi(z_1 \ldots z_N) = \prod_{i<j}^{N} \frac{(z_i - z_j)^{2m}}{|z_i - z_j|^{2m}} \, |\Phi(z_1 \ldots z_N)> \tag{6.6}$$

is a solution to the Schoedringer equation: $\hat{H}'\Psi = E\Psi$. with

$$\hat{H}' = \hat{K}' + \hat{V} \tag{6.7}$$

and

$$\hat{K}' = \frac{1}{2m_e}\sum_{j=1}^{N}\{-i\hbar\vec{\nabla}_j + e[\vec{A}(r_j) - \vec{a}(r_j)]\}^2 \ , \tag{6.8}$$

where $\vec{a}(\vec{r})$ is the "Chern-Simons" vector potential:

$$\vec{a}(\vec{r}) = \frac{2m}{2\pi}\phi_0 \sum_{j=1}^{N} \frac{\vec{z} \times (\vec{r} - \vec{r}_j)}{|\vec{r} - \vec{r}_j|^2} \tag{6.9}$$

and ϕ_0 is the magnetic field flux quantum.

The Chern-Simons magnetic field $\vec{b}(\vec{r})$ associated with the vector potential $\vec{a}(\vec{r})$ is given by:

$$\vec{b}(\vec{r}) = \vec{\nabla} \times \vec{a}(\vec{r}) = 2m\phi_0 \sum_{j=1}^{N} \delta(\vec{r} - \vec{r}_j) = \rho(\vec{r})2m\phi_0 \tag{6.10}$$

where $\rho(\vec{r})$ is the local particle density.

In other words, the Chern-Simons transformation can be described as the exact modeling of an electron as a fermion attached to $2m$ flux quanta.

Assuming a uniform density, the Chern-Simons flux quanta attached to the fermions are smeared out into a uniform magnetic field of magnitude:

$$< \vec{b} >= \rho_e 2m\phi_0 \tag{6.11}$$

with ρ_e the average electronic density.

At some special value of ν, when $|\vec{B}| = | < \vec{b} > | = \rho_e 2m\phi_0$, the applied magnetic field precisely cancels the Chern-Simons flux at the mean field level.

This happens at filling factors

$$\nu = \frac{\phi_0 \rho_e}{B} = 1/(2m) \tag{6.12}$$

At these special filling factors $\nu = 1/(2m)$, $m = 1, 2 \ldots$ the mean field system can be described as fermions in zero magnetic field, and should therefore be a compressible Fermi-looking liquid state.

When ν is away from $1/(2m)$, the applied magnetic field and the Chern-Simons one do not cancel, so a residual field:

$$B^* = B - 2m\phi_0\rho_e = B(1 - 2m\nu) \tag{6.13}$$

is left over.

Thus, the mean field system is decribed as non-interacting fermions in a uniform field B^*. The effective filling factor for these gauge transformed fermions, $p = \rho_e\phi_0/B^*$ is $1, 2 \ldots$ corresponding to the integer quantum Hall effect (IQHE) of these transformed fermions.

The "true" filling factor of the electrons, $\nu = \rho_e\phi_0/B$ is just $\nu = \frac{p}{2mp+1}$, which is precisely the composite fermion (CF) Jain series [25] of FQHE states.

Thus the FQHE at these filling factors is identified with an IQHE of gauge transformed fermions.

The excitation gaps for these quantized Hall states are naturally given by the corresponding effective cyclotron frequency of the CF-s:

$$E_g = \hbar\omega_c^* = \hbar\frac{eB^*}{m^*_{gap}(\nu)} , \tag{6.14}$$

where $m^*_{gap}(\nu)$ is the effective mass.

In the following we concentrate on the filling $\nu = 1/2$, where several related wavefunctions have been employed to incorporate the physics of CF-s on it.

From the Chern-Simons (CS) theory, we know that at exactly $\nu = 1/2$ the fermions see no net magnetic field, so they can form a Fermi sea, which does have a uniform density.

As a consequence we would expect that the half-filled state should be well described by a

Fermi many-electron wavefunction of the form:

$$\Psi_{\nu=1/2}^{Fermi} = \hat{P}_{LLL} \prod_{j<k}^{N} (z_j - z_k)^2 Det\{\varphi_{\vec{k}}(\vec{r})\} \ , \tag{6.15}$$

where $\varphi_{\vec{k}}(\vec{r})$ are normalized plane waves in 2D.

In order to have the correct density of the half filled case, the Fermi surface must have the radius, $k_F = 1/l_0$. Excited states involve creation of quasiparticle-quasihole pairs near this Fermi-like surface and these excitations should have an effective mass $m^*(k)$ determined by inter-electron interactions only.

6.3 The Fermi Hyper-Netted-Chain formalism for half-filling

Let us start the application of the FHNC theory on the half filled state, by computing the (reduced) single–particle density matrix for the dynamically uncorrelated state of the half-filled Fermi wavefunction,

$$\hat{\rho}(\vec{r}_1, \vec{r}_2) = g_s \sum_{|\vec{k}| \leq k_F} n(\vec{k}) \ \varphi_{\vec{k}}^*(\vec{r}_1) \varphi_{\vec{k}}(\vec{r}_2) \tag{6.16}$$

where the ground state occupation number for a fully-spin-polarized (spinless) 2D ideal Fermi gas ($g_s = 1$) is:

$$n(\vec{k}) = \begin{cases} 1 & |\vec{k}| \leq k_F \\ 0 & |\vec{k}| > k_F \end{cases} \tag{6.17}$$

The normalized single particle states of a 2D gas of free electrons occupying an area A, are $\varphi_{\vec{k}}(\vec{r}) = \frac{1}{\sqrt{A}} e^{i\vec{k}\vec{r}}$, and $k_F = 1/l_0$.

A trivial calculation of the statistical exchange factor $l(\vec{r}_1, \vec{r}_2) = \hat{\rho}(\vec{r}_1, \vec{r}_2)/\rho$ gives:

$$l(\vec{r}_1, \vec{r}_2) = 2 \ \frac{J_1(k_F r_{12})}{k_F r_{12}} \tag{6.18}$$

where $r_{12} = |\vec{r}_2 - \vec{r}_1|$ and $J_1(x)$ is the first order Bessel function.

Noting that:

$$\lim_{x \to 0} \frac{J_1(x)}{x} = 1/2 \tag{6.19}$$

we assure ourselves to have correctly described all the main ingredients needed by the FHNC theory.

The FHNC relations given in Appendix A, provide a closed set of equations for the nodal and non-nodal (composite) components only, if the elementary contributions (described by elementary diagrams) are known. Several different approximation schemes are available for an appropriate evaluation of the elementary portions. However, at present we neglect such diagrams adopting the so-called FHNC/0 approximation. In this approximation we set $E_{\alpha,\beta} = 0$, where the indices are (α, β)= (dd), (de), (ee) and (cc).

For convenience, wee substitute: $f(|\vec{r}_i - \vec{r}_j|)^2 = \exp[U(|\vec{r}_i - \vec{r}_j|)]$, in the expression of $|\Psi^{Fermi}_{\nu=1/2}|^2$, and next, we separate the pseudopotential associated with the Jastrow part, $U(r_{12}) = 4\ln(|z_1 - z_2|)$, into a short– and a long–ranged part, respectively,

$$U_s(r_{12}) = -4K_0(Qr_{12}) \ , \tag{6.20}$$

$$U_l(r_{12}) = 4K_0(Qr_{12}) + 4\ln(r_{12}) \ . \tag{6.21}$$

Function $K_0(x)$ is the standard modified Bessel function and the wave number Q is a cut-off parameter of order $1/l_0$. Furthermore, all nodal and non-nodal functions are separated into their respective short– and long–range parts and the FHNC/0 equations are solved by a standard iterative procedure.

6.4 The Effective Hyper-Netted-Chain Method

The EFHNC prescription applied to the $\Psi^{Fermi}_{\nu=1/2}$ wavefunction, leads us to the (pseudo)potential

$$w(r) = \ln[g_{exact}(r)] - \frac{1}{\rho}[\frac{(S_{exact}(k)-1)^2}{S_{exact}(k)}]^{F^{-1}} , \tag{6.22}$$

where the spatial distribution function $g_{exact}(r)$ and the associated structure function $S_{exact}(k)$ correspond to the dynamically uncorrelated 2D ideal Fermi gas.

Employing Eq.(6.18) we have

$$|l(\vec{r}_1,\vec{r}_2)|^2 = |2\frac{J_1(k_F r_{12})}{k_F r_{12}}|^2 , \tag{6.23}$$

and, consequently, for our spin-polarized (spinless) system, $g_s = 1$, we have

$$g_{exact}(r_{12}) = 1 - \frac{1}{g_s}|l(\vec{r}_1,\vec{r}_2)|^2 = 1 - 4|\frac{J_1(k_F r_{12})}{k_F r_{12}}|^2 , \tag{6.24}$$

The static structure factor for the 2D ideal Fermi gas [49] was written as:

$$S_{exact}(k) = \begin{cases} 2/\pi[\arcsin(\frac{k}{2k_F}) + \frac{k}{2k_F}\sqrt{1-(\frac{k}{2k_F})^2}] & k \le 2k_F \\ 1 & k \ge 2k_F \end{cases} \tag{6.25}$$

With these expressions as input, Eq.(6.22) provides an explicit expression for the potential $w(r)$ and, consequently, writing

$$|\Psi^{Fermi}_{\nu=1/2}|^2 = \prod_{i<j}^{N} \exp\left[\tilde{u}(r_{ij})\right] , \tag{6.26}$$

where $\tilde{u}(r_{ij}) = 4\ln(r_{ij}) + w(r_{ij})$.

We may now employ the familiar Bose HNC/0 formalism to perform the calculation of the radial distribution function.

$$\tilde{U}_s(r_{12}) = -4K_0(Qr_{12}) \tag{6.27}$$

$$\tilde{U}_l(r_{12}) = 4K_0(Qr_{12}) + 4\ln(r_{12}) + w(r_{12}) \tag{6.28}$$

Decomposing the function $w(r_{12})$ into a short– and a long–range portion,

$$w(r_{12}) = w_s(r_{12}) + w_l(r_{12}) \ , \tag{6.29}$$

we may write

$$w_s(r_{12}) = \ln\ [g_{exact}(r_{12})\ ] \tag{6.30}$$

and

$$w_l(r_{12}) = -\frac{1}{\rho}\ \{\ \frac{[S_{exact}(k)-1]^2}{S_{exact}(k)}\ \}^{F^{-1}} \ . \tag{6.31}$$

This decomposition achieves an analogous convenient separation $\tilde{u}(r_{12})$ of the pseudopotential,

$$\tilde{u}_s(r_{12}) = -4K_0(Qr_{12}) + w_s(r_{12}) \ , \tag{6.32}$$

$$\tilde{u}_l(r_{12}) = 4K_0(Qr_{12}) + 4\ln(r_{12}) + w_l(r_{12}) \ . \tag{6.33}$$

Consequently, the k-space representation of the long-ranged part of the pseudo-potential $\tilde{u}_l(k)$, may be analytically performed and poses no computational problems for applying standard EFHNC/0 theory.

6.5 The particle-hole excitation spectrum of the Fermi half filled state

In this section we report a new method used to compute the quasiparticle-quasihole Fermi excitations for the Fermi wave function, $\Psi^{Fermi}_{\nu=1/2}$.

For a correlated 2D Fermi gas calculations of the ground state energy E_0 are generally carried out with the wavefunction:

$$\Psi_0 = \hat{C}\ \Phi[n(\vec{k})] \tag{6.34}$$

where $\hat{C}$ is a correlation operator and $\Phi[n(\vec{k})]$ is a 2D Fermi gas wavefunction with occupations $n(\vec{k})$.

Let us compute the energies of a quasiparticle/quasihole state obtained with wavefunctions $\Psi_p(\vec{p})$ for $|\vec{p}| > k_F$ and $\Psi_h(\vec{q})$ for $|\vec{q}| < k_F$:

$$\Psi_p(\vec{p}) = \hat{C}\ \Phi[n(\vec{k}) + \delta_{\vec{p},\vec{k}}] \tag{6.35}$$

$$\Psi_h(\vec{q}) = \hat{C}\ \Phi[n(\vec{k}) - \delta_{\vec{q},\vec{k}}] \tag{6.36}$$

Let $E_p(p)$ and $E_h(q)$ be the energies obtained with these wavefunctions. The energy differences:

$$E_p(p) - E_0 = e(p > k_F) \tag{6.37}$$

$$E_0 - E_h(q) = e(q < k_F) \tag{6.38}$$

give the single particle energy to create a quasiparticle and a quasihole respectevely.

The energy per particle obtained by either adding or removing particles having $k = k_F$ is:

$$e(k_F) = \frac{E_0(\rho)}{N} + \frac{\rho}{N}\frac{\partial}{\partial\rho}E_0(\rho) \tag{6.39}$$

For a Fermi disk filled up to $|\vec{k}| \leq k_F$ the ground state energy of the system is only kinetic given by: $E_0(\rho) = \frac{1}{2}\epsilon_F N$ where $\epsilon_F = \frac{\hbar^2}{2m}\frac{4\pi}{g_s}\rho$. We are dealing with the fully spin polarized (spinless) case so g_s is 1.

It is convenient to calculate $e(p > k_F)$ and $e(q < k_F)$, respectevily the quasiparticle and quasihole excitation energies, by removing a small fraction $x \ll 1$ of particles [41] ($x\ N$ is the number of the removed fermions), from a thin ring at $k = k_F$ and $k = q$ in momentum space, and putting them into a thin ring at $k = p$ and $k = k_F$.

Up to terms linear in x we have:

$$E(x,k)/N = E_0/N + x[\pm e(k) \mp e(k_F)] \tag{6.40}$$

The upper signs are for the quasiparticle case $k = p > k_F$ and the lower signs for the quasihole one, $k = q < k_F$.

The "mixed" density matrix for these occupations is a simple function of x, k and r_{12} :

$$l(x,k,r_{12}) = l(\vec{r}_1,\vec{r}_2) \pm x[J_0(kr_{12}) - J_0(k_F r_{12})] \tag{6.41}$$

E_0/N is the energy per particle of the system described by the wavefunction of Eq.(6.34), where no fermions have been removed from the Fermi disk, while $E(x,k)/N$ is the energy per particle of our system when a small fraction $x \ll 1$ of particles is removed from the Fermi disk and placed on a ring at wave vector k in momentum space.

Both $E(x,k)$ and E_0 are calculated in the same way, by the FHNC method.

Noting $E(x,k)/N = e(x,k)$, $E_0/N = e_0$, and fixing just on the quasiparticle energy we write:

$$e_{qp}(q) = e(k) - e(k_F) = \frac{1}{x}[e(x,k) - e_0] \tag{6.42}$$

where $q = k - k_F > 0$

Then, the effective mass $m^*(k)$ is given by:

$$\frac{m^*(k)}{m_e} = \frac{\hbar^2}{m_e}\frac{k}{\frac{\partial}{\partial q}e_{qp}(q)} \tag{6.43}$$

where m_e is the bare mass of the electron.

6.6 Results

In the present work we applied the Fermi-Hyper-Netted-Chain (FHNC) theory to the half-filled state of FQHE, employing the unprojected Fermi half-filled wave function:

$$\Psi^{Fermi}_{\nu=1/2} = \prod_{j<k}^{N}(z_j - z_k)^2 Det\{\varphi_{\vec{k}}(\vec{r})\} \; . \tag{6.44}$$

The elementary diagrams were neglected, for sake of simplicity, so calculations were performed within the so-called FHNC/0 approximation.

Ground state interaction energy per particle, $u^{Fermi}_{\nu=1/2}$, radial distribution function, $g^{Fermi}_{\nu=1/2}(r)$ and Fermi excitation spectrum were computed for this wavefunction.

The interaction energy per particle was computed from the formula:

$$u^{Fermi}_{\nu=1/2} = \frac{\rho}{2}\int d^2r \; [g^{Fermi}_{\nu=1/2}(r) - 1] \; v(|\vec{r}|) \; . \tag{6.45}$$

The $\Psi^{Fermi}_{\nu=1/2}$ wave function does not lie entirely within the LLL, so the "kinetic energy" per particle,

$$\frac{1}{N}\frac{<\Psi^{Fermi}_{\nu=1/2}|\hat{K}|\Psi^{Fermi}_{\nu=1/2}>}{<\Psi^{Fermi}_{\nu=1/2}|\Psi^{Fermi}_{\nu=1/2}>} > \frac{1}{2}\hbar\omega_c \; . \tag{6.46}$$

The calculation of the "kinetic energy" is not easy to perform within the FHNC approach, so our interest was devoted mainly to the calculation of interaction energy per particle.

As a first step we compute these quantities also for the Laughlin-like Bose wave function,

$$\Psi^{Bose}_{\nu=1/2} = \prod_{j<k}^{N}(z_j - z_k)^2 \prod_{j=1}^{N}\exp(-\frac{|z_j|^2}{4l_0^2}) \tag{6.47}$$

which describes the electrons at a half filled "Bose" state. To do this we employ the Bose HNC method which is rather standard and much easier than the FHNC theory.

As $\Psi^{Bose}_{\nu=1/2}$ lies entirely within the LLL, the "kinetic energy" per particle is:

$$\frac{1}{N}\frac{<\Psi^{Bose}_{\nu=1/2}|\hat{K}|\Psi^{Bose}_{\nu=1/2}>}{<\Psi^{Bose}_{\nu=1/2}|\Psi^{Bose}_{\nu=1/2}>} = \frac{1}{2}\hbar\omega_c \ , \tag{6.48}$$

while the interaction energy per particle is:

$$u^{Bose}_{\nu=1/2} = \frac{\rho}{2}\int d^2r \ [g^{Bose}_{\nu=1/2}(r) - 1] \ v(|\vec{r}|) \ . \tag{6.49}$$

In Fig. 6.1 we plot the radial distribution function $g(r)$, obtained from the unprojected $\Psi^{Fermi}_{\nu=1/2}$ and $\Psi^{Bose}_{\nu=1/2}$ wave functions.

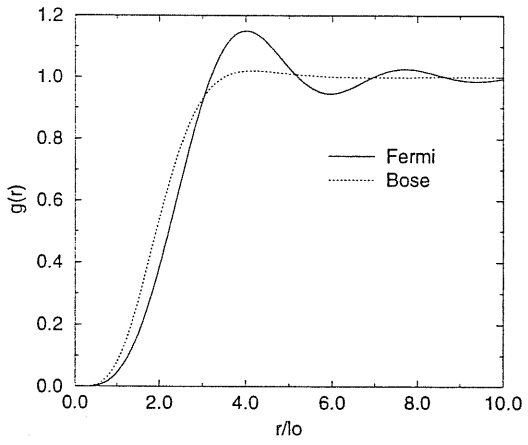

Figure 6.1: Radial distribution function $g(r)$ for the $\nu = 1/2$ state obtained from the unprojected Fermi wavefunction, $\Psi^{Fermi}_{\nu=1/2}$ and the projected Bose Laughlin-like wavefunction $\Psi^{Bose}_{\nu=1/2}$. Calculations were done neglecting the elementary diagrams, namely within the FHNC/0 and HNC/0 approximation, respectively for the Fermi and Bose case

The ground state interaction energy per particle, obtained from $\Psi^{Fermi}_{\nu=1/2}$ and $\Psi^{Bose}_{\nu=1/2}$ are shown in Table 6.1.

Table 6.1: Interaction energies per particle u_ν expressed in units $\frac{1}{4\pi\epsilon_0}\frac{e^2}{\epsilon l_0}$, computed using the unprojected Fermi wavefunction, $\Psi^{Fermi}_{\nu=1/2}$ [second row], the projected Laughlin-like Bose wavefunction $\Psi^{Bose}_{\nu=1/2}$ [third row] and exact diagonalization results of Fano et al. Ref. [50] [forth row]

ν	Wavefunction	Method	u_ν
1/2	$\Psi^{Fermi}_{\nu=1/2}$	FHNC/0	-0.503
1/2	$\Psi^{Bose}_{\nu=1/2}$	HNC/0	-0.480
1/2	Exact diagonalization	Ref. [50]	-0.469 $\pm$ 0.005

The value $u^{Fermi}_{\nu=1/2}$ for the unprojected $\Psi^{Fermi}_{\nu=1/2}$ case is found to be considerably lower than the value suggested from exact diagonalizations of small systems of up to 12 electrons [50] in the spherical geometry, shown in the forth row of Table 6.1. There is no doubt that this discrepancy is due to the missing projection of $\Psi^{Fermi}_{\nu=1/2}$ into the LLL. Without projection, the electrons are not able to avoid each other fairly well and this strongly affects the short-range behaviour of $g(r)$ and as a consequence $u^{Fermi}_{\nu=1/2}$.

Our major interest was concentrated in the unprojected Fermi half filled wave function $\Psi^{Fermi}_{\nu=1/2}$, using the method described previously, we computed the particle-hole excitation spectrum of this state,by adopting a technique previously used in nuclear physics [41]. The suposed-to-be low-energy Fermi excitations should have an effective mass $m^*(k)$ determined by inter-electron interactions only. Once we are able to calculate the interaction ground state energy per particle, for several "mixed" $\Psi^{Fermi}_{\nu=1/2}(\{\vec{r}_i\}, x)$ states, we are able to compute the quasiparticle and quasihole energies.

In Fig. 6.2 we plot the quasiparticle excitation spectrum $e_{qp}(q)$ as a function of $q = k - k_F > 0$.

It was found that in the long wavelength limit ($q \to 0$), the quasiparticle excitation energy

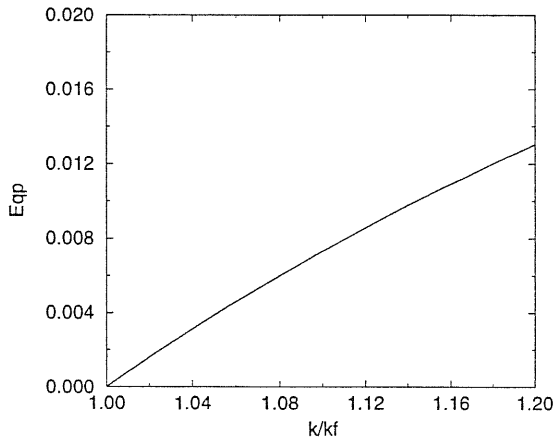

Figure 6.2: The Fermi quasiparticle excitation spectrum for the unprojected half filled Fermi state, $\Psi^{Fermi}_{\nu=1/2}$. The Fermi quasiparticle energy, $E_{qp}(q)$ computed from the inter-electron correlations only and expressed in the units of $\frac{1}{4\pi\epsilon_0}\frac{e^2}{\epsilon l_0}$, is given as a function of k/k_F, where $q = k - k_F$ and k_F is the corresponding Fermi wave vector. For $k/k_F \approx 1$ there is a linear dependence of $E_{qp}(q)$ on q.

expressed in units $\frac{1}{4\pi\epsilon_0}\frac{e^2}{\epsilon l_0}$ is linearly proportional to q expresed in units $\frac{1}{l_0}$ with $\alpha = 0.082$. In this units:

$$e_{qp}(q) = \alpha\, q \tag{6.50}$$

From the above quasiparticle excitation spectrum, we compute the effective mass $m^*(k)$ of the Fermi excitations by applying Eq.(6.43)

Using the dielectric constant $\epsilon = 12.6$ apropiate for GaAs, and the magnetic field $B = 10$ T, taken from Halperin et al. [48] we find with a striking accuracy the result:

$$m^*(k = k_F) = m_e\ , \tag{6.51}$$

in accordance with the mean field prediction of not imposing the LLL constraint.

This is an indication of the high accuracy of the adapted method used to compute the Fermi excitation spectrum, applied for the first time to a 2D problem, like the FQHE is. Further, the urgent need of a LLL projection scheme incorporated to the FHNC theory, is pointed out.

6.7 Conclusions

The Fermi-Hyper-Netted-Chain (FHNC) theory was applied to the study the filling factor $\nu = 1/2$ of the fractional quantum Hall effect (FQHE).

Calculations were done neglecting the elementary diagrams on the cluster expansion of $g(r)$, namely adopting the so-called FHNC/0 approximation.

This technique which has the priority to treat exactly in the thermodynamic limit, the many body correlated systems, was employed to study several unprojected wavefunctions, used to describe this filling factor.

Our main interest was concentrated to the unprojected Fermi wavefunction, $\Psi^{Fermi}_{\nu=1/2}$.

For the Fermi unprojected state $\Psi^{Fermi}_{\nu=1/2}$ we study both ground state and excited state properties.

After computing the Fermi quasiparticle/quasihole excitation spectrum for the unprojected $\Psi^{Fermi}_{\nu=1/2}$ state, the resulting effective mass of the quasiparticles close to the Fermi surface k_F was found to be exactly the bare mass of the electrons, in agreement with the mean-field prediction of not imposing the LLL projection.

The accuracy of the method was tested to be very high, so if a reasonable scheme to perform the LLL projection within the FHNC is found, then the calculation of the effective mass near the Fermi radius, can be done accurately.

7 Overview on ^{4}He and ^{3}He

7.1 Overview

The physics of ^{3}He and ^{4}He has always been a subject of great interest in quantum statistical mechanics and many-body theory. Helium atoms, as components of liquid or solid helium, can be considered as structureless, spherical particles interacting via a two–body potential. The attractive part of the potential causes helium gas to condense into a liquid phase (at a temperature $T_0 = 3.2K^0$ for ^{3}He and $4.2K^0$ for ^{4}He, at normal pressure). In addition, decreasing temperature below T_0, either ^{3}He, or ^{4}He does not solidify unless pressure is applied. This is a genuine quantum effect caused, in part, by the strong zero point motion arising from the small atomic mass, and, in part, by the weakness of the attractive part of the interaction, due to the high symmetry of the atoms. Moreover, quantum effects are responsible for the striking different behaviors of the Fermi ^{3}He system and the Bose ^{4}He one, which emphasize the role played by the exchange symmetry for such low T quantum fluids.

A transition to the crystalline state can only occur at higher pressure. At low T both systems undergo a phase transition to a superfluid phase, of different origin. The Bose ^{4}He undergoes a Bose-Einstein condensation in the liquid phase at the λ temperature ($2.17\ K^0$ at standard pressure), instead for ^{3}He which is Fermi liquid, the transition occurs at a much

lower temperature (some mK) due to a mechanism of pairing that can be described by BCS theory. The phase diagram of ^{3}He is richer and more complicated than that of ^{4}He.

Realistic pair potentials have been extracted from experiments and simulation data to represent the interaction between helium atoms in the condensed systems, from the Lennard-Jones (LJ) potential adopted in early studies to the class of pseudopotentials developed and refined by Aziz and coworkers [51].

Ground state properties of ^{4}He homogeneous phases have been well described by Green Functions Monte Carlo (GFMC) simulations of the liquid and the solid phases [52] and using modern potentials they well reproduce the experimental data [53].

Also at finite temperature a satisfactory description of ^{4}He has been given by exact Path Integral Monte Carlo (PIMC) simulations, even at low T where the statistics and exchanges play an important role. From PIMC simulations the λ-transition, the momentum distribution and the condensate fraction have been studied with precision.

For ^{3}He the situation is less satisfactory as Quantum Monte Carlo results are not as accurate as for ^{4}He; GFMC simulations for the unpolarized system have been performed in the fixed node approximation [54] (employing nodes from accurate variational wave functions), which give an upper bound to the exact energies, and very recenly a PIMC method to treat Fermi systems has been developed by Ceperley [55], who employs a fixed node approximation for the high T density matrix, and has been used to study ^{3}He down to 0.5 K^0 taking into account also the statistics.

In this thesis, we deal with what may seem the less interesting part of this physics, namely normal liquid and solid ^{3}He at temperature T=0 K^0, which does not exist in nature. Actually, ^{3}He becomes superfluid in the millikelvin region, and, therefore, an exact many-body theory should find ^{3}He in its B superfluid phase at T=0 K^0. However, after about thirty years from the discovery of superfluidity in ^{3}He, we are still lacking such microscopic theory.

The experimental data which are commonly used for the normal ^{3}He at $T = 0K$ are extrapolated from those of the true normal fluid at low temperatures, as if the superfluid transition were not taking place. Ab initio calculations on such strongly correlated Fermi system are of fundamental importance, not only to learn about a microscopic theory for ^{3}He and its possible breakthrough in other branches of condensed matter physics, but also to understand several properties of the normal fluid.

The more modern and efficient many–body techniques employed in such calculations, heavily rely on variational theory. The knowledge of realistic trial functions for the ground and the excited states is a fundamental requirement, first of all, to get a realistic picture of the system, but, and more important, for any further developments towards that *exact* microscopic theory, which is viewed as one of the main goals in this field of research.

Variational methods have been employed from the beginning, first in HNC calculations, then in Variational Monte Carlo (VMC) simulations, where wave functions of increasing sophistication have been developed.

VMC is a well known stochastic method, which allows for the exact evaluation of the expectation values of various observables for systems with a finite number of particle in a simulation box with periodical boundary conditions.

Today, VMC studies are also the first necessary step to perform QMC simulations. The simplest wave function is represented as a product of a pair correlations and takes into account correlations due to the excluded volum effect caused by the short range repulsion between He atoms. Triplet and backflow correlations [56] have also shown to play an important role. The crucial parts of a variational method lies in parameters or functional form optimization for the correlations employed in the wave function.

We apply such VMC techniques to the study of liquid and solid ^{3}He, using a new many-body trial wave function which uses the spin-coherent representation to include the spin-spin

correlations into the wave function.

8 Variational Studies on liquid and solid ^{3}He

8.1 Variational Monte Carlo

The Hamiltonian that describes a system of N interacting ^{3}He or ^{4}He particles is

$$\hat{H} = \hat{T} + \hat{V} = -\frac{\hbar^2}{2m}\sum_{i=1}^{N}\nabla_i^2 + \sum_{i<j}^{N} v(|\vec{r}_i - \vec{r}_j|) \,, \tag{8.1}$$

where m is the mass of either ^{3}He or ^{4}He and $v(|\vec{r}|)$ is a potential describing the interaction between the He particles.

It is beleived that the HFDHE2 potential of Aziz et al. [51] provides a realistic description of both liquid and solid ^{3}He, and we employed it in these calculations.

The HFDHE2 potential is writen as follows,

$$v(r) = \epsilon\left\{A\exp[-\alpha\frac{r}{r_m}] - [c_6(\frac{r_m}{r})^6 + c_8(\frac{r_m}{r})^8 + c_{10}(\frac{r_m}{r})^{10}]F(r)\right\} \,, \tag{8.2}$$

where

$$F(r) = \begin{cases} \exp[-(D\frac{r_m}{r} - 1)^2] & \frac{r}{r_m} \leq D \\ 1 & \frac{r}{r_m} > D \end{cases} \tag{8.3}$$

The values of the parameters for the HFDHE2 potential as reported by Aziz et al. [51] are: $A = 0.5448504 \times 10^6$, $\alpha = 13.353384$, $D = 1.241314$, $r_m = 2.9673$ Å, $\epsilon/k_B = 10.8K^o$,

$c_6 = 1.3732412$, $c_8 = 0.4253785$, $c_{10} = 0.178100$.

Employing this potential and using the most sophisticated techniques of microscopic investigation, it has been possible to reproduce most of the experimental results in liquid and solid ^{4}He. In liquid and solid ^{3}He, the available many-body theories do not still allow to check the reliability of the model Hamiltonian Eq.(8.1), with the same accuracy as in ^{4}He. Variational methods represent one of the most succesful approaches to the microscopic study of many-body systems. For any many-body trial wavefunction $\Psi(\vec{R},\vec{\sigma})$ (continuous with a continuous first derivative), satisfying some given boundary condition, the following inequality holds:

$$\frac{<\Psi(\vec{R},\vec{\sigma})|\hat{H}|\Psi(\vec{R},\vec{\sigma})>}{<\Psi(\vec{R},\vec{\sigma})|\Psi(\vec{R},\vec{\sigma})>} \geq E_0 \tag{8.4}$$

where E_0 is the exact ground state energy of the many-body correlated system and $\vec{R}$, $\vec{\sigma}$ denotes the whole set of space and spin coordinates, $\{\vec{r}_1 \ldots \vec{r}_N\}$, $\{\vec{\sigma}_1 \ldots \vec{\sigma}_N\}$.

One can obtain an approximation to this ground state energy (upper bound) by minimizing the parameters of a chosen class of trial wavefunctions. It shoul be noticed that a trial wave function $|\Psi>$, which gives a good variational energy is not guaranteed to be similarly good for the description of other properties of the system.

Apart from very simple cases, the evaluation of the integrals in Eq.(8.4) is impossible from direct numerical integration, and one has to resort to diagramatic techniques or to Monte Carlo methods.

8.2 Trial wavefunctions for liquid and solid ^{3}He

The simplest trial wavefunction to describe ^{3}He liquid is the Jastrow-Slater (JS) wavefunction,

$$|\Psi(\vec{R},\{\sigma\})>=\exp[\sum_{i<j}^{N} u(|\vec{r}_i-\vec{r}_j|)]\; D_\sigma(\vec{R}) \tag{8.5}$$

where

$$D_\sigma(\vec{R}) = D_\uparrow(\vec{r}_1\ldots\vec{r}_{N/2})\; D_\downarrow(\vec{r}_{N/2+1}\ldots\vec{r}_N) \tag{8.6}$$

In the above expression $D_\sigma(\vec{R})$, is the Slater determinant wavefunction of N fermions with spin $\{\sigma = 1/2\}$. The pseudopotential $u(|\vec{r}|)$ is due to McMillan [57] and is written as,

$$u(|\vec{r}|) = -\frac{1}{2}(\frac{b}{|\vec{r}|})^5 \tag{8.7}$$

However, this trial wavefunction gives estimates of energy per particle, which are more than 1.5 K^0, higher than the experimental values at ^{3}He liquid equilibrium density $\rho_{eq} = 0.273/\sigma^3 = 0.01635\mathring{A}^{-3}$.

Because ^{3}He is a Fermi system, the backflow not only provides triplet correlations, but also momentum dependent correlations. The backflow is usually taken into account modifying the plane waves in the determinant $D_\sigma(\vec{R})$, namely considering the following single particle orbitals:

$$\varphi_{\vec{k}}(\vec{r}_i) = \exp(i\vec{k}\vec{r}_i) \rightarrow \exp\left[i\vec{k}\left(\vec{r}_i + \lambda_B \sum_{all j\neq i}^{N} \eta(|\vec{r}_i-\vec{r}_j|)(\vec{r}_i-\vec{r}_j)\right)\right] \tag{8.8}$$

A better trial wavefunction is the one who includes explicit 3-body (triplet) correlations on it, $|\Psi_3(\vec{R},\{\sigma\})>$ which is written as:

$$|\Psi_3(\vec{R},\{\sigma\})>=\exp[\sum_{i<j}^{N} u(|\vec{r}_i-\vec{r}_j|)]\; D_\sigma(\vec{R})\; \exp\left[-\frac{\lambda_T}{2}\sum_{\{P\}}^{N}\xi(|\vec{r}_i-\vec{r}_j|)\xi(|\vec{r}_i-\vec{r}_k|)(\vec{r}_i-\vec{r}_j)(\vec{r}_i-\vec{r}_k)\right] \tag{8.9}$$

where λ_T is a variational parameter and $\{P\}$ are cyclic permutations over the three indexes i, j, and k.

The 3-body pseudopotential in Eq.(8.9) can be rewritten as:

$$\frac{\lambda_T}{2}\sum_{\{P\}}^{N}\xi(|\vec{r}_i-\vec{r}_j|)\xi(|\vec{r}_i-\vec{r}_k|)(\vec{r}_i-\vec{r}_j)(\vec{r}_i-\vec{r}_k) = \frac{\lambda_T}{4}\sum_{l=1}^{N}\vec{G}(\vec{r}_l)\vec{G}(\vec{r}_l) - \frac{\lambda_T}{2}\sum_{i<j}^{N}\xi^2(|\vec{r}_i-\vec{r}_j|)|\vec{r}_i-\vec{r}_j|^2 \tag{8.10}$$

where

$$\vec{G}(\vec{r}_l) = \sum_{all j\neq l}^{N}\xi(|\vec{r}_l-\vec{r}_j|)(\vec{r}_l-\vec{r}_j) \tag{8.11}$$

This expression is more convenient in Monte Carlo computation, because involves only updating the pair form $\vec{G}(\vec{r}_l)$. By including the triplet correlations the Jastrow pseudopotential is modified to $\tilde{u}(|\vec{r}_i-\vec{r}_j|)$, where:

$$\tilde{u}(|\vec{r}_i-\vec{r}_j|) = u(|\vec{r}_i-\vec{r}_j|) + \frac{\lambda_T}{2}\xi^2(|\vec{r}_i-\vec{r}_j|)|\vec{r}_i-\vec{r}_j|^2 \tag{8.12}$$

and the new Jastrow-Slater-Triplet (JST) wavefunction is:

$$|\Psi_3(\vec{R},\{\sigma\})>= \exp[\sum_{i<j}^{N}\tilde{u}(|\vec{r}_i-\vec{r}_j|)]\; D_\sigma(\vec{R})\; \exp\left[-\frac{\lambda_T}{4}\sum_{l=1}^{N}\vec{G}(\vec{r}_l)\vec{G}(\vec{r}_l)\right] \tag{8.13}$$

Table 8.1 reports the results of some variational calculations carried out at density $\rho\sigma^3 = 0.277$, they are compared with the experimental value at the equilibrium density $\rho_{eq}\sigma^3 = 0.273$ which is slightly lower.

A possible parametrization of the function $\xi(|\vec{r}|)$, is that employed in Ref. [56]:

$$\xi(r) = \exp[-(\frac{r-r_T^0}{w_T})^2](\frac{r-R_T}{R_T})^3\ . \tag{8.14}$$

The parameter R_T is a cutoff distance, introduced not to have discontinuties in the logarithmic derivative of the wave function at the border of the simulation box.

Table 8.1: Variational ground-state energies per particle for different trial wavefunctions, used to describe ^{3}He liquid. The values are taken from Ref. [56]

N	$\rho\sigma^3$	Potential	$\|\Psi>$	E/N $\pm\delta E$(K)
54	0.277	HFDHE2	JS	-1.08 ± 0.03
54	0.277	HFDHE2	JST	-1.61 ± 0.03
54	0.277	HFDHE2	JS+B	-1.55 ± 0.04
54	0.277	HFDHE2	JST+B	-1.91 ± 0.04
–	0.273	–	Experiment	-2.47 ± 0.01

Table 8.2: The best Jastrow and triplet variational parameters obtained using a Jastrow-Slater-Triplet (JST) wave function, for ^{3}He liquid. The values are taken from Ref. [56] , $\sigma = 2.556\mathring{A}$

N	$\rho\sigma^3$	Potential	b/σ	$\lambda_T\sigma^2$	r_T^0/σ	w_T/σ
54	0.277	HFDHE2	1.15	-12	0.95	0.6

Other variational parameters are the before mentioned triplet strength, λ_T, the center r_T^0 and width, w_T of the Gaussians.

The triplet correlation provides a localization of the particles at a distance r_T^0, depending on the angles between the directions joining the three particles.

The best triplet variational parameters for liquid ^{3}He, after a VMC simulation for $N = 54$ particles, at a density $\rho\sigma^3 = 0.277$, (higher than the liquid ^{3}He equilibrium density $\rho_{eq}\sigma^3 = 0.273$), obtained using a JST wavefunction are given in Table 8.2.

Much less satisfactory is the situation for ^{3}He solid, where most of the calculations have been performed in terms of mass three bosons, based on the fact that in a crystalline structure,

the exchange effects are small.

In order to have a localization of the particles on the sites of some given lattice, it is, in general necessary to modulate the wave function with a one-body term consisting of Gaussians centered on the appropiate positions. Such factor, known as Nosanow factor [58], must replace the $D_\sigma(\vec{R})$ determinant of the ^{3}He case.

The non-antisymmetrized Jastrow-Nosanow wave function, $\Psi^N_{Solid}(\vec{R})$ is written as a Jastrow multiplying a product of one-body terms:

$$\Psi^N_{Solid}(\vec{R}) = \exp[\sum_{i<j}^{N} u(|\vec{r}_i - \vec{r}_j|)] \prod_{j=1}^{N} \varphi_{\vec{s}_j}(\vec{r}_j) \tag{8.15}$$

where $\varphi_{\vec{s}_j}(\vec{r}_j) = \exp[-C(\vec{r}_j - \vec{s}_j)^2]$ are Gaussians centered at the given lattice sites $\vec{s}_j$ and C is considered as a variational parameter.

The effect of the antisymmetrization of the solid ^{3}He wave function, was discussed for the first time in 1977 by Ceperley et al. [59] using the Lennard-Jones (LJ) potential to describe the interaction of ^{3}He atoms:

$$V_{LJ}(r) = 4\epsilon \left[(\frac{\sigma}{r})^{12} - (\frac{\sigma}{r})^{6} \right] \tag{8.16}$$

where $\epsilon/k_B = 10.22K^o$ and $\sigma = 2.556$ Å.

They performed VMC simulations on solid bcc ^{3}He, using a many-body variational wave function composed of a product of a Jastrow function with a determinant of Gaussians:

$$\Psi_{Solid}(\vec{R}) = \exp[\sum_{i<j}^{N} u(|\vec{r}_i - \vec{r}_j|)] \; Det\{\varphi_{\vec{s}_j}(\vec{r}_i)\} \tag{8.17}$$

where $\vec{r}_i$ are the particle coordinates, and $\vec{s}_j$ are the given bcc lattice sites.

Their results are shown in Table 8.3.

Much earlier, Hansen and Levesque [60], had performed the same calculations on solid ^{3}He, employing the non-antisymmetrized $|\Psi^N_{Solid}(\vec{R})>$ wave function.

Table 8.3: VMC results for solid bcc ^{3}He, obtained with a Jastrow and an antisymmetrized determinant of Nosanow Gaussians centered at given lattice sites after Ref [59]

N	$\rho\sigma^3$	Potential	Wavefunction	b/σ	$C\sigma^2$	E (K)
54	0.427	LJ	$\|\Psi_{Solid}>$	1.092	2	1.57 ± 0.08
128	0.427	LJ	$\|\Psi_{Solid}>$	1.092	2	1.38 ± 0.1

Table 8.4: VMC results for solid bcc ^{3}He, obtained with a Jastrow and a non-antisymmetrized product of Nosanow Gaussians centered at given lattice sites. The values in second row are taken from Ref [60], while those in the third row are taken from Ref [59]

N	$\rho\sigma^3$	Potential	Wavefunction	b/σ	$C\sigma^2$	E (K)
864	0.427	LJ	$\|\Psi^N_{Solid}>$	1.092	2	1.07
864	0.427	LJ	$\|\Psi^N_{Solid}>$	1.092	2	1.07 ± 0.3

In principle this wave function does not have the correct symmetry, but the obtained energies per particle are lower than the values obtained from the properly antisymmetrized deteminant of Gaussians, as confirmed later by Ceperley et al. [59].

In Table 8.4 we show the results of Hansen and Levesque [60] (second row) and Ceperley et al. [59] (third row).

Very recently, Pederiva et al. [61] used the formalism of the Shadow Wave Functions (SWF) to describe the groundstate properties of liquid and solid ^{3}He, but their results for solid ^{3}He are still not in a very good agreement with the exact experimental values.

Periodic boundary conditions are employed to represent an infinite system by means of a few particles, and the continuity of the logarithmic derivative of the wave function must be imposed in order to have a meaningful variational estimate. To this purpose, if only

short range correlations are present in the wave function, they should be cut off continously at a distance equal to $L/2$, where L is the simulation box side, and the minimum image convention has to be used in computing the interactions. If long range correlations are considered, Ewald summation must be used.

The value of the potential energy must be corrected by a tail correction, given from the integral:

$$\frac{\rho}{2}\int_{L/2}^{\infty} d^3r\ v(|\vec{r}|) \tag{8.18}$$

Different estimators can be employed to define the local kinetic energy, as different forms of the kinetic energy operator are possible. The simplest form, called the Pandharipande-Bethe (PB) form, is obtained from the direct evaluation of $\vec{\nabla}_i^2$ on $|\Psi>$,

$$<\hat{T}>_{PB}= -\frac{\hbar^2}{2m}\sum_i^N \int d\vec{R}\ p(\vec{R})\left\{\nabla_i^2 \ln \Psi(\vec{R}) + \left[\vec{\nabla}_i \ln \Psi(\vec{R})\right]^2\right\} \tag{8.19}$$

where

$$p(\vec{R}) = \frac{\Psi^*(\vec{R})\ \Psi(\vec{R})}{\int d\vec{R}\ \Psi^*(\vec{R})\ \Psi(\vec{R})}\ . \tag{8.20}$$

Another form obtained from the Jackson-Feenberg identity

$$\int d\vec{R}\ \Psi^*(\vec{R})\ \nabla_i^2\Psi(\vec{R}) = -\int d\vec{R}\ [\vec{\nabla}_i\Psi^*(\vec{R})]\ [\vec{\nabla}_i\Psi(\vec{R})] \tag{8.21}$$

, after a partial integration is called the Jackson-Feenberg (JF) form of the kinetic energy and is given by:

$$<\hat{T}>_{JF}= \frac{1}{2}\left\{<\hat{T}>_{PB} + \frac{\hbar^2}{2m}\sum_i^N \int d\vec{R}\ p(\vec{R})\ [\vec{\nabla}_i \ln \Psi(\vec{R})]\ [\vec{\nabla}_i \ln \Psi^*(\vec{R})]\right\} \tag{8.22}$$

However the best estimator for the total energy, in terms of lower variance for a fixed number of Monte Carlo steps (MCS), is obtained using the PB kinetic energy. Nevertheless it is useful to monitor both values during the simulation, as they should converge to the same value if the sampling is correct.

9 Coherent State Wavefunction for Systems with Spin-Dependent Correlations

9.1 The coherent state formalism

Finding viable wavefunctions for variational calculations of spin-correlated systems has been a long standing problem in many areas of physics, including quantum liquids and nuclear physics. A simple Jastrow form $\Psi = \hat{F}|\Phi>$ is often used where $|\Phi>$ is a product of single particle wavefunctions that reflects the symmetry of the system and $\hat{F}$ is a correlation operator with state-dependent factors [62]. A particular example of $\hat{F}$ is the Jastrow form:

$$\hat{F} = \exp\left[\sum_{i<j}^{N}\sum_{\alpha} u^{\alpha}(|\vec{r}_i - \vec{r}_j|)\ \hat{O}_{ij}^{\alpha}\right] \tag{9.1}$$

where $\hat{O}_{ij}^{\alpha}$ is an operator of the form $\{1, \vec{\sigma}_i \cdot \vec{\sigma}_j, S_{ij}, \vec{\tau}_i \cdot \vec{\tau}_j, (\vec{\sigma}_i \cdot \vec{\sigma}_j)(\vec{\tau}_i \cdot \vec{\tau}_j), S_{ij}(\vec{\tau}_i \cdot \vec{\tau}_j)\}$ where $S_{ij} = T^{\alpha\beta}(r_{ij})\sigma_i^{\alpha}\sigma_j^{\beta}$ is the tensor operator with $T^{\alpha\beta}(r_{ij}) = 3r_{ij}^{\alpha}r_{ij}^{\beta} - \delta_{\alpha,\beta}r_{ij}^2$. The $\vec{\sigma}_i$ and $\vec{\tau}_i$ are the Pauli matrices for the spin and isospin of particle i. Here we limit the discussion to models which contain only these six or a subset of operators. Many more complicated sets of operators with spin-orbit and other correlations can be added. Summations over α are taken for those operatorial components $\hat{O}^{\alpha}$ which are needed for the particular system under consideration. For example, in nuclear matter calculations, all six components could

be considered; in neutron matter, the isospin terms will drop out and only the first three terms would be used; while a description of ^{3}He could use just the first two. A fundamental problem with the correlation operator approach has been the difficulty in evaluating accurately expectation values required for variational calculations.

For wavefunctions with no spin operators, variational calculations are straightforward to perform. The spatial integrations needed to evaluate expectation values are easily done using Monte Carlo [52, 63] or integral equation methods, such as Fermi hyper-netted-chain (FHNC) [26, 64]. In condensed matter systems, for example, Monte Carlo calculations on hundreds of particles are routine. However, the inclusion of spin variables into the correlation operator severely restricts the system size. This is because the correlation operators are usually nonlocal in spin space. The sign and phase of the resulting terms make it difficult to construct a low variance method for doing these summations. Explicit summation techniques limit the size of systems that can be considered. The largest calculations for liquid ^{3}He with explicit spin dependent wave functions has been for 14 particles [65]. In nuclear physics, only light nuclei (less than about 8 particles) have been considered [66, 67].

Incorporation of cluster expansion techniques into the Monte Carlo method shows some promise; although it remains unclear as to whether the cluster expansion converges at the four- or five-body level where the series is truncated [68, 69].

With these difficulties in mind, we propose a different approach for dealing with spin correlations in variational calculations. In this approach, the wavefunction is constructed using spin coherent states to represent the spin states of particles. In this basis, the states are parametrized by a continuous variable that looks like a classical spin vector. Particularly attractive is that operators can be represented as simple integrals over these "spin variables". Thus, correlation operators that had previously proven cumbersome in variational calculations can be replaced by integrals over c-valued functions. The price for this for-

mulation is that the number of integration variables increases. However, these integrals can be evaluated using standard numerical techniques. With this approach, Monte Carlo calculations for nuclei and larger systems may become feasible. Additionally, since these classical spin variables commute, commutator terms in the FHNC equations do not appear. After briefly reviewing the coherent state formalism, we present the coherent state wavefunction (CSWF). We report results of Monte Carlo calculations on liquid and solid ^{3}He, which agrees very well with standard methods.

In the coherent state formulation, the spin coherent states are a family of spin states created by applying the rotation operator $\hat{R}(\theta,\phi)$ to the maximally spin polarized state $|S,S>$,

$$|\Omega>=\hat{R}(\theta,\phi)|S,S>=e^{i\phi\hat{S}_z}e^{i\theta\hat{S}_y}|S,S> \tag{9.2}$$

where $|\Omega>$ is a unit vector on the sphere with coordinates $|1,\theta,\phi\rangle$, $0\leq\theta\leq\pi$ and $0\leq\phi<2\pi$ and the state $|S,S\rangle$ is the eigenstate of $\hat{S}_z$ with the largest possible eigenvalue. With this definition, there is a one-to-one correspondence between the coherent states and points on the unit sphere except for the case of the south pole.

For spin $S=1/2$ which is the case we will consider here, the expansion is especially simple

$$|\Omega\rangle=\omega_\uparrow(\Omega)|\uparrow\rangle+\omega_\downarrow(\Omega)|\downarrow\rangle \tag{9.3}$$

where the coefficients are given by

$$\omega_\uparrow(\Omega)=\langle\uparrow|\Omega\rangle=\cos(\frac{\theta}{2}\hbar)\exp(\frac{i}{2}\phi\hbar) \tag{9.4}$$

$$\omega_\downarrow(\Omega)=\langle\downarrow|\Omega\rangle=\sin(\frac{\theta}{2}\hbar)\exp(-\frac{i}{2}\phi\hbar)\ . \tag{9.5}$$

From these definitions, the overlap of two coherent states can be easily found

$$\langle\Omega'|\Omega\rangle=\omega_\uparrow(\Omega')\omega_\uparrow(\Omega)+\omega_\downarrow(\Omega')\omega_\downarrow(\Omega). \tag{9.6}$$

The Hilbert space spanned by the coherent states is distinguished by two properties: the individual states are not orthogonal and the set $\{|\Omega\rangle\}$ is overcomplete. A number of useful results follows from the overcompleteness, $\int \frac{d\vec{\Omega}}{2\pi}|\Omega\rangle\langle\Omega| = \hat{1}$.

For example, any operator $\hat{O}$ can be represented in a form that looks like a diagonal operator

$$\hat{O} = \int \frac{d\vec{\Omega}}{2\pi}|\Omega\rangle f(\Omega)\langle\Omega|. \tag{9.7}$$

Here, $f(\Omega)$ is, in general, a non-unique, c-valued function of the angles (θ, ϕ). For example, the Pauli matrices find the following representation in the coherent state basis

$$\hbar\hat{\vec{\sigma}} = \int \frac{d\vec{\Omega}}{2\pi}|\Omega\rangle\ 3\ \vec{\Omega}\ \langle\Omega|. \tag{9.8}$$

In general, if the operator $\hat{O}$ is linear in $\hbar\vec{\sigma}$, then the corresponding $f(\Omega)$ is also linear in $\vec{\Omega}$. For example, $\vec{\sigma}_i \cdot \vec{\sigma}_j$ goes over to $\vec{\Omega}_i \cdot \vec{\Omega}_j$.

In the following, we limit our discussion to the case of liquid ^{3}He. The helium interaction has no tensor force, so the total spin of the system is conserved, and no tensor correlations occur.

9.2 The Coherent State Wave Function

In a recent paper the above authors [70] have proposed a variational wave function which uses coherent states to represent the spin state of the particles. Spin states are parametrized by a continuous variable that looks like a classical spin vector, so that spin operators are represented as simple integrals without commutation terms. A standard variational Monte Carlo (VMC) technique was employed to compute groundstate energy per particle for liquid ^{3}He. This new wave function takes explicitely into account the spin-spin correlation among the particles, a quantity neglected in all previous VMC calculations.

In this work we apply such a variational wave function not only to liquid ^{3}He, but also to solid ^{3}He. Furthermore, we include also triplet correlations on it, which are essential in

bringing the equilibrium density ρ_{eq} and energy per particle $E(\rho_{eq})/N$ close to the experimental values.

A coherent state wave function (CSWF) for liquid ^{3}He includes a trivial Jastrow, a spin-spin correlation part (written in the coherent state representation) and a modified Slater determinant:

$$|\Psi_{CS}(\vec{R})>=\int d\vec{\Omega}(N)|\Omega(N)>\exp\left[\sum_{j>i}^{N}u(|\vec{r}_i-\vec{r}_j|)+\sum_{j>i}^{N}u^{\sigma}(|\vec{r}_i-\vec{r}_j|)\vec{\Omega}_i\vec{\Omega}_j\right]<\Omega(N)|\Phi> \tag{9.9}$$

We use a short-hand notation where $|\Omega(N)>$ represents the many-spin state:$|\Omega_1\ldots\Omega_N>$, $d\vec{\Omega}(N)$ is the whole set of variables $d\vec{\Omega}_1\ldots d\vec{\Omega}_N$, $\vec{\Omega}_i$ is a classical unit vector specified in spherical coordinates (θ_i,ϕ_i) and $<\Omega(N)|\Phi>$ is the modified Slater determinant. For each particle, the spin state is specified as being $|\uparrow>$ or $|\downarrow>$. The full overlap $<\Omega(N)|\Phi>$ is expressed as a determinant of modified single-particle orbitals of the form:

$$<\Omega(N)|\Phi>=Det(M_{ij})\ , \tag{9.10}$$

where $M_{ij}=\psi_j(\vec{r_i})<\Omega_i|s_j>$ and

$$s_j=\begin{cases}\uparrow & j=1,\ldots\frac{N}{2}\\ \downarrow & j=\frac{N}{2}+1,\ldots N\end{cases} \tag{9.11}$$

The single particle wavefunctions $\psi_j(\vec{r_i})$ where particle i occupies the j-th orbital are taken as plane waves of the form:

$$\psi_{\vec{k}_j}(\vec{r}_i)=\sqrt{\frac{1}{L^3}}\exp(i\vec{k}_j\vec{r}_i)\quad |\vec{k_j}|\leq k_F \tag{9.12}$$

where $j=1,\ldots N$, L is the size of the cubic simulation cell and N is the number of the particles in the simulation. The spin-spin pseudopotential has been taken of the Backflow

form, as suggested by [70]:

$$u^{\sigma}(r) = -\lambda \exp[-(\frac{r - r_0}{w})^2](\frac{L/2 - r}{L/2})^3 \tag{9.13}$$

Calculations were performed for N=14 particles in a periodic box. We compare results for the ground state energies for liquid ^{3}He using $|\Psi_{CS}\rangle$ with those obtained using both a Jastrow–Slater (JS) trial function and a Jastrow–Slater function with backflow correlations (JSB), where to include backflow, the plane waves in the Slater determinant are modified as in Eq.(8.8).

At the two-body level spin singlet pairs and spin triplet pairs are correlated differently in the CSWF. The effect can be similar to backflow which correlates states with different wave vectors differently. Recent calculations have shown that spin correlations can give results quantitatively similar to backflow[65]. The fact that the CS wavefunction results agree very well when compared to the Jastrow-Slater form with backflow (JSB) indicates that $|\Psi_{CS}\rangle$ provides a good representation of the true spin correlations. The inclusion of the triplet correlations on the CS wave function (CSWF) is done using the same formalism as in the previous section, namely by modifying the Jastrow pseudopotential to:

$$\tilde{u}(|\vec{r}_i - \vec{r}_j|) = u(|\vec{r}_i - \vec{r}_j|) + \frac{\lambda_T}{2}\xi^2(|\vec{r}_i - \vec{r}_j|)|\vec{r}_i - \vec{r}_j|^2 \tag{9.14}$$

and adding the term:

$$\exp\left[-\frac{\lambda_T}{4}\sum_{l=1}^{N}\vec{G}(\vec{r}_l)\vec{G}(\vec{r}_l)\right] \tag{9.15}$$

in the wave function. There are three parameters in the triplet correlation, namely the strength λ_T, the position r_T^0, and the width w_T of the Gaussians. The cut off R_T should be chosen equal to $L/3$ in order to avoid counting different images of the same triplet, but as $\xi(|\vec{r}|)$ is very short ranged and is almost zero at $L/3$, even larger cut off values, as reported in literature, can be used without trouble.

9.3 The Variational Monte Carlo technique

As an explicit test of this wavefunction, we present the results of a VMC calculation for liquid and solid ^{3}He. This is an appropriate test system because it has been the subject of extensive numerical investigation [63]. In addition, strong evidence suggests that spin-correlations can play a major role in determining its ground state properties.

Our VMC simulations on liquid ^{3}He are performed considering periodic boundary conditions. These conditions determine the wavevectors $\vec{k}_j = \frac{2\pi}{L}\vec{n}_j$, where $\vec{n}_j$ are the allowed quantum nembers $(0,0,0), (0,0,\pm 1)\ldots$

To ensure the correct ground state symmetries for the wave function, we consider in the simulations a number of particles N, that fill a complete shell in momentum space.

Let us use the simplified notation: $\vec{\Omega}^{L,R} = \{\vec{\Omega}_1^{L,R},\ldots\vec{\Omega}_N^{L,R}\}$, $d\vec{\Omega}^{L,R} = d\vec{\Omega}_1^{L,R}\ldots d\vec{\Omega}_N^{L,R}$, $d\vec{R} = d\vec{r}_1\ldots d\vec{r}_N$, where the superscripts L and R stands for "left" and "right" index. The ground-state expectation value of the Hamiltonian and other operators are many-body integrals.

These integrals can be evaluated by either FHNC or Monte Carlo methods. They depend not only on the interparticle distance $|\vec{r}_i - \vec{r}_j|$, but also on the angular variables $\vec{\Omega}_i^L, \vec{\Omega}_j^L, \vec{\Omega}_i^R, \vec{\Omega}_j^R$. Such dependence is due to the fact that $|\Psi_{CS}^R\rangle$ involves integrals of $\{\vec{\Omega}_i^R\}$ and similarly $\langle\Psi_{CS}^L|$ on $\{\vec{\Omega}_i^L\}$. Thus, in a given matrix element, there are two angles to be integrated for each particle $\vec{\Omega}_i^L, \vec{\Omega}_i^R$, left and right.

The expectation value of Hamiltonian $\hat{H}$ is written :

$$\frac{<\Psi_{CS}^L(\vec{R})|\hat{H}|\Psi_{CS}^R(\vec{R})>}{<\Psi_{CS}^L(\vec{R})|\Psi_{CS}^R(\vec{R})>} = \frac{\int d\vec{R}d\vec{\Omega}^L d\vec{\Omega}^R\ |p(\vec{R},\vec{\Omega}^L,\vec{\Omega}^R)|\ w(\vec{R},\vec{\Omega}^L,\vec{\Omega}^R)\ \frac{\hat{H}|\Psi_{CS}^R(\vec{R})>}{\Psi_{CS}^R(\vec{R})}}{\int d\vec{R}d\vec{\Omega}^L d\vec{\Omega}^R\ |p(\vec{R},\vec{\Omega}^L,\vec{\Omega}^R)|\ w(\vec{R},\vec{\Omega}^L,\vec{\Omega}^R)} \tag{9.16}$$

where

$$w(\vec{R},\vec{\Omega}^L,\vec{\Omega}^R) = \frac{p(\vec{R},\vec{\Omega}^L,\vec{\Omega}^R)}{|p(\vec{R},\vec{\Omega}^L,\vec{\Omega}^R)|}\ , \tag{9.17}$$

and

$$p(\vec{R},\vec{\Omega}^L,\vec{\Omega}^R) = \exp\left\{2\sum_{j>i}^{N} u(|\vec{r}_i-\vec{r}_j|) + \sum_{j>i}^{N} u^{\sigma}(|\vec{r}_i-\vec{r}_j|)(\vec{\Omega}_i^L\cdot\vec{\Omega}_j^L + \vec{\Omega}_i^R\cdot\vec{\Omega}_j^R)\right\}$$
$$< \Omega^L(N)|\Omega^R(N) > Det(M^L)Det(M^R) \quad (9.18)$$

Such expectation value is computed by generating a set $\{\vec{R},\vec{\Omega}^L,\vec{\Omega}^R\}$ of M configurations $\{\vec{R}_i,\vec{\Omega}_i^L,\vec{\Omega}_i^R\}$, $i = 1,2,\ldots M$, sampled from the probability: $|p(\vec{R},\vec{\Omega}^L,\vec{\Omega}^R)|$.

Calculations were peformed using the Metropolis algorithm [71]. Initial coordinates are chosen for each particle; typically there are either on a lattice or are a result of a previous Monte Carlo run. The particles are then moved one by one to new trial positions. The probability to accept the Metropolis move p is given by :

$$p = \frac{|p(\vec{R}_{new},\vec{\Omega}^L_{new},\vec{\Omega}^R_{new})|}{|p(\vec{R}_{old},\vec{\Omega}^L_{old},\vec{\Omega}^R_{old})|} \quad (9.19)$$

and the expectation value of Eq.(9.16) is found averaging the quantity:

$$\frac{\sum_i^M w(\vec{R}_i,\vec{\Omega}_i^L,\vec{\Omega}_i^R)\; E_L(\vec{R}_i,\vec{\Omega}_i^L,\vec{\Omega}_i^R)}{\sum_i^M w(\vec{R}_i,\vec{\Omega}_i^L,\vec{\Omega}_i^R)} \quad (9.20)$$

where the local energy $E_L(\vec{R}_i,\vec{\Omega}_i^L,\vec{\Omega}_i^R)$ is:

$$E_L(\vec{R}_i,\vec{\Omega}_i^L,\vec{\Omega}_i^R) = \frac{\hat{H}|\Psi^R_{CS}(\vec{R})>}{\Psi^R_{CS}(\vec{R})} = \sum_{j>i}^{N} v(|\vec{r}_i-\vec{r}_j|) - \frac{\hbar^2}{2m}\sum_{i=1}^{N}\frac{(\vec{\nabla}_i)^2\Psi^R_{CS}(\vec{R})}{\Psi^R_{CS}(\vec{R})} =$$
$$\sum_{j>i}^{N} v(|\vec{r}_i-\vec{r}_j|) - \frac{\hbar^2}{2m}\sum_{i=1}^{N}\left[h_i(\vec{R},\vec{\Omega}^L,\vec{\Omega}^R) - \vec{g}_i(\vec{R},\vec{\Omega}^L,\vec{\Omega}^R)\vec{g}_i(\vec{R},\vec{\Omega}^L,\vec{\Omega}^R)\right] \quad (9.21)$$

The laplacian and the gradient are respectevely:

$$h_i(\vec{R},\vec{\Omega}^L,\vec{\Omega}^R) = (\vec{\nabla}_i)^2 \ln\left[\Psi^R_{CS}(\vec{R})\right] \quad (9.22)$$

$$\vec{g}_i(\vec{R},\vec{\Omega^L},\vec{\Omega^R}) = (\vec{\nabla}_i)\ln\left[\Psi^R_{CS}(\vec{R})\right] \quad (9.23)$$

The pseudopotential $u(|\vec{r_i} - \vec{r_j}|)$ for the 2-body Jastrow correlation between particle i and particle j is taken of McMillan form [57],

$$u(|\vec{r}|) = -\frac{1}{2}(\frac{b}{|\vec{r}|})^5 \tag{9.24}$$

where b is variationally chosen.

In these calculations, the phase $w(\vec{R}, \vec{\Omega}^L, \vec{\Omega}^R)$ limits the size of the system that can be currently handled with low variance, so for the liquid ^{3}He, the calculations were possible only for $N = 14$ particles.

9.4 Results on liquid ^{3}He

We have performed VMC calculations on liquid ^{3}He using the Coherent State Wave Function (CSWF), $|\Psi_{CS}(\vec{R}) >$ of Eq.(9.9).

In our Monte Carlo calculations, we have used a number N=14 of particles. For a higher number of particles, N=54, we were not able to have a statistically stable result, because of the sign problem.

For the liquid densities we considered, the size of the cubic simulation box was taken $L(N) = (N/\rho)^{1/3}$ compatible with N=14.

For the McMillan pseudopotential $u(|\vec{r}|) = -\frac{1}{2}(\frac{b}{|\vec{r}|})^5$, the best variational b was: $b = 2.94\mathring{A}$.

The spin-spin pseudopotential $u^\sigma(r)$ was taken as in Eq.(9.13). The best variational values were found to be the same as those reported by Lawson et al. [70], namely: $\lambda = -6$, $b = 2.94\mathring{A}$, $r_0 = 2.4\mathring{A}$ and $w = 1.3\mathring{A}$.

For the liquid ^{3}He case, we computed the total radial distribution function $g(r) = g^{\uparrow\uparrow}(r) + g^{\uparrow\downarrow}(r)$ and the spin-resolved ones, $g^{\uparrow\uparrow}(r)$ and $g^{\uparrow\downarrow}(r)$, at given densities.

Starting from the definition of the pair distribution function :

$$\rho g(\vec{r}) = \frac{1}{N}\left\langle \sum_{i=1}^{N}\sum_{j\neq i}^{N} \delta\left[\vec{r} - (\vec{r}_i - \vec{r}_j)\right]\right\rangle \tag{9.25}$$

for a homogeneous and isotropic liquid as the ^{3}He case, we have:

$$\rho g(r) = \frac{2}{N}\left\langle \sum_{j>i}^{N} \delta\left[r - |\vec{r}_i - \vec{r}_j|\right]\right\rangle \tag{9.26}$$

where $r = |\vec{r}|$. The normalization of $g(r)$ is obtained by integrating over all possible separations of 2 atoms, namely:

$$\rho \int d^3r\ g(r) = N - 1 \tag{9.27}$$

To evaluate $g(r)$ from the simulation data we rewrite Eq.(9.27) as:

$$\rho \sum_{dr} g(r)\Omega(r,dr) = \frac{2}{N}\sum_{dr}\left\langle \sum_{j>i}^{N} \delta\left[r - |\vec{r}_i - \vec{r}_j|\right]\Omega(r,dr)\right\rangle\ , \tag{9.28}$$

where $\Omega(r,dr)$ is a spherical shell of radius r and thickness dr.

The quantity $N(r,dr) = \sum_{j>i}^{N} \delta\left[r - |\vec{r}_i - \vec{r}_j|\right]\ \Omega(r,dr)$ is a counting operator which gives the number of atoms found in the sperical shell $\Omega(r,dr)$, with the shell centered on another atom.

Term by term we must have:

$$g(r) = \frac{< N(r,dr) >}{\frac{N}{2}\ \rho\ \Omega(r,dr)} \tag{9.29}$$

and this is the most suitable form to compute $g(r)$ in a MC simulation.

Similarly $g^{\uparrow\uparrow}(r) = \frac{<N^{\uparrow\uparrow}(r,dr)>}{\frac{N}{2}\rho\Omega(r,dr)}$ and $g^{\uparrow\downarrow}(r) = \frac{<N^{\uparrow\downarrow}(r,dr)>}{\frac{N}{2}\rho\Omega(r,dr)}$.

In the coherent state representation the operator $\hat{P}_{ij}^{\uparrow\uparrow}(r) = \frac{1+\vec{\sigma}_i\vec{\sigma}_j}{2}$ provides to be 1 only when the spins of the particles i and j, are parallel at a given distance r between them . Otherwise this operator is always 0.

Similarly $\hat{P}_{ij}^{\uparrow\downarrow}(r) = \frac{1-\hat{\vec{\sigma}}_i\hat{\vec{\sigma}}_j}{2}$ does the same thing for the anti-parallel spins.

Keeping this in mind it is not difficult to compute:

$$< N^{\uparrow\uparrow}(r,dr) >= \frac{< \Psi_{CS}^L|\hat{P}_{ij}^{\uparrow\uparrow}(r)|\Psi_{CS}^R >}{< \Psi_{CS}^L|\Psi_{CS}^R >} = \frac{1}{2}\left[1 + \frac{< \Psi_{CS}^L|\vec{\sigma}_i\vec{\sigma}_j|\Psi_{CS}^R >}{< \Psi_{CS}^L|\Psi_{CS}^R >}\right] =$$
$$\frac{1}{2}\left[1 + \frac{\int d\vec{R}d\vec{\Omega}^L d\vec{\Omega}^R \; |p(\vec{R},\vec{\Omega}^L,\vec{\Omega}^R)| \; w(\vec{R},\vec{\Omega}^L,\vec{\Omega}^R) \; \frac{<\Omega^L(N)|\vec{\sigma}_i\vec{\sigma}_j|\Omega^R(N)>}{<\Omega^L(N)|\Omega^R(N)>}}{\int d\vec{R}d\vec{\Omega}^L d\vec{\Omega}^R \; |p(\vec{R},\vec{\Omega}^L,\vec{\Omega}^R)| \; w(\vec{R},\vec{\Omega}^L,\vec{\Omega}^R)}\right] \tag{9.30}$$

The same formula is obtained for $< N^{\uparrow\downarrow}(r,dr) >$, where the sign of the second term within the brackets must be changed from + to −.

The quantity $\frac{<\Omega^L(N)|\hat{\vec{\sigma}}_i\hat{\vec{\sigma}}_j|\Omega^R(N)>}{<\Omega^L(N)|\Omega^R(N)>}$ is written as follows

$$\frac{< \Omega^L(N)|\hat{\vec{\sigma}}_i\hat{\vec{\sigma}}_j|\Omega^R(N) >}{< \Omega^L(N)|\Omega^R(N) >} = \frac{< \Omega_i^L|\sigma_i^z|\Omega_i^R >}{< \Omega_i^L|\Omega_i^R >}\frac{< \Omega_j^L|\sigma_j^z|\Omega_j^R >}{< \Omega_j^L|\Omega_j^R >} +$$
$$\frac{< \Omega_i^L|\sigma_i^x|\Omega_i^R >}{< \Omega_i^L|\Omega_i^R >}\frac{< \Omega_j^L|\sigma_j^x|\Omega_j^R >}{< \Omega_j^L|\Omega_j^R >} + \frac{< \Omega_i^L|\sigma_i^y|\Omega_i^R >}{< \Omega_i^L|\Omega_i^R >}\frac{< \Omega_j^L|\sigma_j^y|\Omega_j^R >}{< \Omega_j^L|\Omega_j^R >} \tag{9.31}$$

In the coherent state representation expectation values like $< \Omega_i^L|\sigma_i^z|\Omega_i^R > \ldots$ are straightforward and easily implemented in the code.

In Fig. 9.1 we show the spin parallel and spin anti-parallel radial distribution functions obtained for liquid ^{3}He at a density $\rho = 0.01660\mathring{A}^{-3}$, using the CSWF.

In Table 9.1 we show the values of the energy per particle obtained from the CSWF, after a VMC simulation on liquid ^{3}He, with $N = 14$ particles. The last row refers to the CSWF+Triplet results.

The inclusion of the triplet correlations is done modifying the Jastrow pseudopotential as in Eq.(9.14) and adding the term Eq.(9.15) in the CSWF.

The parametrization of $\xi(r)$ is done as in Eq.(8.14), but we must bear in mind that:

$$\xi(r) = \exp[-(\frac{r - r_T^0}{w_T})^2](\frac{r - R_T(N)}{R_T(N)})^3 \tag{9.32}$$

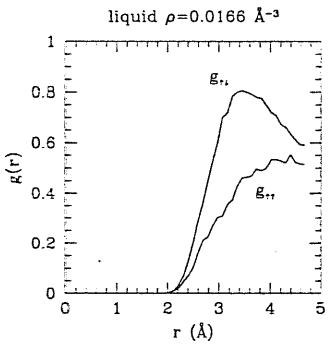

Figure 9.1: Radial distribution function $g^{\uparrow\uparrow}(r)$ and $g^{\uparrow\downarrow}(r)$ for liquid ^{3}He at the density $\rho = 0.01660\mathring{A}^{-3}$, after a simulation with N=14 particles using the coherent state representation to include the spin-spin correlations into the wave function (CSWF)

and their values in Table 8.2 are compatible with $N = 54$.

Using the same variational values for the triplet as those of Table 8.2, we have different cut-off-s for $N = 14$ and $N = 54$, namely

$$\frac{R_T(N=14)}{R_T(N=54)} = (\frac{14}{54})^{1/3} \tag{9.33}$$

In Fig. 9.2, we plot $\sqrt{|\lambda_T|}\ \xi(r)$ for $N = 14$ and $N = 54$, using the same variational parameters $\lambda_T\sigma^2 = -12$, $r_T^0/\sigma = 0.95$, $w_T/\sigma = 0.6$. In the case of Fig. 9.2 the cut-off for the triplet correlation $\xi(r)$ is taken at $R_T(N) = \frac{L(N)}{2} = \frac{1}{2}(\frac{N}{\rho})^{1/3}$ and not at $R_T(N) = \frac{L(N)}{3}$.

Table 9.1: Variational ground-state energies per particle after a VMC simulation on ^{3}He liquid. Our simulations were done using the Coherent State Wave function (CSWF) for N=14 particles. Later on, also triplet correlations were included in the wavefunction (CSWF+T).

N	$\rho\sigma^3$	$\rho(\mathring{A}^{-3})$	Potential	$\|\Psi>$	E/N (K)
14	0.273	0.01635	HFDHE2	CSWF	-1.49 ± 0.03
14	–	0.01797	HFDHE2	CSWF	-1.22 ± 0.03
14	0.325	0.01946	HFDHE2	CSWF	-0.71 ± 0.03
14	0.277	0.01659	HFDHE2	CSWF	-1.41 ± 0.01
14	0.277	0.01659	HFDHE2	CSWF+T	-0.00000 ± 0.00000

9.5 Results on solid ^{3}He

Solid ^{3}He is very interesting for its magnetic properties. From experiment it is known that below a temperature of the order of mK^0, a nuclear-spin ordering of the up-up-down-down (u2d2) form becomes stable, namely there is a stacking of two planes of the body-centered-cubic (bcc) crystal with "up" spins, followed by two planes with "down" spins (u2d2).
Such order is due to a competetion between two, three, or more atomic exchanges in solid ^{3}He and can hardly be observed in a standard simulation.
We describe solid ^{3}He by an anti-symmetrized many-body wavefunction $|\Psi_{CS}^{Solid}(\vec{R})>$ which includes explicitely the spin-spin correlations through the coherent state representation:

$$|\Psi_{CS}^{Solid}(\vec{R})>=\int d\vec{\Omega}(N)\,|\Omega(N)>\exp[\sum_{i<j}^{N}u(|\vec{r}_i-\vec{r}_j|)]\exp[\sum_{i<j}^{N}u^{\sigma}(|\vec{r}_i-\vec{r}_j|)\vec{\Omega}_i\vec{\Omega}_j]\;<\Omega(N)|Det\{\varphi_{\vec{s}_j}(\vec{r}_i)\}> \tag{9.34}$$

The single-particle states $\varphi_{\vec{s}_j}(\vec{r}_i)=\exp[-C(\vec{r}_i-\vec{s}_j)^2]$ of the determinant of Gaussians are modified as in the ^{3}He liquid case by the $<\Omega_i|s_j>$ angular factors, where $s_j=\uparrow$ for

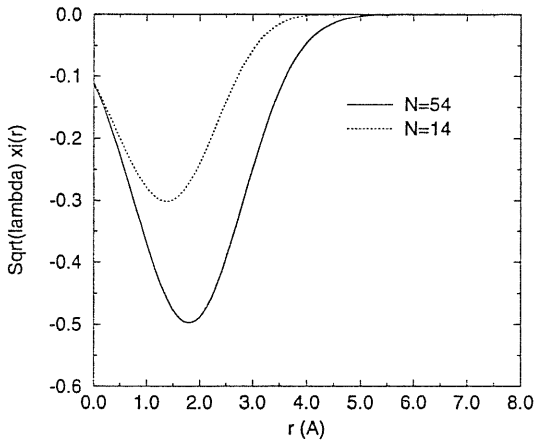

Figure 9.2: The triplet correlation $\xi(r)$ multiplied by the the square of the modulus of the triplet strength $|\lambda_T|$, drawn with the same variational parameters $\lambda_T = -1.83769\mathring{A}^{-2}$, $r_T^0 = 2.4282\mathring{A}$, $w_T = 1.5336\mathring{A}$ for the N=14 and N=54 particle case. The above numbers are the best values for the triplet correlation from a VMC simulation with N=54

$j = 1 \ldots N/2$, and $s_j = \downarrow$ otherwise.

We have performed VMC simulations at several densities of solid ^{3}He, using $N = 16$ and later $N = 54$ particles.

Differently from the liquid ^{3}He case, for the solid ^{3}He the simulations were statistically stable also for $N = 54$.

For $N = 16$, we started the simulation from an initial configuration of bcc type with an anti-ferromagnetic (AF) nuclear-spin ordering and optimized the parameters of $|\Psi_{CS}^{Solid}(\vec{R})>$ The optimal values for $N = 16$ were as follows, for the Jastrow pseudopotential $b = 2.84\mathring{A}$; for the spin-spin pseudopotential $\lambda = -5$, $r_0 = 2.4\mathring{A}$, $w = 1.3\mathring{A}$ and for the determinant

Table 9.2: Variational ground-state energies per particle after a VMC simulation on ^{3}He solid. Our simulations were done using the Coherent State Wave function (CSWF). The results at the last two rows were obtained with a Shadow-Slater-Backflow wave function of Ref [61].

N	$\rho\sigma^3$	$\rho(\mathring{A}^{-3})$	Potential	$\|\Psi>$	E/N(K)
16	–	0.02509	HFDHE2	$\|\Psi_{CS}^{Solid}>$	0.69 ± 0.03
16	0.427	0.02570	HFDHE2	$\|\Psi_{CS}^{Solid}>$	0.79 ± 0.02
16	–	0.02618	HFDHE2	$\|\Psi_{CS}^{Solid}>$	1.03 ± 0.03
16	–	0.02867	HFDHE2	$\|\Psi_{CS}^{Solid}>$	2.43 ± 0.03
16	–	0.03011	HFDHE2	$\|\Psi_{CS}^{Solid}>$	3.61 ± 0.05
54	0.427	0.02570	HFDHE2	ShSB-NAF	0.955 ± 0.033
54	0.427	0.02570	HFDHE2	ShSB+Exchange	2.057 ± 0.039

of Gaussians $C = 0.40\mathring{A}^{-2}$.

Either for the bcc-AF, or for the bcc-u2d2 spin ordering, the energy per particle obtained from the simulation, was the same within the statistical error bars.

From further tests it comes out that the CSWF does not have the pathologic behaviour of the Shadow-Slater-Backflow Wave Function (ShSB) of Pederiva et al. [61], when the exchange moves are turned on.

In Table 9.2 we report the values obtained from a VMC simulation of $N = 16$ particles of solid ^{3}He at 5 different densities, and compare are data with those of Ref. [61].

The spin parallel and spin anti-parallel radial distribution function $g^{\uparrow\uparrow}(r)$ and $g^{\uparrow\downarrow}(r)$ are plotted in Fig. 9.3 for the solid ^{3}He bcc at the density $\rho = 0.02509\mathring{A}^{-3}$.

Changing the form of the spin-spin pseudopotential $u^{\sigma}(r)$ as shown in Fig. 9.4, we were able to obtain quite visible changes in the radial distribution functions too.

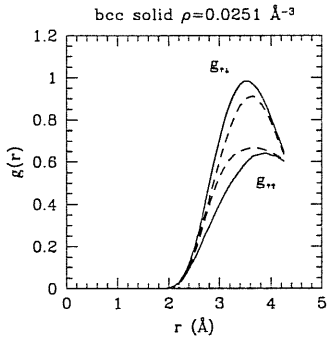

Figure 9.3: The spin parallel and spin anti-parallel radial distribution function $g^{\uparrow\uparrow}(r)$ and $g^{\uparrow\downarrow}(r)$ for the bcc solid ^{3}He at the density $\rho = 0.02509\mathring{A}^{-3}$ plotted for two different spin-spin pseudopotentials. The simulations were done with N=16 particles.

When we extended the calculation to the $N = 54$ case, using the same wave function, we had to reoptimize the variational values we used before.

For the simulation on solid ^{3}He using $N = 54$ particles at the density $\rho = 0.02570\mathring{A}^{-3}$ ($\rho\sigma^3 = 0.427$), the best variational estimates were found to be: $b = 2.82\mathring{A}$ for the Jastrow part, $\lambda = -2.1$, $r_0 = 1.8\mathring{A}$, $w = 1.3\mathring{A}$ for the spin-spin pseudopotential and $C = 0.40\mathring{A}^{-2}$ for the single particle Gaussians of the determinant.

The inclusion of the triplet correlations on the solid ^{3}He study with the $|\Psi_{CS}^{Solid}(\vec{R})>$ as a trial variational many-body wave function, was done modifying the Jastrow pseudopotential and adding the triplet term as in the liquid ^{3}He case.

The optimal values of the triplet correlation parameters for solid ^{3}He, after a VMC simu-

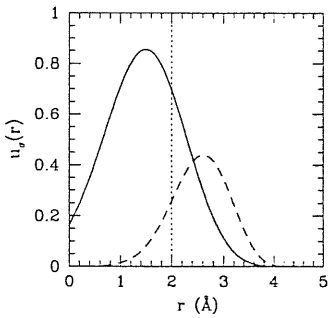

Figure 9.4: The two different spin-spin pseudopotentials $u^\sigma(r)$ refered in the previous graph. The simulations were done with N=16 particles.

lation with $N = 54$ particles were found to be: $\lambda_T = -0.00000\mathring{A}^{-2}$, $r_T^0 = 0.00000\mathring{A}$ and $w_T = 0.0000000\mathring{A}$.

In Table 9.3 we show the CSWF+Triplet (CSWF+T) results after a simulation with $N = 54$ particles for solid ^{3}He at the density $\rho = 0.02570\mathring{A}^{-3}$.

Table 9.3: Variational ground-state energies per particle after a VMC simulation on ^{3}He solid. Our simulations were done using the Coherent State Wave function (CSWF). For the case N=54 also the triplet correlations were included in the wavefunction (CSWF+T). The results at the last two rows were obtained with a Shadow-Slater-Backflow wave function and with N=54.

N	$\rho\sigma^3$	$\rho(\mathring{A}^{-3})$	Potential	$\|\Psi>$	E/N(K)
16	0.427	0.02570	HFDHE2	CSWF	0.79 ± 0.02
54	0.427	0.02570	HFDHE2	CSWF+T	0.0000 ± 0.0000
54	0.427	0.02570	HFDHE2	ShSB-NAF	0.955 ± 0.033
54	0.427	0.02570	HFDHE2	ShSB+Exchange	2.057 ± 0.039

Acknowledgments

I would like to express my gratitude to my supervisor, Prof. Stefano Fantoni, for introducing and guiding me in this new field of research. I deeply thank Prof. Erio Tosatti not only for suggesting many "physical" ideas, but also for his wonderful behaviour and friendship.

I am very grateful to Dr. Saverio Moroni and Dr. Klaus Gernoth for their help on responding with the utmost patience to all my questions.

I want to thank my class friends with whom I started the Phd studies in SISSA, and these are (in strict alphabetic order!) Alice Ruini, Carlo Cavazzoni, Claudio Tebaldi, Daniele Passerone and Marco Saitta.

Special thanks to Lu Zhong Yi and Francesco Di Tolla with whom, together with Carlo and Daniele, I shared also the working room in different times.

While living in Trieste, I frequently used to move from one place to another and the people with whom I shared the house and part of the failures during my research cannot be forgotten. Let me remember them starting from Kristi Pance and going on with D. Jamayanna, H. Odbadrakh , Lorenzo de Santis and Leonardo Guidoni.

I do not want to forget Frank Celestini, Stefano Serra and Dario Alfe with whom I shared nice time in Kanzas City.

With Stefano Giovanazzi I shared many interesting discussions and a good friendship.

I thank also Alessandro Laio, Augusto Smerzi, Abdullah Al-Sharif, Matteo Calandra and

so many others for their stimulating discussions.

Finally, I thank all the people who were close to me with their encouragements and love: my parents, my brother and especially my wife, Irena, which was always by me during this period.

Appendix A

The Fermi Hyper-Netted-Chain Equations

In the Appendix we present the explicit expressions of the quantities entering the FHNC equations.

The sums of non-nodal (composite) diagrams of the four types are given by

$$X_{dd}(r) = f^2(r)\, e^{N_{dd}(r)+E_{dd}(r)} - N_{dd}(r) - 1 \,, \tag{A.1}$$

$$X_{de}(r) = f^2(r)\, e^{N_{dd}(r)+E_{dd}(r)}[N_{de}(r) + E_{de}(r)] - N_{de}(r) \,, \tag{A.2}$$

$$X_{ee}(r) = f^2(r)\, e^{N_{dd}(r)+E_{dd}(r)}[N_{ee}(r) + E_{ee}(r) + |N_{de}(r) + E_{de}(r)|^2 - g_s|N_{cc}(r) + E_{cc}(r) - l(r)/g_s|^2] - N_{ee}(r) \,, \tag{A.3}$$

$$X_{cc}(r) = f^2(r)\, e^{N_{dd}(r)+E_{dd}(r)}[N_{cc}(r) + E_{cc}(r) - l(r)/g_s] + l(r)/g_s - N_{cc}(r) \,. \tag{A.4}$$

The chain formation of the nodal diagrams is generated by convolution equations,

$$N_{dd}(r_{12}) = \rho \int d\vec{r}_3 [X_{dd}(r_{13}) + N_{dd}(r_{13})] P(r_{32}) \,, \tag{A.5}$$

$$N_{de}(r_{12}) = \rho \int d\vec{r}_3[X_{dd}(r_{13})X_{ee}(r_{32}) - X_{de}(r_{13})X_{de}(r_{32}) + [X_{de}(r_{13}) + N_{de}(r_{13})]P(r_{32})] \ , \tag{A.6}$$

$$N_{ee}(r_{12}) = \rho \int d\vec{r}_3[X_{de}(r_{13})X_{de}(r_{32}) - X_{dd}(r_{13})X_{ee}(r_{32}) + [X_{ee}(r_{13}) + N_{ee}(r_{13})]P(r_{32})] \ , \tag{A.7}$$

$$N_{cc}(r_{12}) = \rho \int d\vec{r}_3[-l(r_{13})/g_s + X_{cc}(r_{13}) + N_{cc}(r_{13})]X_{cc}(r_{32}) \ , \tag{A.8}$$

with

$$P(r_{ij}) = X_{dd}(r_{ij}) + 2X_{de}(r_{ij}) + \rho \int d\vec{r}_k[X_{dd}(r_{ik})X_{ee}(r_{kj}) - X_{de}(r_{ik})X_{de}(r_{kj})] \ . \tag{A.9}$$

As a final result the radial distribution function is composed from the components

$$g(r) = 1 + X_{dd}(r) + N_{dd}(r) + 2[X_{de}(r) + N_{de}(r)] + X_{ee}(r) + N_{ee}(r) \ . \tag{A.10}$$

Bibliography

[1] T. Chakraborty, P. Pietaläinen, *The Fractional Quantum Hall Effect*, (Springer–Verlag, New York 1988).

[2] R.B. Laughlin, in *The Quantum Hall effect*, R. Prange and S. Girvin eds., (Springer–Verlag, New York, 1987).

[3] D.C. Tsui, H.L. Stormer, A.C. Gossard, Phys. Rev. Lett. **48**, 1559 (1982).

[4] R.B. Laughlin, Phys. Rev. Lett. **50**, 1395 (1983).

[5] J.M. Caillol, D. Levesque, J.J. Weis, J.P. Hansen, J. Stat.Phys. **28**, 325 (1982).

[6] B. Yancovici, Phys. Rev. Lett. **46**, 386 (1981).

[7] D. Levesque, J.J. Weis, and A.H. MacDonald, Phys. Rev. B **30**, 1056 (1984).

[8] S.M. Girvin, Phys. Rev. B **30**, 558 (1984).

[9] S. Fantoni, S. Rosati, Nucl. Phys. A, **328**, 478 (1979).

[10] Q.N. Usmani, B. Friedman, V.R. Pandharipande, Phys. Rev. B **25**, 4502 (1982).

[11] S.M. Girvin, A.H. Macdonald, P.M. Platzman, Phys. Rev. B **33**,2481 (1986).

[12] S.M. Girvin, A.H. Macdonald, P.M. Platzman, Phys. Rev. Lett . **54**, 581 (1985).

[13] S. Vitiello, K. Runge, and M.H. Kalos , Phys. Rev. Lett. **60**, 728 (1988).

[14] L. Reatto and G.L. Masserini, Phys. Rev. B **38**, 4516 (1988).

[15] A. Ferrante, M. Bernasconi, X.Q. Wang, S. Fantoni, and E. Tossati, in *Recent Progress in Many-Body Theories,* Vol. 3, edited by T.L. Ainsworth, C.E. Campbell, B.E. Clements, and E. Krotscheck (Plenum Press, New York and London, 1992).

[16] F.D.M. Haldane, Phys. Rev. Lett. **51**, 605 (1983).

[17] B.I. Halperin, Phys. Rev. Lett. **52**, 1583, (1984).

[18] A.H. MacDonald, G.C. Aers, and M.W.C Dharma-wardana, Phys. Rev. B **31**, 5529 (1985).

[19] S.M. Girvin, Phys. Rev. B **29**, 6012 (1984).

[20] R. Morf and B.I. Halperin, Phys. Rev. B **33**, 2221 (1986).

[21] O. Ciftja, S. Fantoni, K.A. Gernoth, Phys. Rev. B **55**, 13739 (1997).

[22] D. Yoshioka, Phys. Rev. B **29**, 6833 (1984).

[23] M.W.C Dharma-wardana, Phys. Rev. B **51**, 1653 (1995).

[24] O. Ciftja and S. Fantoni, Europhys. Lett., **36** (9), 663 (1996).

[25] J.K. Jain, Phys. Rev. Lett. **63**, 199 (1989).

[26] S. Fantoni, S. Rosati, Nuovo Cim. Lett. **10** 545 (1974) ; S. Fantoni, S. Rosati, Nuovo Cim. **A25** 593 (1975).

[27] J.P. Hansen, D. Levesque, J. Phys. C**14**, L603 (1981).

[28] E. Krotscheck, M. L. Ristig, Phys. Lett. **48A**, 17 (1974) ; E. Krotscheck, M. L. Ristig, Nucl. Phys. A **242**, 389 (1975).

[29] T. Chakraborty,Phys. Rev. B **31**, 4026 (1985).

[30] P. Pietilainen , T. Chakraborty, Europhys. Lett. **5** (2), 157 (1988).

[31] J.W. Kim, Diploma Thesis, Institut für Theoretische Physik, Universität zu Köln, 1992 (unpublished).

[32] F. Lado, J. Chem. Phys. **47** 5369 (1967).

[33] J.G. Zabolitzky, Phys. Rev. B **22**, 2353 (1980).

[34] N.E. Bonesteel, Phys. Rev. B **51**, 9917 (1995).

[35] J.K. Jain, Phys. Rev. B. **41**, 7653 (1990).

[36] G. Dev and J.K. Jain, Phys. Rev. Lett. **69**, 2483 (1992).

[37] X. G. Wu, G. Dev and J.K. Jain, Phys. Rev. Lett. **71**, 153 (1993).

[38] O. Ciftja, S. Fantoni, J. W. Kim and M. L. Ristig, to appear in Journal of Low Temperature Physics.

[39] N. Trivedi, J.K. Jain, Mod. Phys. Lett. B **5**, 503 (1993).

[40] E. Manuosakis, S. Fantoni, V.R. Pandharipande and Q.N. Usmani, Phys. Rev. B. **28**, 3770 (1983).

[41] B. Friedman, V.R. Pandharipande, Phys. Lett. **100B** 3 (1981).

[42] J.K. Jain and R.K. Kamilla, Phys. Rev. B **55**, R4895 (1997).

[43] O. Ciftja, S. Fantoni, to appear in Physical Review B.

[44] G. Fano, F. Ortolani, E. Colombo, Phys. Rev. B **34**, 2670 (1986).

[45] R.L. Willett, J.P. Eisenstein, H.L. Stormer, D.C. Tsui, A.C. Gossard, J.H. English Phys. Rev. Lett. **59**, 1776 (1987).

[46] R.L. Willett, M.A. Paalanen, R.R. Ruel, K.W. West, L.N. Pfeiffer, D.J. Bishop Phys. Rev. Lett. **65**, 112 (1990).

[47] F.D.M. Haldane, Phys. Rev. Lett. **55**, 2095 (1985).

[48] B.I. Halperin, P.A. Lee, N. Read, Phys. Rev. B **47**, 7312 (1993).

[49] M. Jonson, J. Phys. C: Solid State Phys. **9** 3055 (1976).

[50] G. Fano, F. Ortolani, E. Tosatti Nuovo Cimento 9D, 1337 (1987).

[51] R.A. Aziz, V.P.S. Nain, J.S. Carley, W.L. Taylor, G.T. McConville, J. Chem. Phys. **70**, 4330, (1979).

[52] M.H. Kalos, M.A. Lee, P.A. Withlock, G.V. Chester, Phys. Rev. B **24**, 115, (1981).

[53] P.A. Withlock, M.H. Kalos, G.V. Chester, D.M. Ceperley, Phys. Rev. B **21**, 999, (1980).

[54] M.A. Lee, K.E. Schmidt, M.H. Kalos, G.V. Chester, Phys. Rev. Lett. **46**, 728, (1981).

[55] D.M. Ceperley, Phys. Rev. Lett. **69**, 331, (1992).

[56] K.E. Schmidt, M.H. Kalos, M.A. Lee, G.V. Chester, Phys. Rev. Lett. **47**, 807, (1981).

[57] W.L. McMillan, Phys. Rev. **138A** , 442, (1965).

[58] L.H. Nosanow, Phys. Rev. Lett. **13** , 270, (1964).

[59] D.M. Ceperley, G.V. Chester, M.H. Kalos, Phys. Rev. B. **16**, 3081, (1977).

[60] J.P. Hansen, D. Levesque, Physical Review. **165**, 293, (1968).

[61] F. Pederiva, S.A. Vitiello, K. Gernoth, S. Fantoni, L. Reatto, Phys. Rev. B. **53**, 15129, (1996).

[62] V.R. Pandharipande and R.B. Wiringa, Rev. Mod. Phys. 51, 821 (1979).

[63] K.E. Schmidt and D. Ceperley in *The Monte Carlo Method in Condensed Matter Physics*, (K. Binder, ed.), Springer-Verlag, Berlin, (1992).

[64] J.W. Clark, *Progress in Particle and Nuclear Physics*, 2, (D.H.Wilkinson, ed.), 89, Oxford, (1979) S. Rosati, *From Nuclei to Particles*, course LXXIX, (A. Molinari, ed.), 73, North Holland, Amsterdam, (1981) J.G. Zabolitzky, Phys. Rev. A 16, 1258, (1977).

[65] S.A. Vitiello, K.E. Schmidt and S. Fantoni, Phys. Rev. B **55**, 5647 (1997).

[66] B. S. Pudliner, A. Smerzi, J. Carlson, V. R. Pandharipande, Steven C. Pieper, and D. G. Ravenhall, Phys. Rev. Lett. 76, 2416 (1996).

[67] B. S. Pudliner, V. R. Pandharipande, J. Carlson, and R. B. Wiringa, Phys. Rev. Lett. 74, 4396 (1995).

[68] Steven Pieper, R.B. Wiringa, and V.R. Pandharipande Phys. Rev C 46, 1741 (1992).

[69] J. Carlson and M.H. Kalos, Phys. Rev. C 32, 2105 (1985).

[70] J.W. Lawson, S.A. Vitiello, K.E. Schmidt, S. Fantoni, Phys. Rev. Lett. **78**, 1846, (1997).

[71] N. Metropolis, A.W. Rosenbluth, M.N. Rosenbluth, A.M. Teller, E. Teller, J. Chem. Phys. **21**, 1087, (1953).